Ground Vibration Measurements:
Study Case of Simultaneous HVSR and SASW for Site Characterization

By:

Yesenia S. Pérez Soto

A project submitted in partial fulfillment of the requirements for the degree of

MASTER OF ENGINEERING
in
CIVIL ENGINEERING

UNIVERSITY OF PUERTO RICO
MAYAGÜEZ CAMPUS

2019

Approved by:

_____	_____
Carlos Huerta López, Ph.D. President, Graduate Committee	Date
_____	_____
Beatriz Camacho Padrón, Ph.D. Member, Graduate Committee	Date
_____	_____
Ricardo Ramos Cabeza, Ph.D. Member, Graduate Committee	Date
_____	_____
Víctor Huérfano, Ph.D. Graduate School Representative	Date
_____	_____
Ismael Pagán Trinidad, M.S.C.E. Chair, Department of Civil Engineering and Surveying	Date

Abstract

In civil engineering, the properties of the soils are important for design and construction of a project. Therefore, it is necessary to know the different properties of the soil layers, the hydraulic and mechanical, so that the engineering process is effective. Some geophysical methods can be used to obtain the properties needed to do a proper engineering design.

The Spectral Analysis of Surface Wave (SASW) is a geophysical method that can be used to obtain the soil characterization. SASW method analyzes the dispersive characteristic of Rayleigh-waves in a homogeneous and non-homogeneous medium. The main objective is to estimate the profile of shear wave velocity versus depth to obtain a soil-site characterization without the need of a borehole. Another method is the Nakamura method, which used the spectral ratio of horizontal and vertical components (HVSR); which estimates the effect of the surface geology on seismic motion using microtremors. This procedure is suitable for areas with low seismic activity.

In this investigation a study and validation of the SASW and HVSR methods were done at the University of Puerto Rico at Mayagüez. From this, an estimation of the shear wave velocity (*Vs*) versus depth profile, and the fundamental frequency of the soil were obtained. To be able to validate the methods, Standard Penetration Test (SPT) test results were compared with the soil site characterization obtained with the SASW method; and the result of the HVSR-Nakamura method was also compared with the obtained results of Vázquez (2014).

According to the results obtained the soil classification for the different layers present in the studied area corresponds to soft soils type E of AASHTO. The estimated dominant fundamental vibration frequency of the studied area is 1.358 Hz.

The obtained results allowed us to validate how effective are the non-invasive geophysical methods (SASW and HVSR), as a reliable alternative to obtain soil site characterization and the fundamental frequency of the soils.

Resumen

En ingeniería civil, las propiedades de los suelos son importantes, tanto en el diseño como en la construcción de un proyecto. Por lo tanto, es necesario conocer las diferentes propiedades de las capas del suelo, la hidráulica y la mecánica, para que el proceso de ingeniería sea efectivo. Se pueden utilizar algunos métodos geofísicos para obtener las propiedades necesarias para realizar un diseño de ingeniería adecuado.

El Análisis Espectral de Ondas de Superficie (SASW, por sus siglas en inglés) es un método geofísico que se utiliza para obtener la caracterización de suelo. El método SASW analiza la característica dispersiva de las ondas Rayleigh en un medio homogéneo y no homogéneo. El objetivo principal es estimar la velocidad de la onda de corte versus al perfil de profundidad para obtener la caracterización de sitio de un área, sin la necesidad de un barrenado. Otro método es el método de relación espectral de componentes horizontales y verticales (HVSR, por sus siglas en inglés); que estima el efecto de la geología de la superficie sobre el movimiento sísmico utilizando microtremores. Este procedimiento es adecuado para áreas con baja actividad sísmica.

En esta investigación se realizó un estudio y validación de los métodos de SASW y HVSR en la Universidad de Puerto Rico en Mayagüez. Se obtuvo la frecuencia fundamental del suelo y la estimación de la velocidad de la onda de corte (*Vs*) del área estudiada para clasificar el tipo de suelo. Para poder validar los métodos, los resultados fueron comparados con las Pruebas de Penetración Estándar (SPT, por sus siglas en ingles). Mientras que el resultado del método HVSR-Nakamura también fue comparados con los resultados de Vázquez (2014).

De acuerdo con los resultados obtenidos, la clasificación del suelo para las diferentes capas presentes en el área estudiada corresponde a suelos blandos, tipo E según AASHTO. Mientras que la frecuencia fundamental de vibración dominante estimada del área es 1.358 Hz.

Los resultados obtenidos nos permitieron validar cuán efectivos son los métodos geofísicos no invasivos (SASW y HVSR), como una alternativa confiable para obtener la caracterización del sitio y la frecuencia fundamental de los suelos.

Acknowledgement

First, I would like to thank God for blessing me all this time. I would also like to thank my family for all their love and support; especially to my mother, Sol M. Soto, for all her sacrifice and for the values she has instilled in me. Special thanks to my sisters, Jessica, Yailin and Sol, for helping me during this process and for encouraging me to never give.

Thanks to my advisor Dr. Carlos Huerta López for all his guidance and help through the process. A big thank you to the members of my committee: Beatriz Camacho Padrón and Dr. Ricardo Ramos Cabeza for all their guidance. I would be eternally grateful for their guidance in my master's degree.

Thanks to my friends who supported me and make me smile in difficult times: Amil Font, Denny Mariana Torres, Carlos Calderon, Daniel Santiago. Special thanks to Alan Rivera who give me a lot of support with this project. Alan, thank you for helping me with the MatLab programs and for all your help during all this time.

Finally, I would also like to thank the personnel of the Department of Civil Engineering of the University of Puerto Rico in Mayagüez, specials thanks to all the professors that gave me the base, help and guidance to be able to do and finish my master's degree.

Table of Contents

List of Figures

List of Tables

Chapter 1. Introduction

For a proper design and construction of civil structures it is imperative to know the properties and composition of the site sub-soil conditions which are necessary to effectively identify and to address risks attributable to the site ground motions. In construction, the properties of the soils are important since it is used as a base for construction. Therefore, it is necessary to know the different properties of the soil layers, the hydraulic and mechanical properties, so that the engineering process is effective. Since the ground is used as the base of a construction, it is necessary to meet the requirements dictated in the project and the codes. To meet the requirements, there are different geotechnical and geophysical techniques for site physical properties and geometry (thickness) characterization.

Some of the most popular invasive and intrusive in-situ soil properties estimation geotechnical methods are: i) the Standard Penetration Test (SPT), and ii) the Static Cone Penetration Test (SCPT). The samples are supposed to represent the natural properties (pressure, moisture content, temperature, among others) of the site and depth where they were extracted. Therefore, if they are extracted for a laboratory study, they must be handled with great care and the results of the different tests must be corrected in the calculations since the sample lost its natural properties.

Other methods to obtain in-situ soil properties, are the geophysical methods. Within these methods there are invasive and non-invasive methods. Some invasive methods are the Cross-Hole and Down-Hole tests. Contrary, some non-intrusive geophysical methods are: i) the direct interpretation of the Fourier spectrum, ii) the calculation of the relative spectral ratio of a site, iii)

H/V Spectral Ratio (HVSR) using ambient vibration, iv) the Spectral Analysis of Surface Waves (SASW), and v) the Multichannel Analysis of Surface Waves (MASW). For applications in civil engineering, these methods can be used for the subsurface explorations, up to the depths of 100 to 150 m below ground level (Lai and Rix, 1998). Using these methods will improve the way the site characterization is done in civil engineering, since they are non-intrusive methods.

For this project, the HVSR and SASW methods were applied for site characterization in terms of the subsoil properties and geometry, as well as the dynamic properties. Our results were compared with the ones obtained with the SPT test conducted nearby our study site.

1.1 Research Goals and Objectives

The goal of this investigation is to study and validate the use of the: (i) spectral ratio of horizontal and vertical components (HVSR) of ambient vibration measurements, and (ii) the Spectral Analysis of Surface Waves (SASW) for site characterization in terms of the physical properties and geometry of the soil layers. To achieve this goal, the following objectives were established and conducted in an experimental site located at UPR-Mayagüez Campus:

a) collect ambient and induced vibrations in seismic arrays for HVSR and SASW,
b) processing / analysis and interpretation of collected data,
c) compute HVSR and the dispersion curve of SASW to characterize the site in terms of its fundamental vibration frequency and the Rayleigh-wave propagation velocity,
d) estimate the shear wave velocity profile versus depth by means of the SASW dispersion curve, and finally

e) compare the results obtained with the SPT study from 3 bore-holes, located nearby our studied site.

1.2 Content / Organization

This document consists of six chapters and four appendices (A, B, C and D) describing the work conducted to meet the objectives. The systematic content of each chapter is as follows:

- Chapter 1 presents the introduction, goals, objectives and justification of this research, and this document organization.
- Chapter 2 presents a literature review where the concepts of wave propagation theory are explained. Also, the SASW, HVSR and SPT method are addressed.
- Chapter 3 presents the site geological conditions and field methodologies used during this research.
- Chapter 4 present the data analysis and results HVSR (fundamental frequency) and SASW (soil site characterization) methods.
- Chapter 5 present the discussion of results and conclusions for this research.
- Chapter 6 presents recommendations for future works.
- The list of references used for this research is provided.

Chapter 2. Literature Review

This chapter provide details and information related to; (i) wave propagation theory and concepts, (ii) geophysical / seismic methods: (ii.1) Nakamura method of horizontal to vertical spectral ratio (HVSR), (ii.2) Spectral Analysis of Surface Waves (SASW) and (iii) the traditional geotechnical Standard Penetration Test (SPT). The above-mentioned methods are some of the methods used for site characterization in terms of the soil-layers geometry (thickness), physical and dynamic properties.

2.1 Geophysical / Seismic methods

Non-invasive, non-intrusive geophysical methods are cost-effective and rapid methods performed from the ground surface, to estimate geotechnical sub-soil properties for engineering investigations, which may include: i) subsurface characterization, ii) engineering properties of earth materials, iii) highway subsidence, and iv) locating buried human-made objects, among others.

They may also provide information about the nature and variability of the subsurface characteristics. Other advantages are site accessibility, portability, noninvasiveness, and operator safety. The equipment can often be deployed beneath bridges, in urban areas, on pavement or rock, and in other areas that might not be easily accessible (Anderson et al., 2008).

Despite the benefits of the geophysical methods, they may have some complexity in the data analysis. Also, most of the instruments are not capable of imaging small targets at shallow depths, but only large targets at greater depths (Anderson et al., 2008). It may occur that the target

can’t be identified because its properties (like density) are not significantly different from those around it.

2.2 Properties of seismic waves

When an earthquake occurs, elastic waves are propagated in all directions. These waves are detected by seismographs and used to study the wave propagation phenomena. Seismic waves are divided in two groups, body-waves and surface-waves are generated. The controlling parameters for their propagation velocity are elastic properties (elastic modulus) and density of the media in which they propagate through. Overall, waves propagate faster at a rate that increases with depth if the velocity of the media increases with depth.

2.2.1 Body-waves

Body-waves are of two types: compressional or primary (P) waves and shear or secondary (S) waves. P- and S-waves are called "body-waves" because they can travel through the interior of a body such as the Earth's inner layers. Compared to the Surface waves, Body-waves are the fastest and the first to be recorded by seismographs.

The P-waves, have a compression (push-pull particle motion) in direction at which the wave propagates (Nazarian and Stoke II, 1986) as presented in Figure 1a. P-waves are the fastest waves and are the first ones to be observed in a seismogram. Typically, its amplitude is lower than the S- and Surface waves, and have a higher frequency than the S-waves. The equation to estimate its velocity is,

$$V_p = \sqrt{\frac{\lambda+2\mu}{\rho}} \tag{2.1}$$

where:

V_p = velocity of P-waves, λ = lame's parameter (elastic modulus), μ = shear modulus, and ρ = density.

The shear waves (S-waves) generate a perpendicular particle motion concerning its direction of propagation, as shown in Figure 1b (Nazarian and Stoke II, 1986). The particle motion can be decomposed in two components, vertical and horizontal (*SV* and *SH*). S-waves do not propagate in fluids; consequently, they do not spread through the outer core of the Earth. As previously mentioned, the velocity of P-waves is higher than the S-wave, ($V_S < V_P$). Therefore, the shear wave arrives at the seismograph after the P-waves. With equation 2.2 the shear wave velocity can be estimated.

$$V_s = \sqrt{\frac{\mu}{\rho}} \tag{2.2}$$

where:

V_s = velocity of S-waves, μ = shear modulus, and ρ = density.

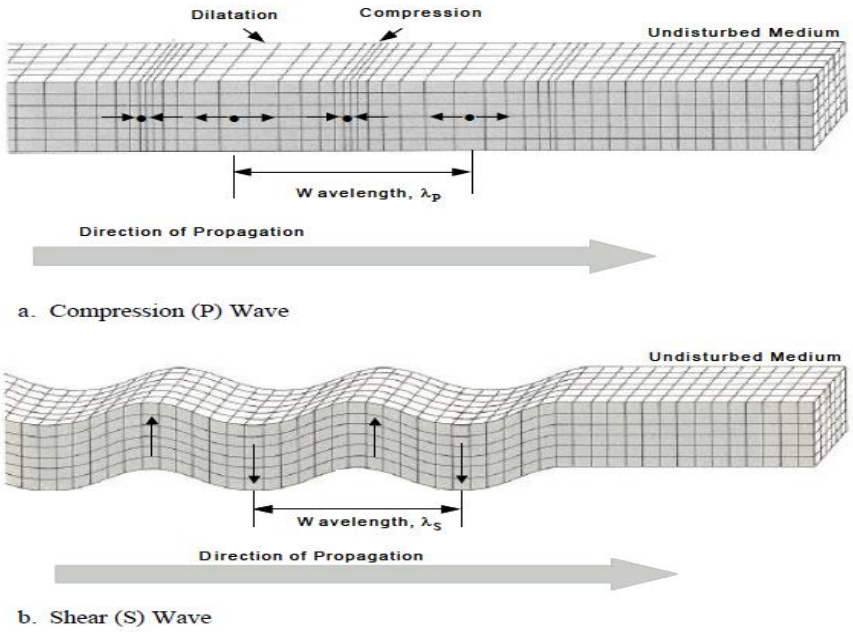

Figure 1. Body-wave - characteristic motion. a) P-waves, and b) S-waves (Foti, 2000)

The waves propagation velocities can be expressed as function of the elastic properties. An example of this is the Poisson's ratio (υ), since it can be expressed in terms of the elastics properties that can be measured in the field, like S- and P- wave velocities. Equations 2.1 and 2.2 can be used to relate V_P, V_S and Poisson's ratio by rewriting it as (Nazarian and Stoke II, 1986):

$$\frac{V_P}{V_S} = \sqrt{\frac{(1-\upsilon)}{(0.5-\upsilon)}} \tag{2.3}$$

where:

V_s = velocity of S-waves, V_p = velocity of P-waves, and υ = the Poisson's ratio.

2.2.2 Surface-waves

There are two types of surface waves: Love-waves (L_Q) and Rayleigh-waves (L_R). For a vertical energy source, Surface waves have the most amount of energy (Nazarian and Stoke II, 1986; Woods, 1968) and slowest propagation velocity. This type of waves propagates on the Earth surface (land and water). Surface waves propagate along a cylindrical wave front as they spread out from the source (Anderson et al., 2008). If the wavelength increases, the particle displacement is going to be deeper. Both, Love- and Rayleigh-waves are dispersive waves, whose amplitude decreases with depth.

Love- waves are generated at the interface of two media. The particle motion perpendicular to the direction of propagation of the wave, parallel to the earth's surface (Figure 2, Vázquez, 2014). Love-wave have low frequency and long wavelength. Is important to add that Love wave's velocity is inversely proportional to frequency (Foti, 2000).

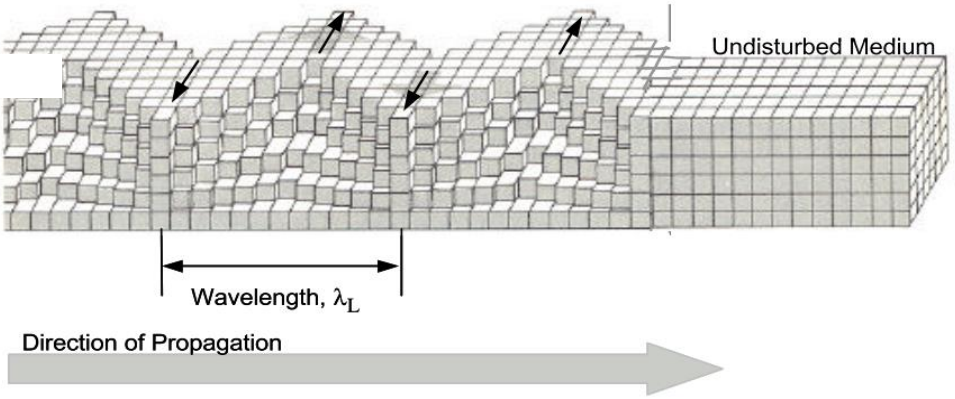

Figure 2. Characteristic ground motion of Love-wave
(Stokoe and Santamarina, 2000)

On the other hand, Rayleigh-waves travel near the surface of solids and have a longitudinal and transverse particle motion that will convert to a prograde ellipse at greater depths. Figure 3 shows the combined motions that forms a retrograde ellipse close to the surface (Nazarian and Stokoe II, 1986).

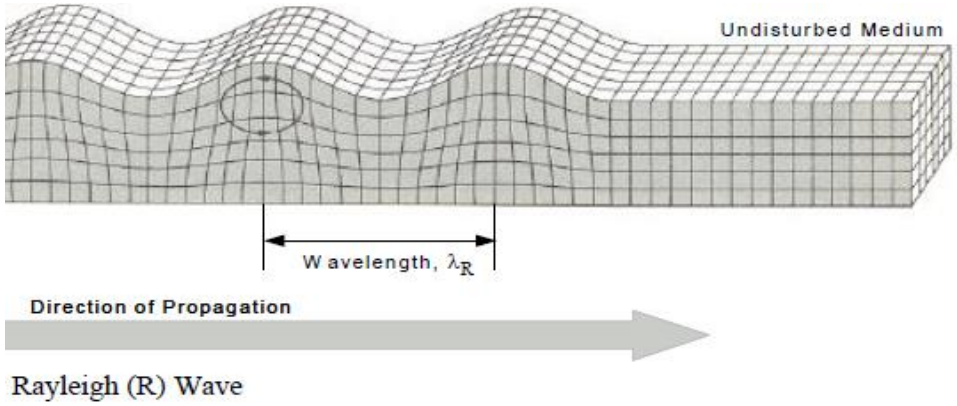

Figure 3. Characteristic ground motion of Rayleigh-waves
(Stokoe and Santamarina, 2000)

Equation 2.4 is used to estimate Rayleigh's wave velocity.

$$V_R = f * L_R \tag{2.4}$$

where:

V_R = velocity of R-waves, f = frequency, and L_R = wavelength.

Since V_R is a product of the interaction between P- and S-waves; it is assumed that the relation between V_R and V_S are related through a V_S/V_R ratio of approximately 1.1 for a Poisson ratio of 0.25. As previously explained, the different wave velocities can be expressed as a function of Poisson's ratio. Figure 4 show the behavior of the normalized wave velocities, with respect to V_S, increase with Poisson's ratio, for V_P and V_R, while V_S remain constant at every value of υ. If

the material is incompressible, then υ=0.5 and V_R/V_S is equal to 0.955 (Stokoe and Santamarina, 2000).

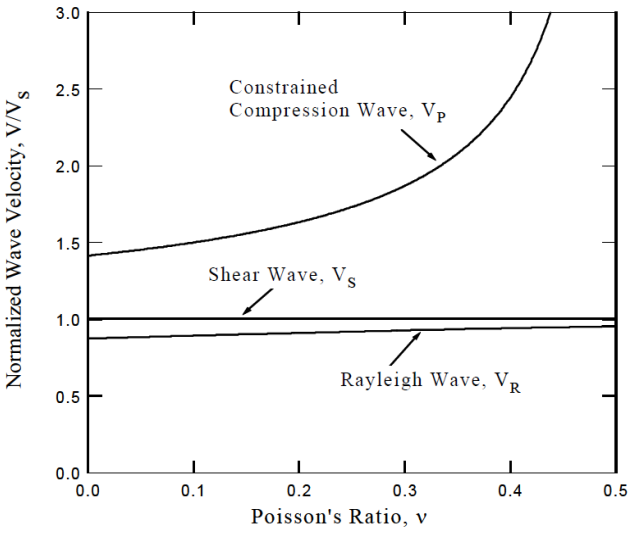

Figure 4. Relationship between V_P, V_S and V_R wave velocity and Poisson's ratio (Stokoe and Santamarina, 2000)

Figure 5 shows the normalized vertical and horizontal displacement with normalized depth. This data shows that the surface wave propagation has an exponential decay of displacement with depth. Also, as the wave length increases the particle displacement is extended to greater depths (Stokoe and Santamarina, 2000). Because of the polarity of the horizontal component, the particle displacement becomes vertical (Villagómez, 2016).

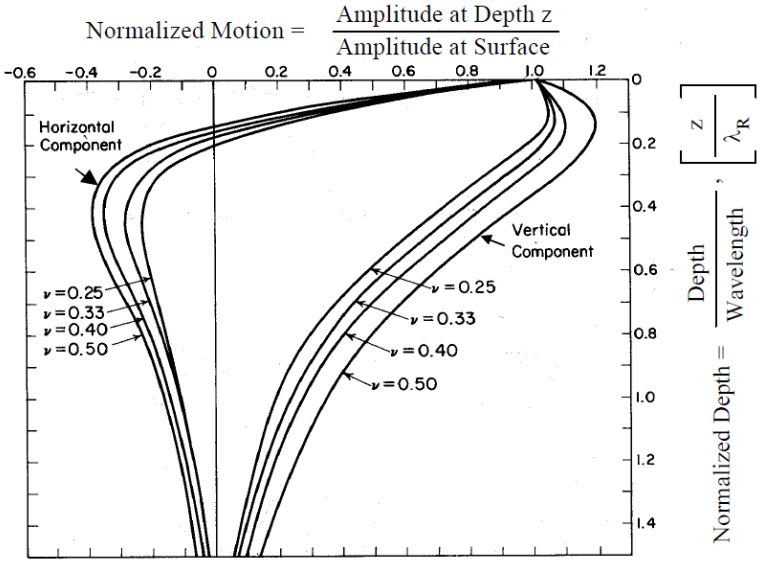

Figure 5. Variation of vertical and radial displacement with normalized depth (Stokoe and Santamarina, 2000)

Surface waves are easy to measure because they have more energy in the surface due to the way they propagate as shown in Figure 6. The amplitudes of the vertical and horizontal movement decay with depth. Surface wave predominates with 67% of its energy that is generated by a vertical acting load at the surface (Stokoe and Santamarina, 2000). Table 1 shows the energy distribution in percentage in a vertical acting load.

Table 1. Distribution of wave energy by a vertical source (Stokoe and Santamarina, 2000)

Wave Type	**Total Energy (%)**
Surface (Rayleigh)	67
Shear	26
Compression	7

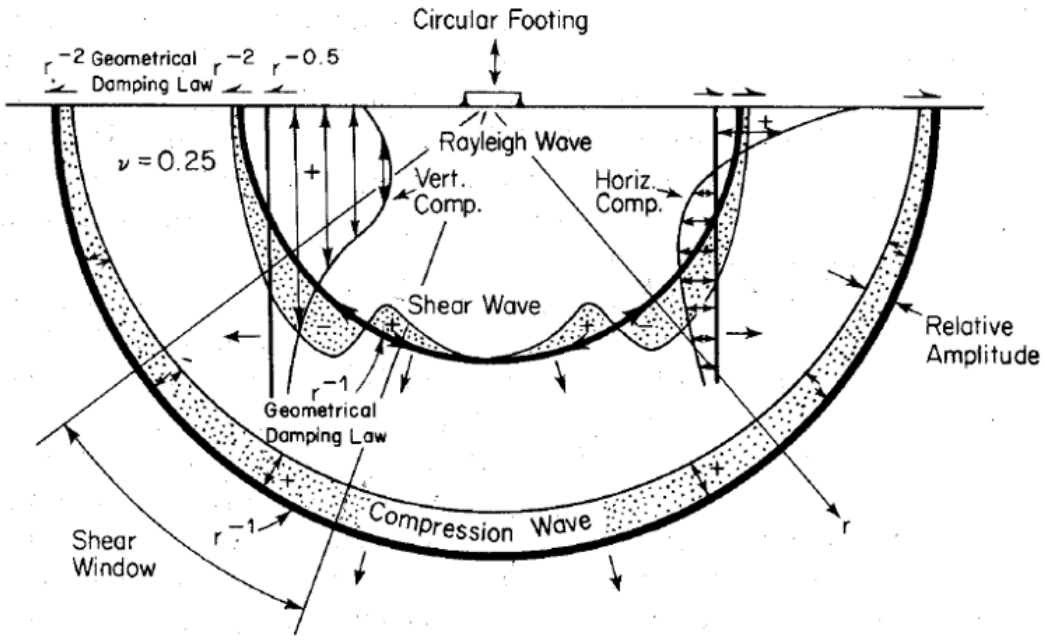

Figure 6. Energy distribution of Rayleigh, Shear and Compression waves (Nazarian and Stoke II, 1986)

2.3 Soil site characterization methods

To build safely, it is essential to estimate the soils properties and to properly characterize the site. The site characterization can be done using Geotechnical and Geophysical methods. Some of the most commonly used geotechnical methods in Puerto Rico and the United States are the Standard Penetration Test (SPT), and the Static Cone Penetration Test (SCPT). On the other hand, non-invasive geophysical methods used for soil properties estimation are: i) the direct interpretation of the Fourier spectrum, ii) the calculation of the relative spectral ratio of a site (Seekins et al., 1996), iii) H/V Spectral Ratio method (HVSR) - Nakamura method, and iv) the SASW method. Some of these methods will be explained in more details in this chapter.

2.3.1 Spectral analysis of surface waves method (SASW)

The Spectral Analysis of Surface Wave method was created in the 1980's and its predecessor is the Steady-State Rayleigh Wave method (Rix et al., 1991). It is a geophysical method for soil characterization that analyze the dispersive characteristic of Rayleigh-waves in a homogeneous and nonhomogeneous medium. It is a non-destructive method, where all the instruments are placed at the soil surface. The method is based on the analysis of the signals in the frequency domain and the main objective is to determine the Rayleigh-wave propagation to finally estimate a shear wave velocity profile vs. depth without the need of a borehole.

This method was developed to determine the shear velocity and shear modulus profiles at soil sites (Nazarian & Stoke II, 1986). There are two assumptions in this method: 1) the only parameter measured is a plane surface wave, and 2) only first mode of surface waves energy is measured in the field (Rix et al., 1991).

The SASW method is performed using two receivers aligned with an active source. The distance between the source and the first receiver, normally, is equal to the distance between both receivers. When performing the test for a single position of the receivers and the source, the dispersion curve can be calculated for a range of frequencies, therefore, the position of the receivers and / or the source should be modified throughout the test. This way, the dispersion curve for different frequency ranges can be obtained. Figure 7 shows the typical configurations used for the SASW method, and the variation of the positions of the receivers and / or source throughout the test. The SASW method is divided in three parts, 1) data acquisition, 2) dispersion curves calculations, and 3) V_s versus depth by doing and inversion or modeling of the dispersion curve (Rix et al. 1991).

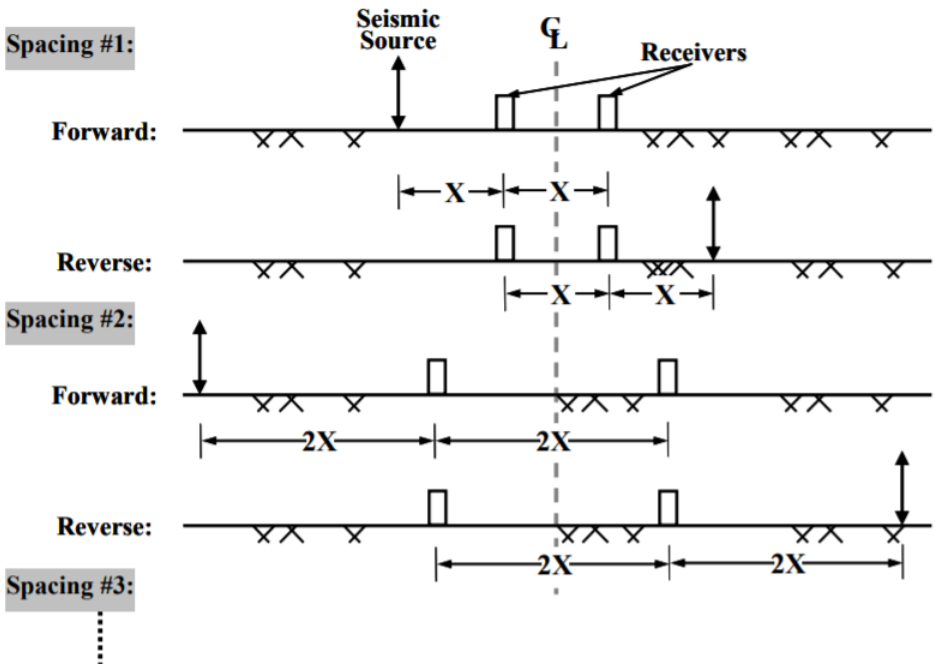

Figure 7. Typical configuration of the equipment / recivers for the SASW method (Lin, 2007)

The dispersion curve shows how the velocity of propagation varies with the frequency or the wavelength. Figure 8 shows the simplified behaviors of the different dispersion curves. In Figure 8(a) the surface wave phase velocity is constant, because the material is uniform. Figure 8(b) shows the surface wave velocity increasing with depth and wavelength. This type of behavior represents a layered soil system resting in a half space where the material of each layer is different, and the velocity of the layers increase with depth. A soil layered system and rock site are examples of this type of behavior. Finally, in Figure 8(c) the velocity is decreasing with larger wavelength. This is because each layer is composed of a different material where the wavelength encounters a smaller velocity as the wavelength increases (Rix et al., 1991).

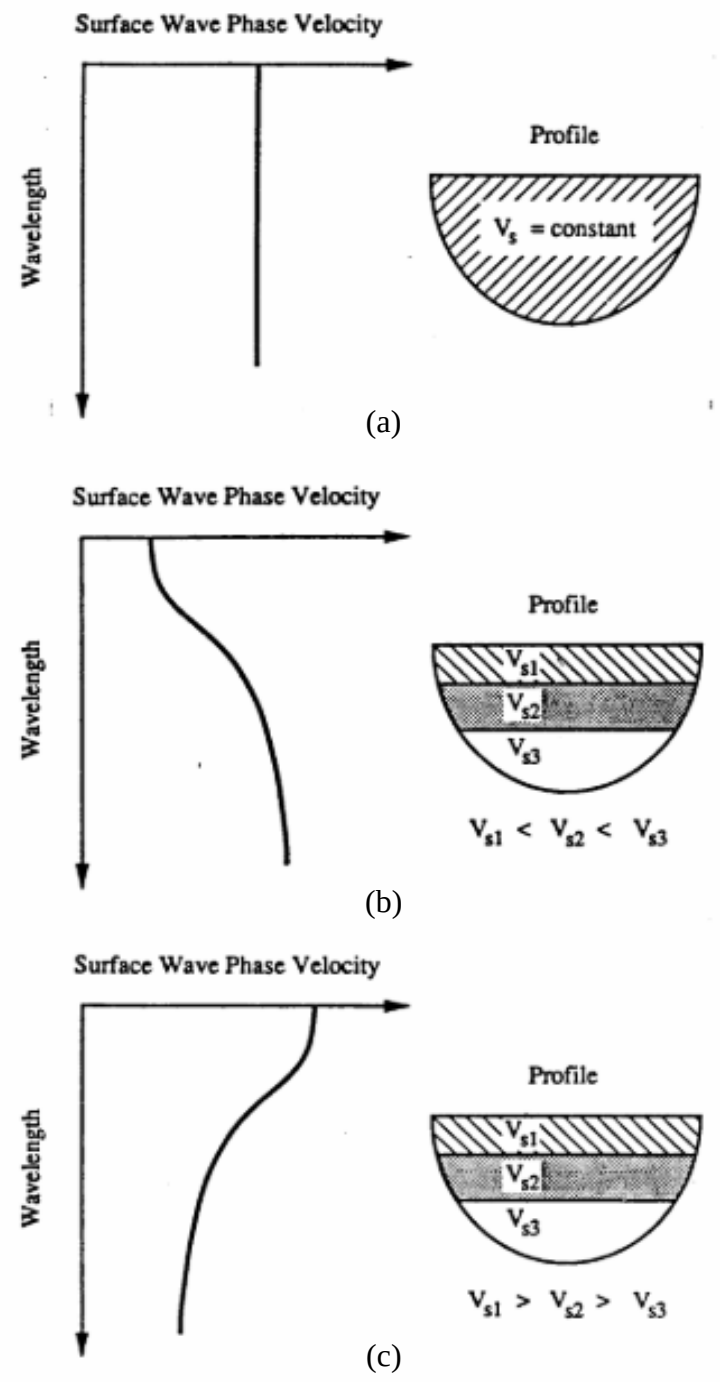

Figure 8. Dispersion curves (a) for an uniform half space, (b) layered half space where the velocity increases with depth, and (c) layered half space where the velocity decreases with depth (Rix et al., 1991)

2.3.2 Ambient vibration horizontal to vertical spectral ratio method

The HVSR method estimate the effect of the surface geology on seismic motion using microtremors. The fundamental hypothesis for this methodology, as developed by Nakamura (1989), is that the layered soil system transfer function can be estimated using ambient vibrations measurements of a single site on the surface through the spectral ratio between horizontal and vertical components (H/V).

Microtremors are vibrations generated by nature (ocean waves, wind, and others.) and artificial/anthropogenic (cars, factories, construction, etc.) sources. They are compose of body-waves (P- and S-waves) and surfaces waves (Rayleigh-waves), and propagate in a soft layer of sediments that rests on a layer of rock, Vázquez (2014).

The hypothesis of the Nakamura method is based on the consideration that the ratio of the horizontal and the vertical spectral ratio of the ambient vibrations recorded at the surface will provide the dominant preferential vibration of the soil system, these, eliminating the need of having records at the base of the sedimentary layer, (Huerta, 2016). The Amplitude Fourier Spectrum of the horizontal component of ground motion at the surface contains local and sources effects that can be expressed as follows:

$$H_S(f)=F_H(f)*F_R(f)*S(f) \tag{2.5}$$

where,

$H_S(f)$ = Amplitude of Fourier spectrum in the horizontal component at the surface, $F_H(f)$ = Amplitude of Fourier spectrum of polarized horizontal body-waves, $F_R(f)$ = Amplitude of Fourier spectrum of the Rayleigh-waves, and $S(f)$ = Amplitude of Fourier spectrum of site effects.

Since the Fourier spectrum in a horizontal component does not have the effect of Rayleigh-waves, equation 2.5 can be rearranged into Equation 2.6. Similarly, the vertical component is not disturbed by the local effects (Equation 2.7).

$$H_B(f)=F_H(f) \tag{2.6}$$

where,

$H_B(f)$ = Amplitude of the Fourier spectrum in the horizontal component.

$$V_S(f)=F_V(f)*F_R(f) \tag{2.7}$$

where,

$V_S(f)$ = Amplitude of Fourier spectrum in the vertical component in the surface, $F_R(f)$ = Amplitude of Fourier spectrum of the Rayleigh-waves, and $F_V(f)$ = Amplitude of Fourier spectrum of the vertical body-waves.

$$V_B(f)=F_V(f) \tag{2.8}$$

where,

$V_B(f)$ = Amplitude of Fourier spectrum in the vertical component at the base.

If the distant sources are eliminated from de microtremors, the site characterization ($C^*(f)$) is given by the spectral quotient between the horizontal and vertical movement.

$$C^*(f) = \frac{H_S(f)}{H_B(f)} \tag{2.9}$$

where,

$C^*(f)$ = site effect of the sedimentary layer, without considering the effects of the body-waves.

If equation 2.5 and 2.6 are substituted in Equation 2.9, the site characterization can be expressed with equation 2.10 as follows:

$$C^*(f) = \frac{F_H(f)*F_R(f)*S(f)}{F_H(f)} = F_R(f) * S(f) \quad (2.10)$$

Using the ratio of the vertical components of the microtremors measurements, the effect of Rayleigh-waves is corrected to isolate the site effect as shown in Equation 2.11:

$$F_R(f) = \frac{V_S(f)}{V_B(f)} \quad (2.11)$$

Substituting equations 2.7 and 2.8 into equation 2.11 leads to the relationship presented by Equation 2.12.

$$F_R(f) = \frac{F_V(f)*F_R(f)}{F_V(f)} \quad (2.12)$$

To estimate the transfer function, the effect of Rayleigh-waves must be eliminated by substituting Equation 2.10 into Equation 2.12, leading to expression presented by Equation 2.13.

$$C(f) = \frac{C^*(f)}{F_R(f)} = \frac{F_R(f)*S(f)}{F_R(f)} = S(f) \quad (2.13)$$

Expressing the equation 2.13 in terms of the spectral components, results into Equation 2.14.

$$C(f) = \frac{\frac{H_S(f)}{H_B(f)}}{\frac{V_S(f)}{V_B(f)}} = \frac{H_S(f)*V_B(f)}{H_B(f)*V_S(f)} \quad (2.14)$$

Nakamura (1989) establish that the ratio of $H_B(f) / V_B(f)$ approximately equals to one, to obtain the site effect(Vázquez 2014). Therefore, Equation 2.14 can be simplified into Equation 2.15, and the site effect obtained as:

$$C(f) = \frac{H_S(f)}{V_S(f)} \quad (2.15)$$

where,

$C(f)$ = site effect, $H_S(f)$ = Amplitude of Fourier spectrum in the horizontal component at the surface, $V_S(f)$ = Amplitude of Fourier spectrum in the vertical component at the surface.

Summarizing, the HVSR method can be applied to obtain site characterization in terms of the fundamental resonant frequency of a sedimentary layer. With this method the effect of seismic motion can be attain without geological information.

2.3.3 Standard penetration test (SPT)

The Standard Penetration Test (SPT) dated back to 1902 when Charles R. Gow started making borings to obtain soil samples with a 1 inch (in). diameter that were driven by hammer blows. The hammer weight was 110 pounds (lb). Later, Harry Mohr determined that the average driving weight should be 140lb with an average drop of 30 in (Rogers, 2006).

This method was standardized in 1940, by Jul Hyorsley at the University of Harvard where he published ‘‘*The Present Status of the Art of Obtaining Undisturbed Samples of Soils’’*. The numbers of blows that take to drive the sampler is defined as the N-value, is the representation of the soil resistance, (ASTM-D1586, 2011). Terzaghi and Harry Mohr developed correlations between the number of blows (N) and the properties of soils, such as density of sand, compressive strength of clays, and the allowable bearing pressure on sands and clays (Rogers, 2006).

Chapter 3. Site Geological Conditions and Methodology

This chapter provides a summary of the site surface geology conditions of the study area, located at the University of Puerto Rico at Mayagüez (UPRM). In addition, the site field work for data acquisition is presented, for the methods used in this project: i) Spectral Analysis of Surface Waves (SASW), and ii) Horizontal and Vertical Spectral Ratio (HVSR).

3.1 Study area

3.1.1 Location

The UPRM is located on the west coast of Puerto Rico. The University is located at the municipality of Mayagüez (Figure 9) in the Miradero neighborhood. The site used for this investigation is located at the middle of the walking track next to the Rafael A. Mangual Coliseum at UPRM. The black star in Figure 10 shows the location of the portion of the Campus considered for the study.

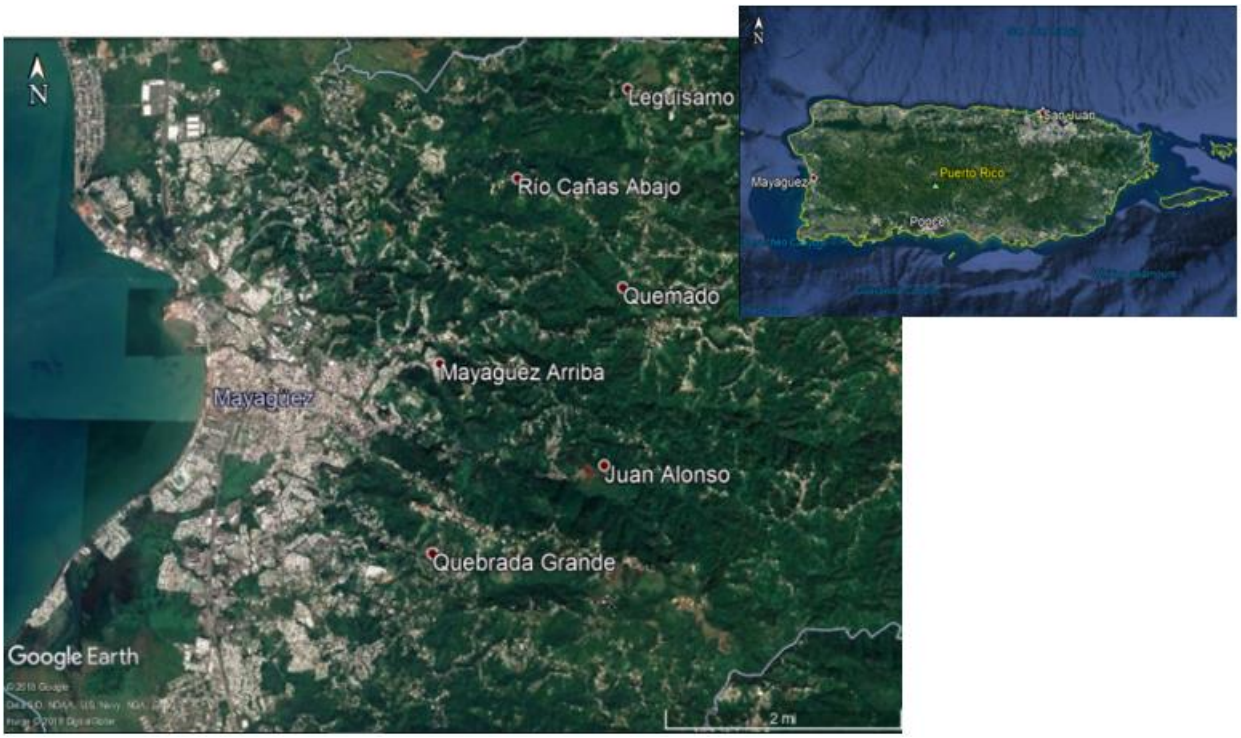

Figure 9. Municipality of Mayagüez

3.1.2 Geology

The UPR, Mayagüez Campus, has a geological composition dominated by alluvial deposits (Qal) and Yauco formation (Ky) which is formed of siltstone, claystone; sandstone, limestone, and conglomerate ("Yauco Formation, Puerto Rico geologic unit TKy"). The area of study contains alluvial deposits (Qal), that are composed of sand, silt and gravel, and include rockfalls and landslide deposits. Figure10 presents the geological map corresponding to the UPR, Mayagüez Campus.

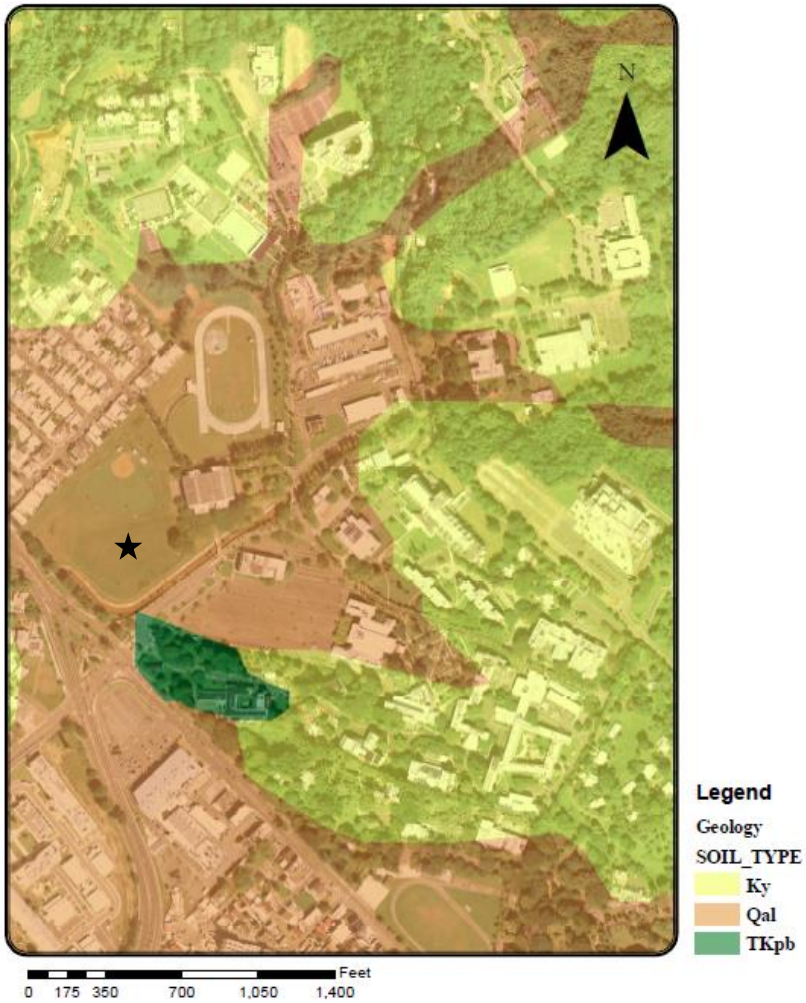

Figure 10. Geological map of the University of Puerto Rico, Mayagüez Campus and study area shown with the star (Curet, 1986; Vázquez, 2014)

3.2 Equipment

For this investigation four accelerographs, equipped with three recording channels, an internal triaxial accelerometer, a memory card and ports to connect the GPS and the computer cable where used. The sensor had a full-scale of ±0.25g. On Table 2 the instruments characteristics and recording parameters are provided. The recording parameters were configured using the communication protocol "*Quick Talk*", a computer program, that establish the communication

between the instruments and the computer. Finally, for the instrument geographic location, a handheld GPS with the North American Datum 1983 (NAD83) was used.

Table 2. Main characteristics of the instruments used during this investigation

		Instrument #1	**Instrument #2**	**Instrument #3**	**Instrument #4**
Serial number		6903	6542	6543	6904
Sensor	**Channels**	3	3	3	3
	Full scale range	± 0.25g	± 0.25g	± 0.25g	± 0.25g
	Bandwidth	DC to 200 Hz	DC to 200 Hz	DC to 200 Hz	DC to 200 Hz
	Dynamic range	155 dB+	155 dB+	155 dB+	155 dB+
Recorder	**Sampling rate**	250 sps	250 sps	250 sps	250 sps
	Input range	± 2.5V	± 2.5V	± 2.5V	± 2.5V
Coordinates	**Latitude N (°)**	18.21229	18.21231	18.21232	18.21236
	Longitude W (°)	67.14486	67.14483	67.14481	67.14478
GPS		Ok	Ok	Ok	Ok

3.3 Array deployment

Four accelerographs were installed on the field to record the vibrations at the study site at the University of Puerto Rico at Mayaguez.

To install the equipment the grass carpet was removed, and the equipment was placed directly on the ground, as can be observed in Figure 11. The instruments were leveled and oriented to the magnetic north with a compass, using as reference the instruments *Y* axis pointing to the north. Table 3, show the distance used between all the instruments and the sources while Figure 12 shows the arrangement used during this investigation. As shown in Table 3, the distances used between the sources and the closest instruments was approximately twice the minimum distance recommended. Carlos Huerta said, that due to his previous researches, this is the best arrangement he has found for this method. Huerta said that having greater distance the wavelength will be

greater and larger depths will be reached (Huerta, 2018). Once the instruments were place, the handheld GPS was used to take their respective coordinates. When all the instruments were in position, leveled, oriented and the GPS connected, they were all turned on and connected to the computer to synchronize the instrument clock. Using the "*Quick Talk"* program, the recording parameters where specified to be able to obtain properly standardized time series. The sampling intervals were 250 samples per second, and no filtering was applied. Finally, the recording was started, and the instruments were left recording until the test was fished.

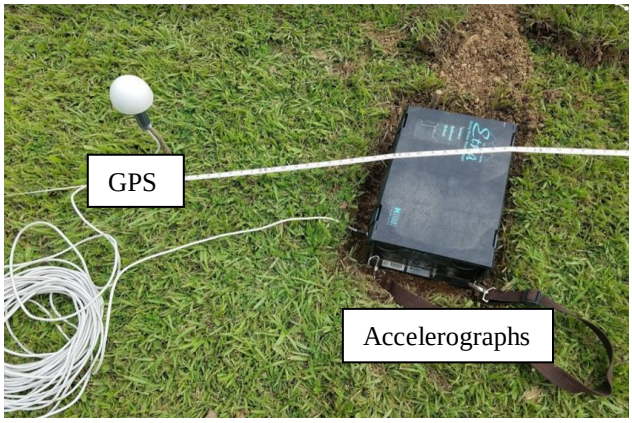

Figure 11. Instruments used, accelerographs (ETNA) and GPS

Table 3. Distances between instruments (stations)

Instuments		**Distance (ft)**
Sta. #	**Sta. #**	
1	2	13.08
1	3	25.33
1	4	38.67
2	3	12.25
2	4	25.58
3	4	13.33
Source A	4	80.00
Source B	1	80.00

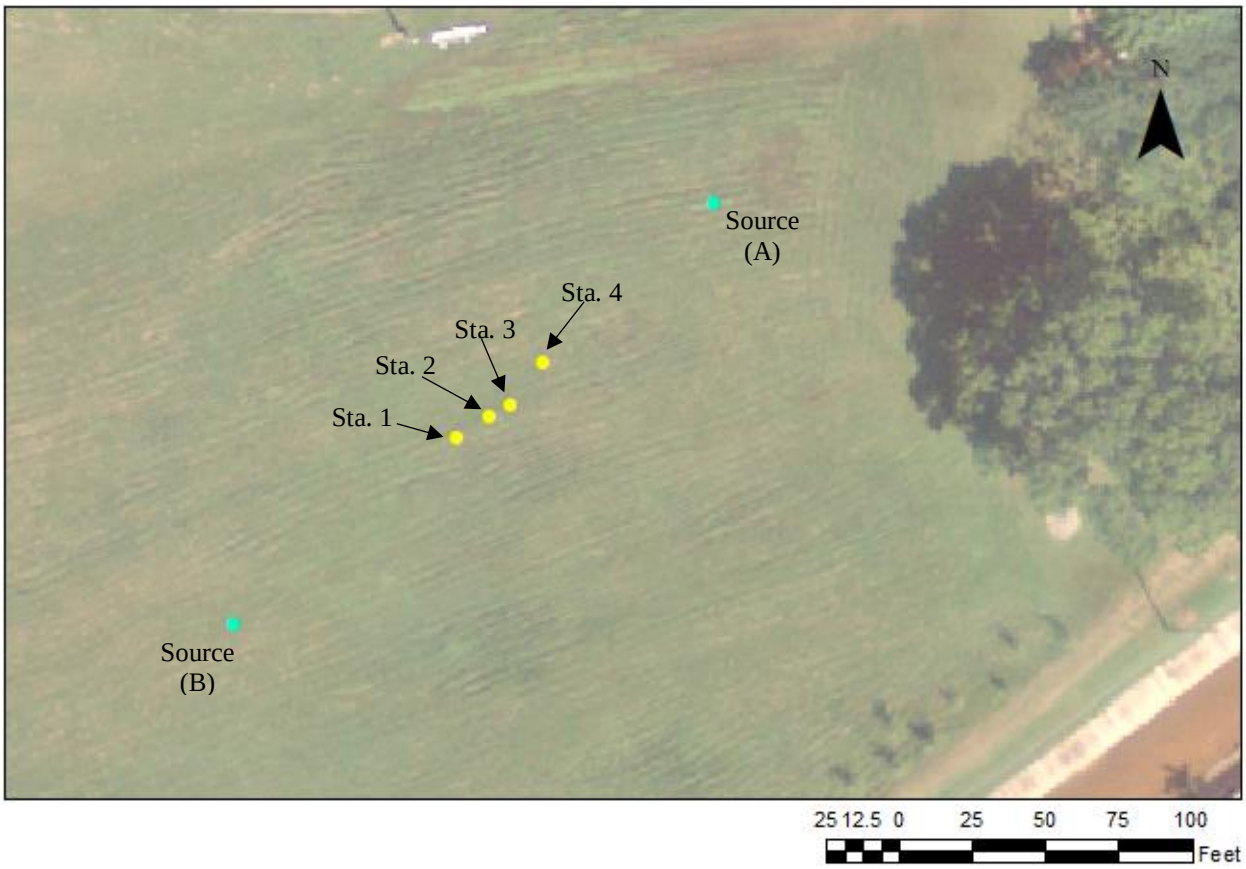

Figure 12. Arrangement of instrument and sources
Instruments Sources

3.4 SASW data acquisition

The first measurements were taken from source A, and the second were taken in the opposite side, source B. The source consisted of a 33 lb weight that was dropped to free fall from a height of approximately 6.6 ft. The metal cylinder hung from a homemade wooden tripod and fall into a metal plate (Figure 13), that was placed on the surface to receive the impacts.

Figure 13. Tripod and weight used as a source

The sources impacted the plate about 6 times each to generate 6 pulses in the seismogram. This was repeated two times, one in each direction, to have a total of 12 pulses per source. To separate the impacts, 1 minute was left between each one. The data acquisition was simultaneously recorded for all the instruments.

3.5 SASW data processing

The SASW data processing followed three main steps, (i) data preparation, (ii) data process selection, and (iii) data processing as described in this section.

The data preparation consisted in obtaining the time series with synchronized common starting and ending time from the collected data (see Figure 14). The data-pulse selection consisted in the identification and portion selection of the induced pulses for the different combinations of the instruments (see Figure 15 and 16). A displacement was made on the vertical axis to have a better visualization of the signals.

Following the description provided in section 2.3.1, the data processing to obtain the dispersion curve for the different distance combinations is next described:

i) first, the data was prepared using the parameters in Table 4. The basic equations for obtaining the auto power spectra, the cross-power spectra, the coherence function and the phase function, are presented in Equations 3.1 through 3.4 (Rix et al., 1991).

$$G_{y1y1} = Y_1^*(f) * Y_1(f) \tag{3.1}$$

$$G_{y2y2} = Y_2^*(f) * Y_2(f) \tag{3.2}$$

$$G_{y1y2} = Y_1^*(f) * Y_2(f) \tag{3.3}$$

$$(Y_{y1y2})^2 = |G_{y1y2}|^2 / (G_{y1y1} * G_{y2y2}) \tag{3.4}$$

where:

G_{y1y1} = auto power spectrum of receiver #1, G_{y2y2} = auto power spectrum of receiver #2, G_{y1y2} = cross power spectrum between receivers 1 and 2, $(Y_{y1y2})^2$ = coherence function between signal 1 and 2, and | | = denotes the magnitude of a complex number.

ii) To calculate the phase velocity, the phase of the cross-power spectrum is needed. The Equation used to obtain the phase cross-power spectrum is:

$$\theta_{y1y2} = tan^{-1}\left(\frac{Im(G_{y1y2})}{Re(G_{y1y2})}\right) \quad (3.5)$$

where:

θ_{y1y2} = phase of the cross-power spectrum in degrees, *Im* = imaginary part of a complex number, and *Re* = real part of a complex number.

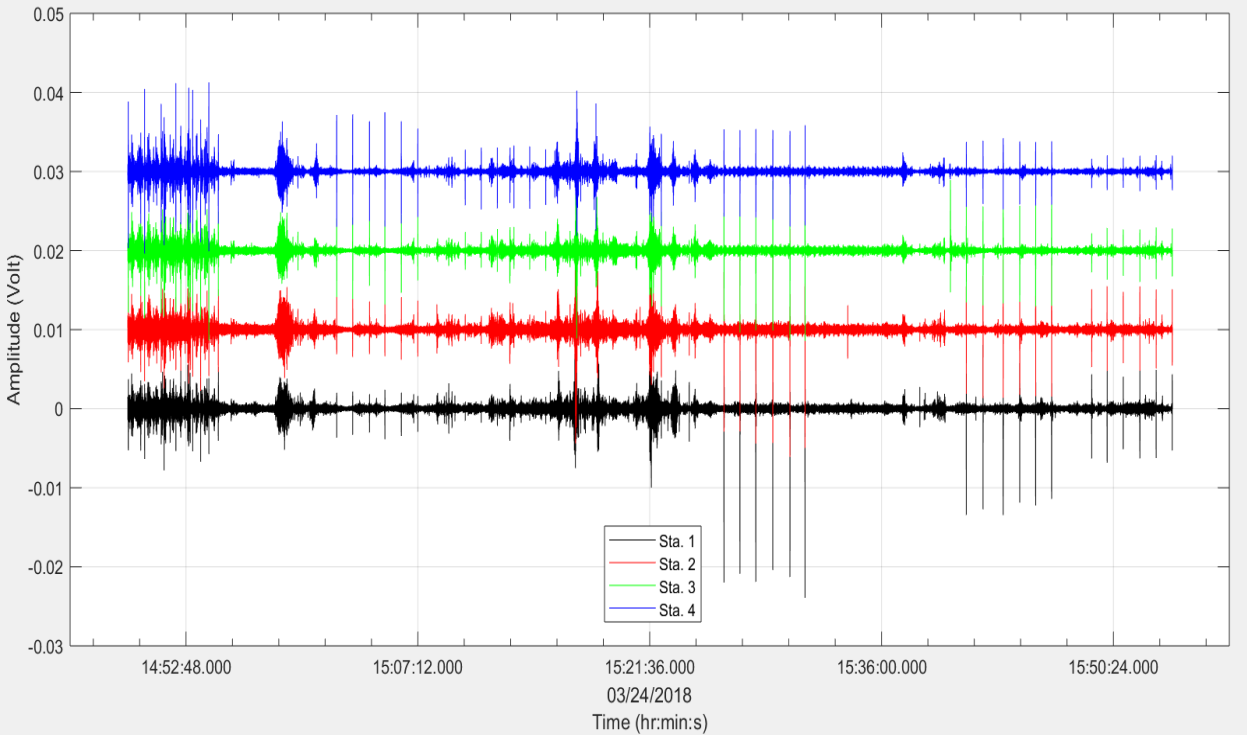

Figure 14. Recorded signals.
The signals were displaced in the vertical axis to observe and study them better

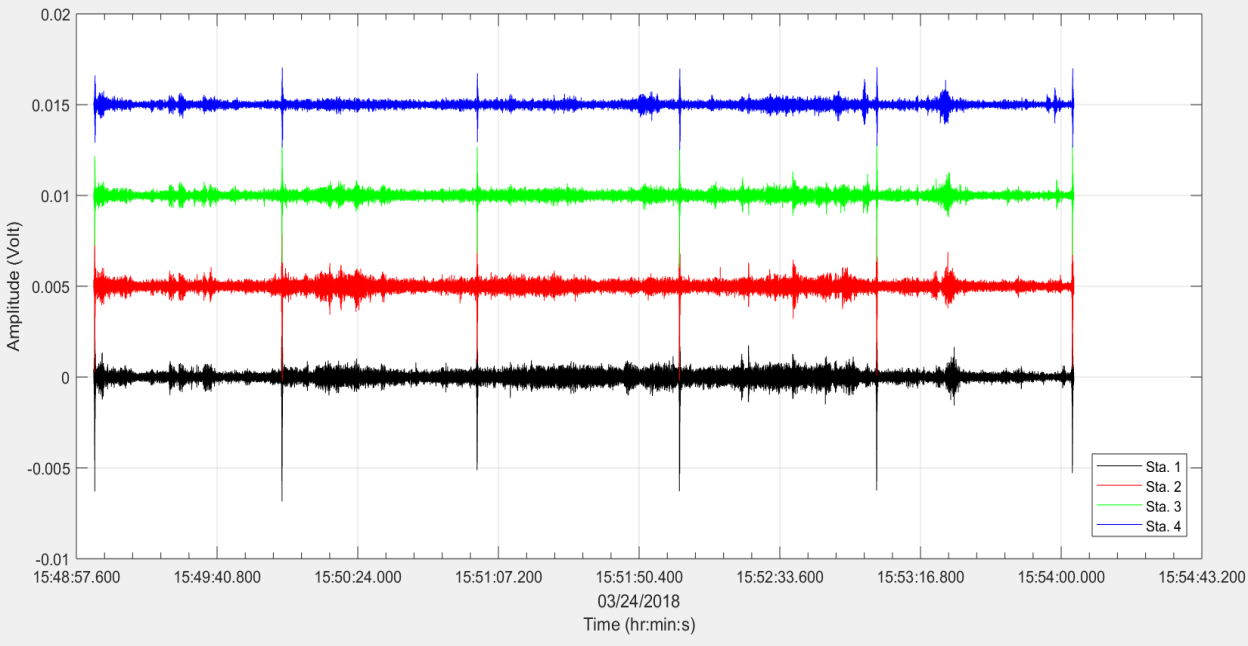

Figure 15. Example of group pulse cut (source: weight in the reverse direction, channel 3). The signals were displaced in the vertical axis to observe and study them better

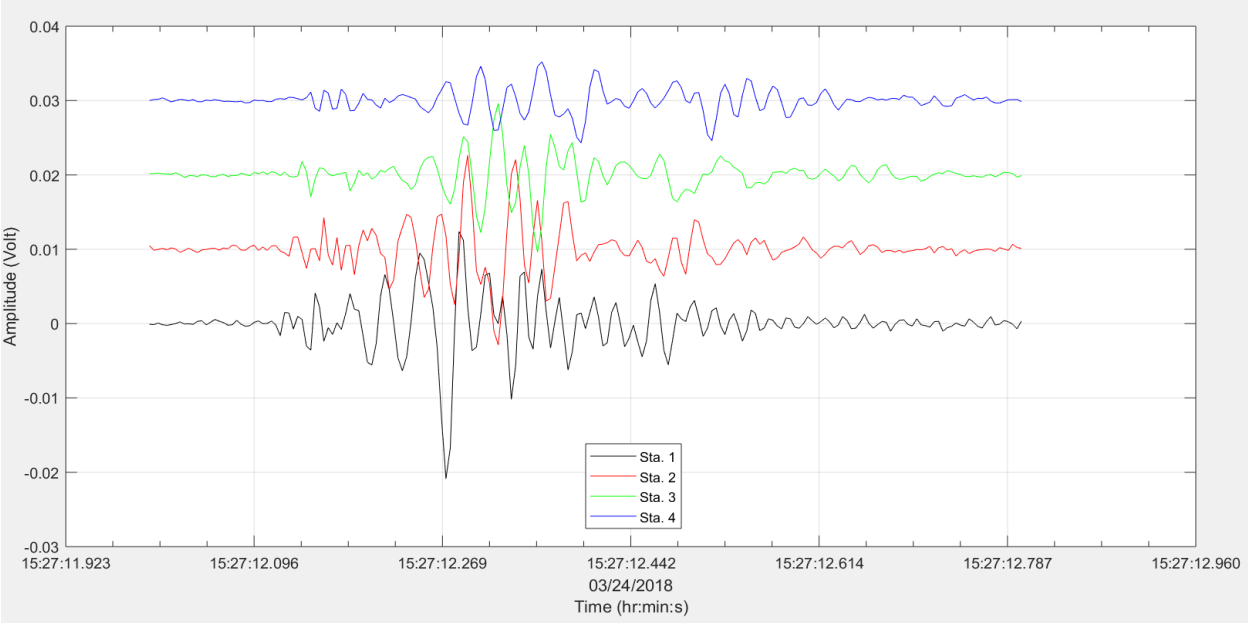

Figure 16. Example of a single pulse signal, channel 3 (vertical). The signals were displaced in the vertical axis to observe and study them better

Table 4. Parameters used for the SASW processig method

File name	Pulse	# Samples	Overlap (fraction)	Segment length	Coherence
allsta_1ww1	**1-A**	201	0.50	128	0.75
allsta_1ww2	**2-A**	201	0.50	128	0.70
allsta_1ww3	**3-A**	201	0.45	128	0.75
allsta_1ww4	**4-A**	201	0.70	128	0.75
allsta_1ww5	**5-A**	201	0.45	128	0.80
allsta_1ww6	**6-A**	201	0.50	128	0.75
allsta_2ww1	**1-B**	201	0.50	128	0.80
allsta_2ww2	**2-B**	201	0.50	128	0.70
allsta_2ww3	**3-B**	201	0.45	128	0.75
allsta_2ww4	**4-B**	201	0.70	128	0.75
allsta_2ww5	**5-B**	201	0.45	128	0.80
allsta_2ww6	**6-B**	201	0.50	128	0.75

Where **A** = direct and **B** = reverse direction of pulses.
File name: allsta_*X*ww*Y* = all stations, *X* (1= direct and 2= reverse directions), ww (weight source), and *Y* (# pulse)

iii) Other parameter to obtain the dispersion curve, is the coherence between the signals of the cross-power spectra. To attain a good dispersion curve, a coherence was specified. With the remaining data, the phase spectral function was unwrapped, and each segment was rearranged. Then, the time delay between receivers was calculated as a function of frequency using Equation 3.6 (Rix et al., 1991).

$$t(f) = \frac{\theta_{y1y2}(f)}{360° * f} \tag{3.6}$$

where:

t(f) = time delay between receivers.

Rayleigh-wave velocity as function of frequency is calculated by mean of Equation 3.7:

$$V_R(f) = \frac{D}{t(f)} \tag{3.7}$$

$$V_{12} = \lambda_{12} f \tag{3.8}$$

where:

V_R = surface wave phase velocity, V_{12} = surface wave phase velocity between instruments 1 and 2, f = frequency, λ_{12} = wave length between instruments 1 and 2, and D = distance between receivers.

Finally, the wave length (λ_R) was computed with equation 3.9.

$$\lambda_R = \frac{V_R}{f} \tag{3.9}$$

This calculation was repeated for each recorded data. At the end, all the data was combined to obtain the composite dispersion curve. The dispersion curve diagram was created with a graph that show the frequency (in Hz) versus the Rayleigh-wave phase velocity (in m/sec).

3.6 HVSR (Nakamura) method

3.6.1 Data acquisition

For this method, time series of ambient vibration were collected, using the deployed instrument array shown in Figure 17. For this method, the installment and arrangement of the instruments were the same as the SASW method. The instruments recorded ambient vibration for approximately two hours.

Figure 17. Arrangement of the equipment in the field.

3.6.2 HVSR data processing

Data was first baseline corrected and then trimmed to time synchronization all the recorded time series (Figure 18), a file containing different columns was created, each representing the time and the sensors, with its sample rates. A MatLab code (*code_plot_hv*) was used to plot the recorded data in the time domain *a(t)*. Figure 18 shows the trimmed data for all the stations used. Table 5 shows the parameters used to trim and process the data for the HVSR testing method.

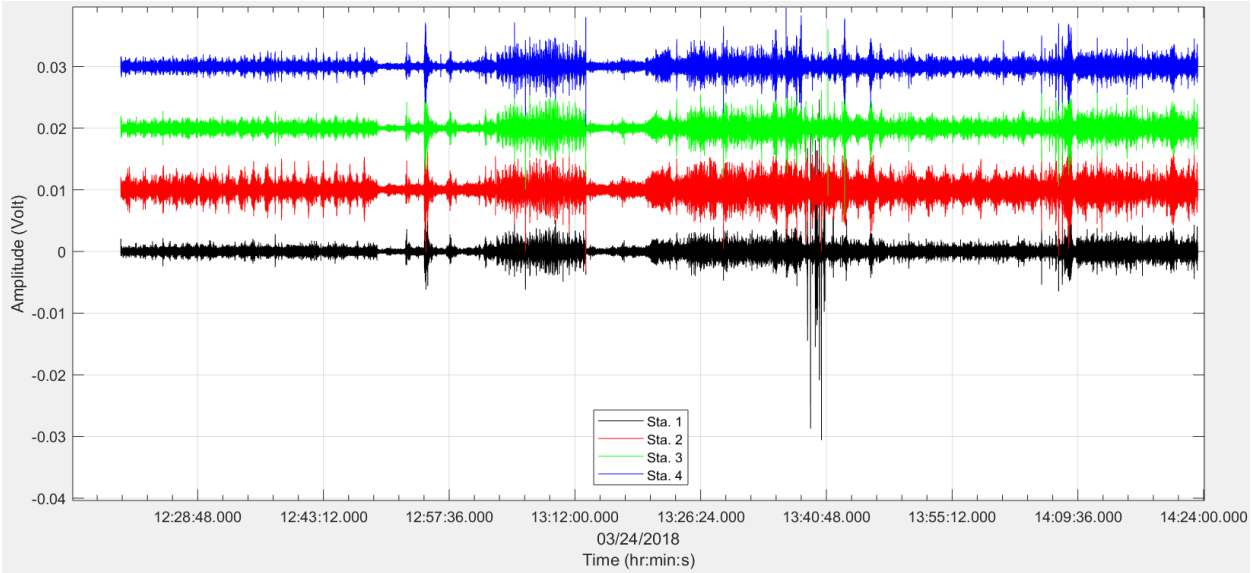

Figure 18. Trimmed data for the East-West horizontal component (channel 2). The signals were displaced in the vertical axis to observe and study them better

Table 5. Parameters used for HVSR method

File name	Overlap (fraction)	Segment length (# Samples)
allsta_trim_001	0.5	16384
allsta_trim_002	0.5	16384

To obtain the signal in the frequency domain *A(f)*, the Fourier transform was computed for each component of the collected data (N-S, E-W and vertical) using Equation 3.10.

$$A(f) = \int_{-\infty}^{\infty} a(t)e^{-2\pi ift}dt \tag{3.10}$$

Using Equation 3.11, the power spectra (A_{PSD}) was then computed for all the components

$$A_{PSD}(f) = A(f) * A^{*}(f) \tag{3.11}$$

where:

A(f)* = conjugate complex of the signal in the frequency domain.

The power spectral density (*PSD*) was computed for all the component, using an average of all the power spectral (A_{PSD}), as presented in Equation 3.2.

$$PSD = \sum_{n}^{i=1} \frac{A_{i\_psd}(f)}{n} \tag{3.12}$$

Next, the spectral ratios ($H_{E\text{-}O}/V$, $H_{N\text{-}S}/V$) were computed using the *PSD*. Finally, the fundamental frequency was obtained according to equation 3.13.

$$\frac{H}{V} = \frac{H_{N-S}+H_{E-W}}{2*V} \tag{3.13}$$

where:

$H_{N\text{-}S}$ and $H_{E\text{-}O}$ = the power spectral ratios of both horizontal components, and V = power spectral ratio of the vertical component.

3.7 Shear-waves versus depth velocity profile

The Shear-wave versus depth velocity profile is obtained by direct-modeling or inversion of the dispersion (phase velocity) curve. The genetic algorithm (Matlab code - free software) used for the inversion process of the phase velocity curve in this investigation was developed by Rix and Lai (2004). In this method the analyst iterates until the theoretical dispersion curve match with the experimental curve obtained from the SASW method. The experimental site was modeled as homogeneous layers, defined by the thickness, shear wave velocity, Poisson's ratio and mass density. Using the procedure described in Figure 19, the initial step was to propose an initial soil model and obtain the theoretical dispersion curve. When each theoretical solution was generated, it was compared with the experimental one, and if the comparison between both curves was not satisfactory, the curves did not match, then the parameters of the model (thickness, shear waves velocity, etc.) were changed and the procedure repeated until a satisfactory adjustment between both curves was obtained. Once the best adjustment of the theoretical and experimental curves was obtained, the solution of the shear wave versus depth velocity profile was granted as the best solution.

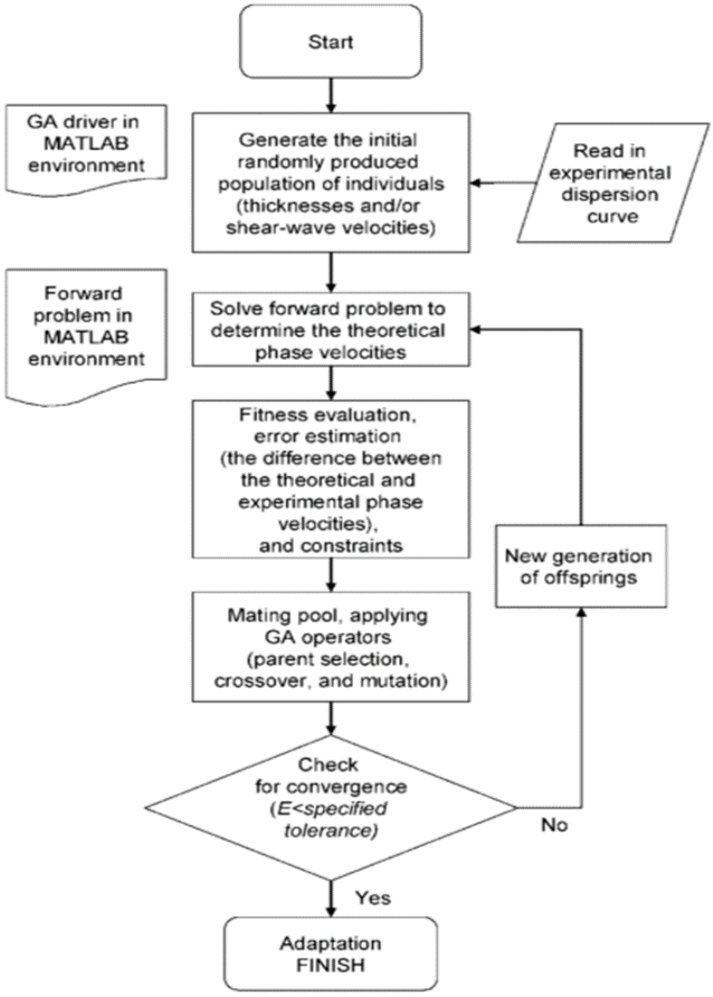

Figure 19. Flow chart of the inversion process (Pezeshk and Zarrabi, 2005)

Chapter 4. Data Analysis and Results

This chapter present the analysis and results of the data collected for this study.

4.1 SASW Method

4.1.1 Dispersion Curve

To obtain the composite dispersion curve, first is necessary to generate a dispersion curve for each distance and impact combination. This curve is normally present either as a function of wavelength or frequency. Figure 20 shows dispersion curves for each distance combination, for the first pulse, and Figure 21 shows all the dispersion curves for one distance combination, all weight drops. The tendency observed in this figure is that the velocity decrease as the frequency is decreased. Figure 22 shows the composite dispersion curve (all distance combinations – all weight drops) of the Rayleigh-wave phase velocity in which the velocity decrease as the frequency also decrease. The behavior previously mentioned corresponds to the case in which an inversion of the velocity descends due to the presence of soft-layers at depth, the tendency of this curve corresponds to Figure 8c (explained in section 2.3.1).

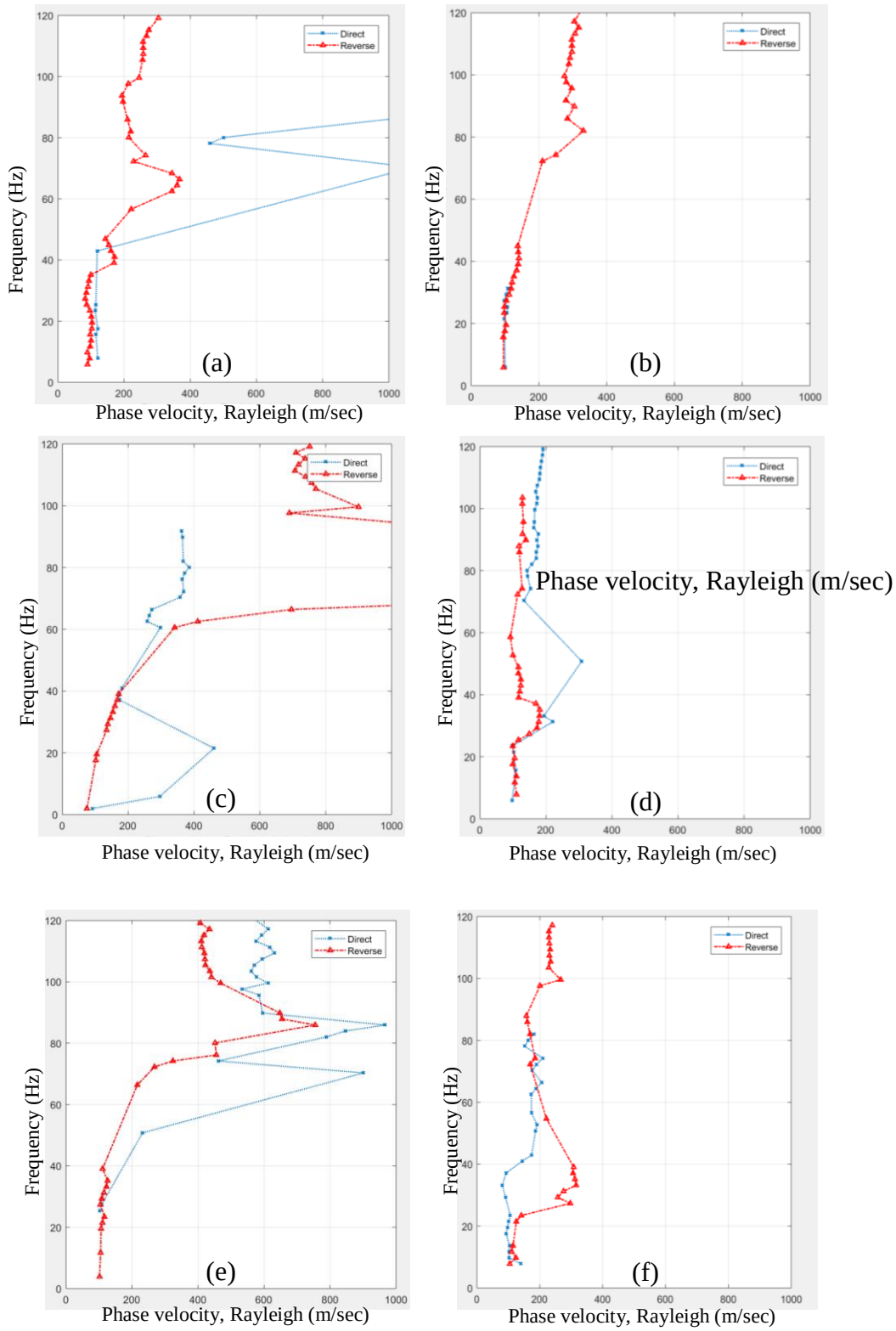

Figure 20. Example of dispersion curve for each distance combination. Combinations (a) Inst. #1 to #2, (b) Inst. #1 to #3, (c) Inst. #1 to 4, (d) Inst. #2 to 3, (e) Inst. #2 to 4 and (f) Inst. #3 to 4

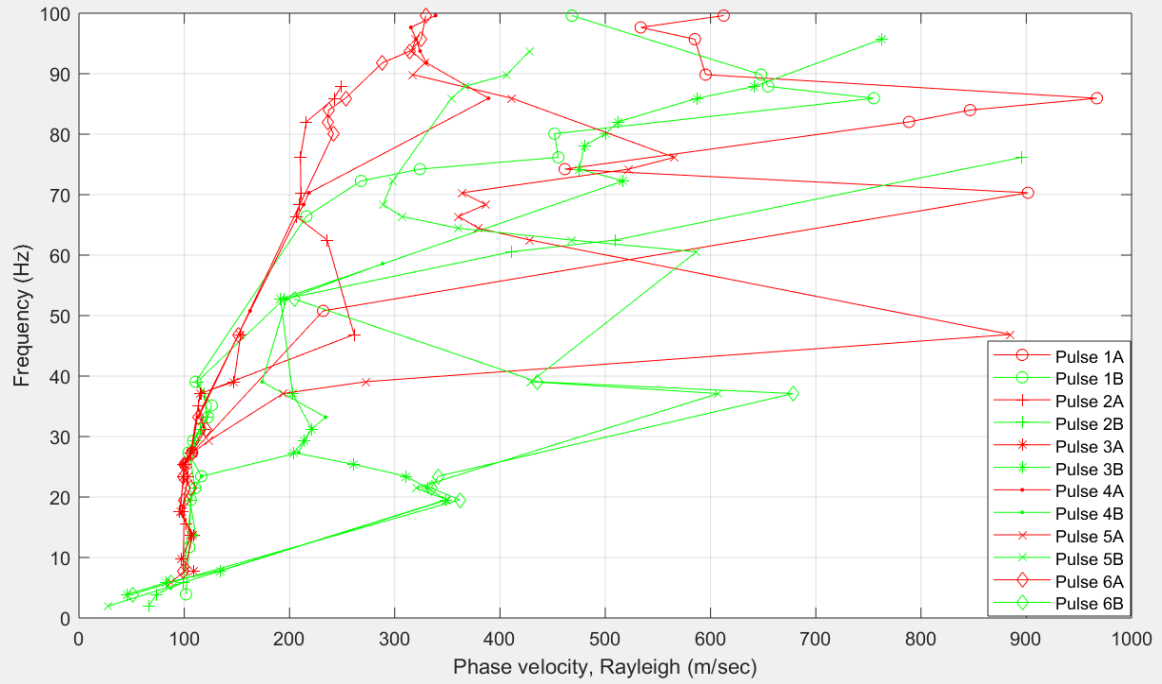

Figure 21. Example of dispersion curve one distance combination (station 2 and 4), all weight drops

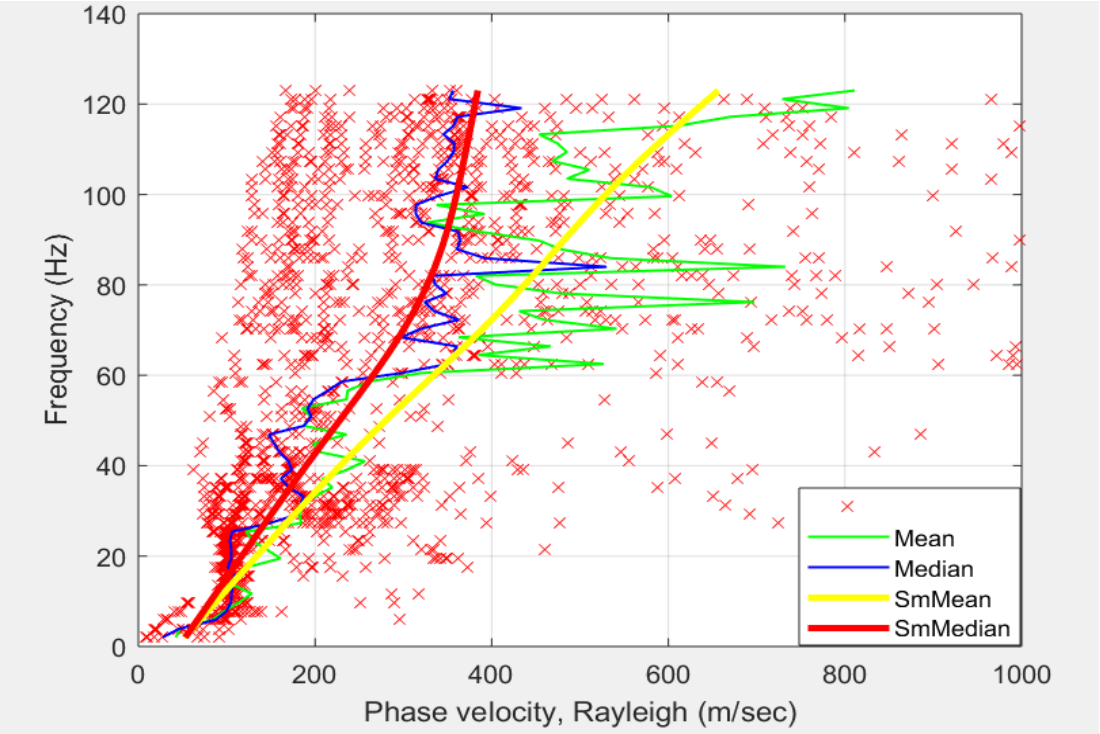

Figure 22. Composite dispersion curve of all distance combinations – all weight drops

Figure 23 and 24 shows separately the composite dispersion curves when the pulses were generated at both sides of the sensors linear array. Figure 23 show the curve in the direct (A) direction and Figure 24 shows the same information but for the reverse direction (B). It is important to mention that, Figures 22, 23 and 24 show the mean curve, the median curve and the smoothed curves for the mean and the median. As previously stated, the behavior presented in these curves corresponds to a soil profile where the Surface-Rayleigh-wave velocity decrease with frequency.

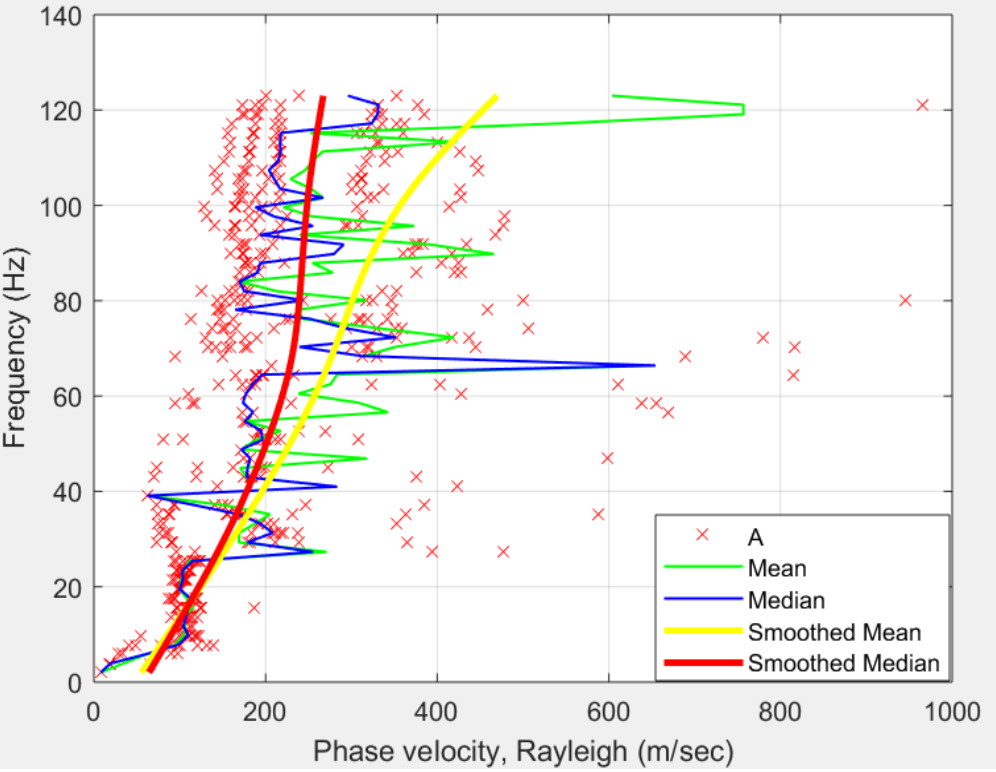

Figure 23. Composite dispersion curve for the direct direction (A)

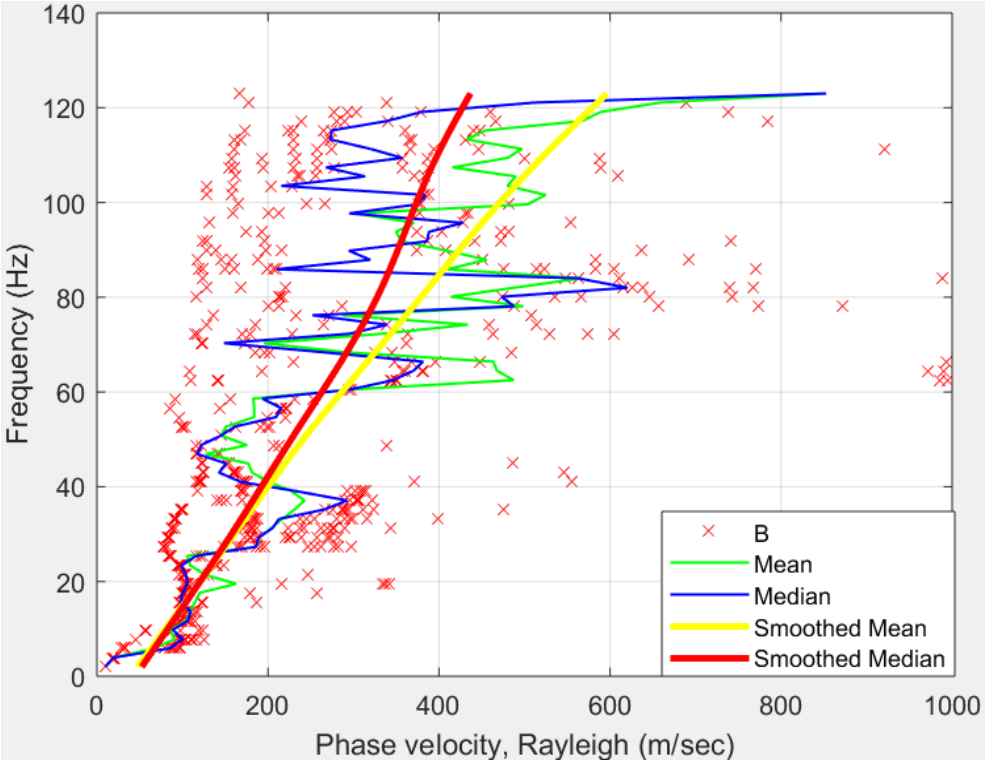

Figure 24. Composite dispersion curve for the reverse direction (B)

4.1.2 Profile Shear-wave velocity versus depth

For the estimation of the of Shear-wave velocity (V_s) versus depth profile, the smoothed medians of the composite dispersion curves were used. The genetic algorithm, explained in section 3.7, was applied for the theoretical estimation of the Rayleigh-wave dispersion curves.

To start the process, the algorithm requests an initial model, that would create a theoretical dispersion curve. This model is defined by the thickness of the soil layers, the density of the soil, Poisson's ratio, and the initial Shear-wave velocity of each layer. Table 6 show the initial model parameters used for the direct and reverse directions. The experimental and theoretical dispersion curves are shown in Figure 25, in which the fit of the best solution can be appreciated, when both curves match each other. The profile of Shear-wave velocity (V_s) versus depth obtained from these

solutions are shown in Figures 26 and 27, showing that the Shear-wave velocity for both cases, direct and reverse measurement, decreases with depth. The average shear waves velocity profile, presented in Figure 28, was used to characterize the site studied during this investigation. The discussion about extreme V_s low values will be addressed in chapter 5.

Table 6. Initial model parameters used for the inversion process

Direction	Layer	Thickness (m)	Density (g/cm^3)	Poisson's ratio (v)	Initial Vs (m/s)
Direct (A)	**1**	1.0	1.1	0.18	110
	2	1.0	1.2	0.20	190
	3	2.0	1.2	0.20	160
	4	1.5	1.3	0.20	190
	5	1.5	1.3	0.20	200
	6	1.0	1.4	0.20	180
	7	9.0	1.6	0.20	180
	8	7.0	1.6	0.20	200
	9	8.0	1.8	0.22	300
	Half-space		2.3	0.22	900
Reverse (B)	**1**	1.0	1.1	0.18	120
	2	1.0	1.2	0.20	180
	3	2.0	1.2	0.20	150
	4	1.5	1.3	0.20	150
	5	1.5	1.3	0.20	150
	6	1.0	1.4	0.20	150
	7	9.0	1.6	0.20	180
	8	7.0	1.6	0.20	190
	9	8.0	1.8	0.22	300
	Half-space		2.3	0.25	900

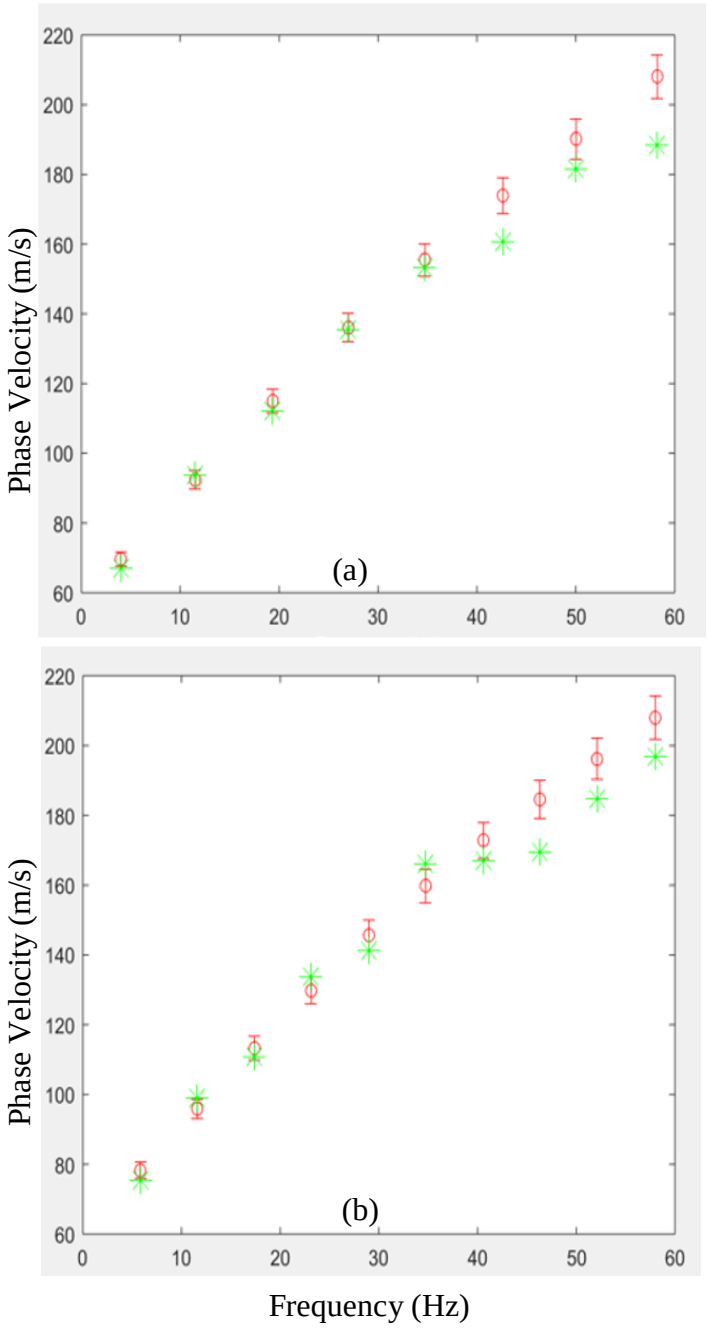

Figure 25. Theoretical (red) and experimental (green) composite dispersion curves, (a) direct direction (A), and (b) reverse direction (B),

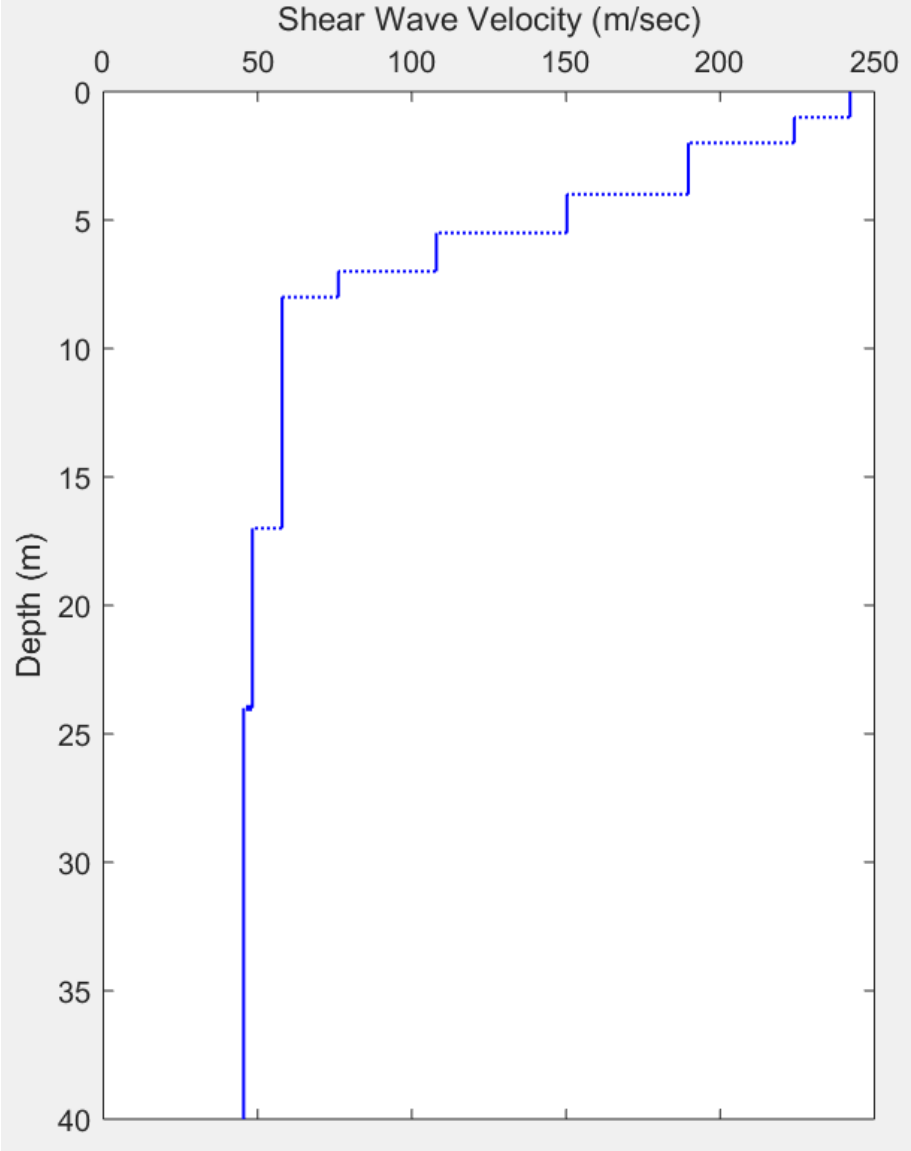

Figure 26. Estimated Shear-wave velocity (Vs) versus depth profile, direct direction (A)

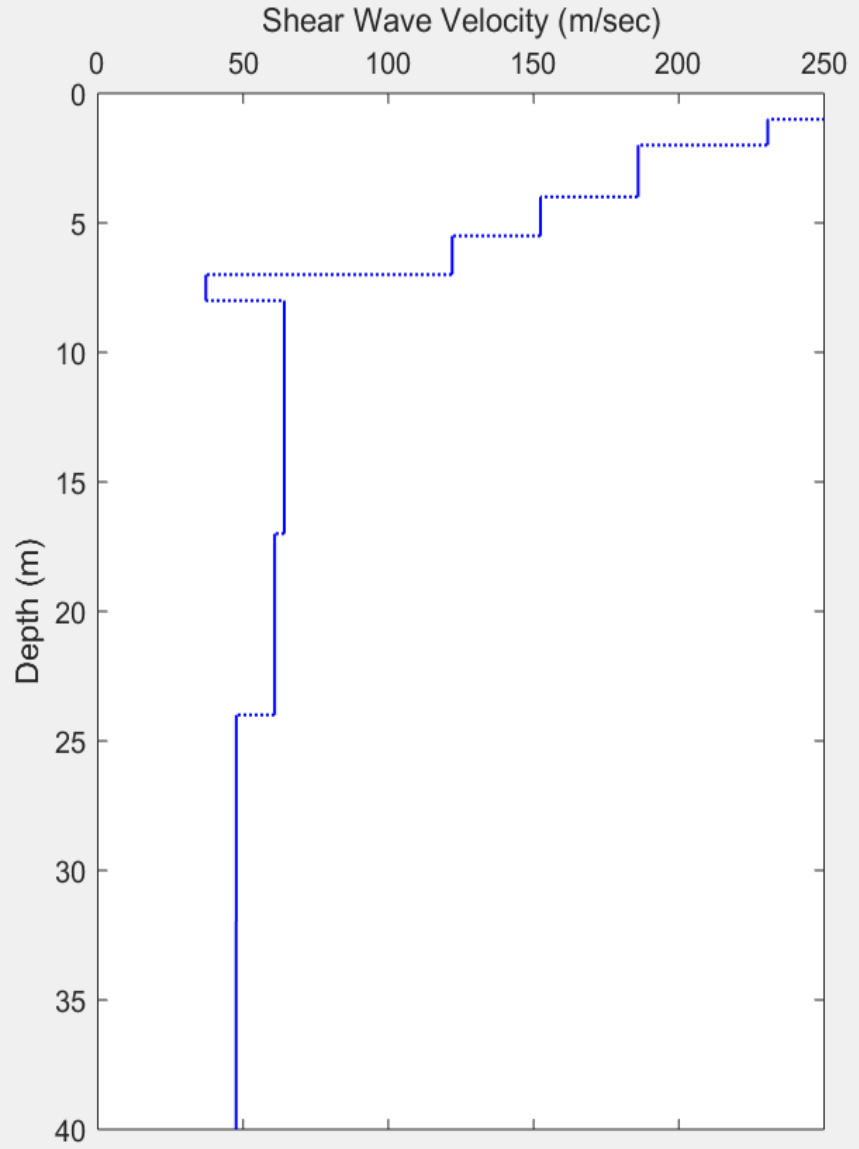

Figure 27. Estimated Shear-wave velocity (Vs) versus depth profile, reverse direction (B)

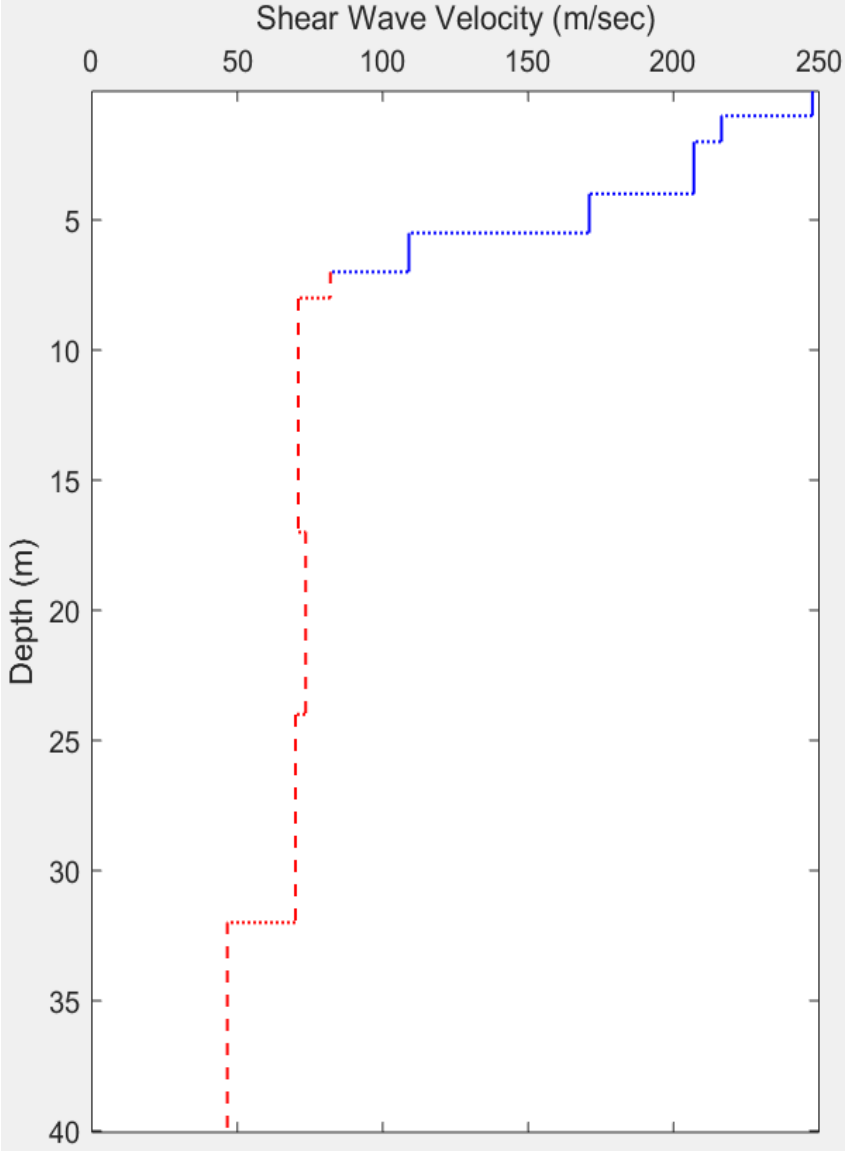

Figure 28. Average Shear-wave velocity (Vs) versus depth profile. V_s values shown in red-dashed line are discuted in chapter 5

4.4 HVSR Nakamura's method

The site fundamental vibration frequency was successfully obtained for the study area using the Nakamura's H/V method. To obtain the fundamental frequency, the power spectral density (PSD) where obtained for the east-west and north-south ($H_{E\text{-}W}/V$, $H_{N\text{-}S}/V$) directions (Figure 29). The fundamental frequency of the site was found to be 1.358 Hz (Figure 30). According to

the results obtained by Vázquez (2014) in her study of microzonation of fundamental vibration mode in the area that we conducted our study, the estimated fundamental vibration mode was in the range of 1.465– 2.190 Hz, for the closest points she measured to our experimental site. Table 7 shows the fundamental frequency results measured by Vázquez (2014). Figure 31 show the location of the instruments used in this project and the location of the nearest sites (approximately 13m from the studied area) measured by Vázquez (2014).

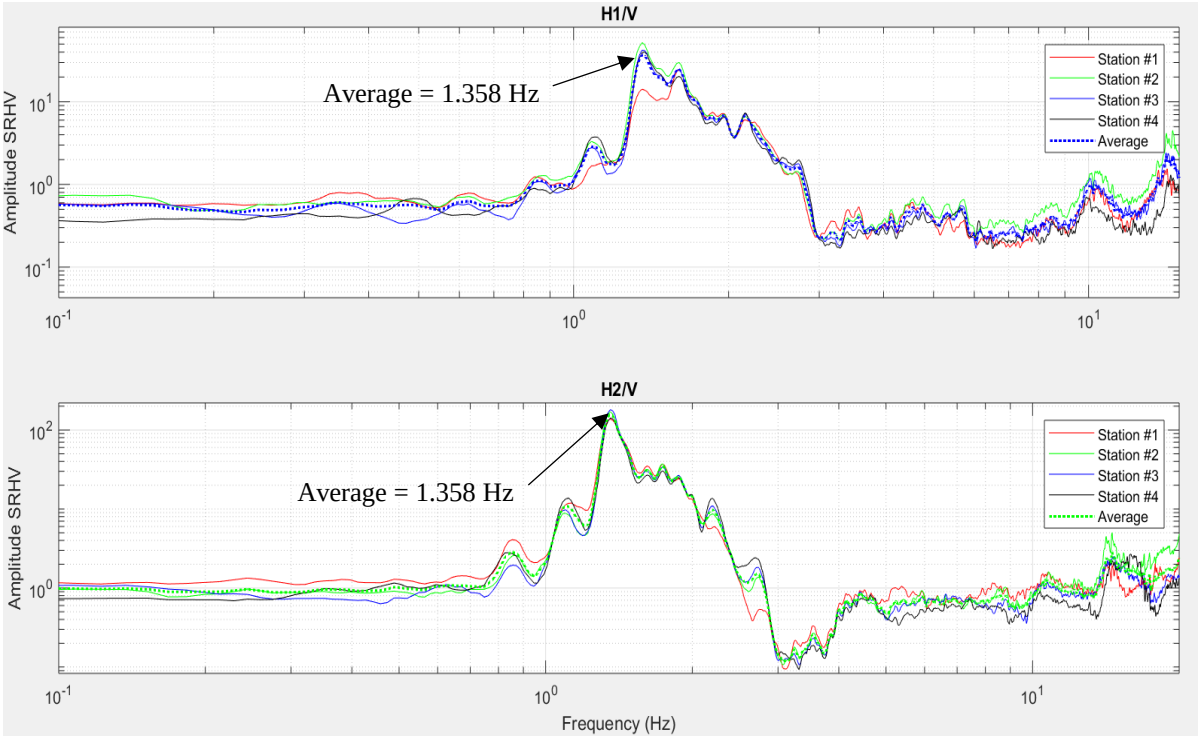

Figure 29. Results and averages of the Fourier spectral quotients for both horizontal directions (H1/V = $H_{N\text{-}S}/V$ and H2/V = $H_{E\text{-}W}/V$)

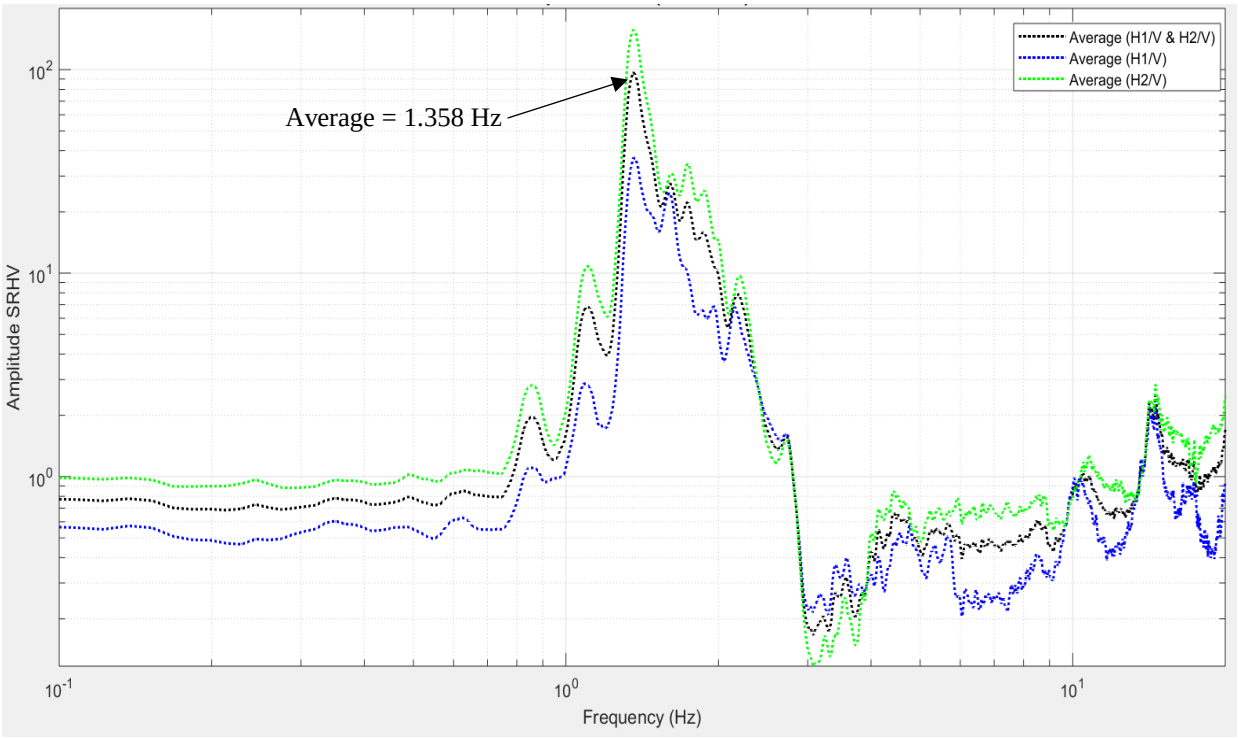

Figure 30. Fundamental frequency results

Table 7. Fundamental frequency results, (Vázquez, 2014)

Identification Number	Latitude (˚) N	Longitude (˚) W	Frequency (Hz)	Period (sec.)
PP11	18.211750	-67.144833	1.807	0.553
PP12	18.212383	-67.146067	2.190	0.457
PP120	18.212470	-67.144780	1.539	0.650
PP127	18.212767	-67.144400	1.709	0.585
PP128	18.211800	-67.145133	2.124	0.471
PP137	18.212861	-67.145306	1.465	0.683

Considering the surface geological conditions of the site, it is expected that soft soils will vibrate in the range of low values of the fundamental vibration frequency. On the other hand, rigid soil conditions may be in the range of high frequency vibrations of fundamental mode. The

description proided above, is consistent with the site surface geological conditions, and with the borings of the SPT studies previously conducted near the studied site by Vázquez (2014).

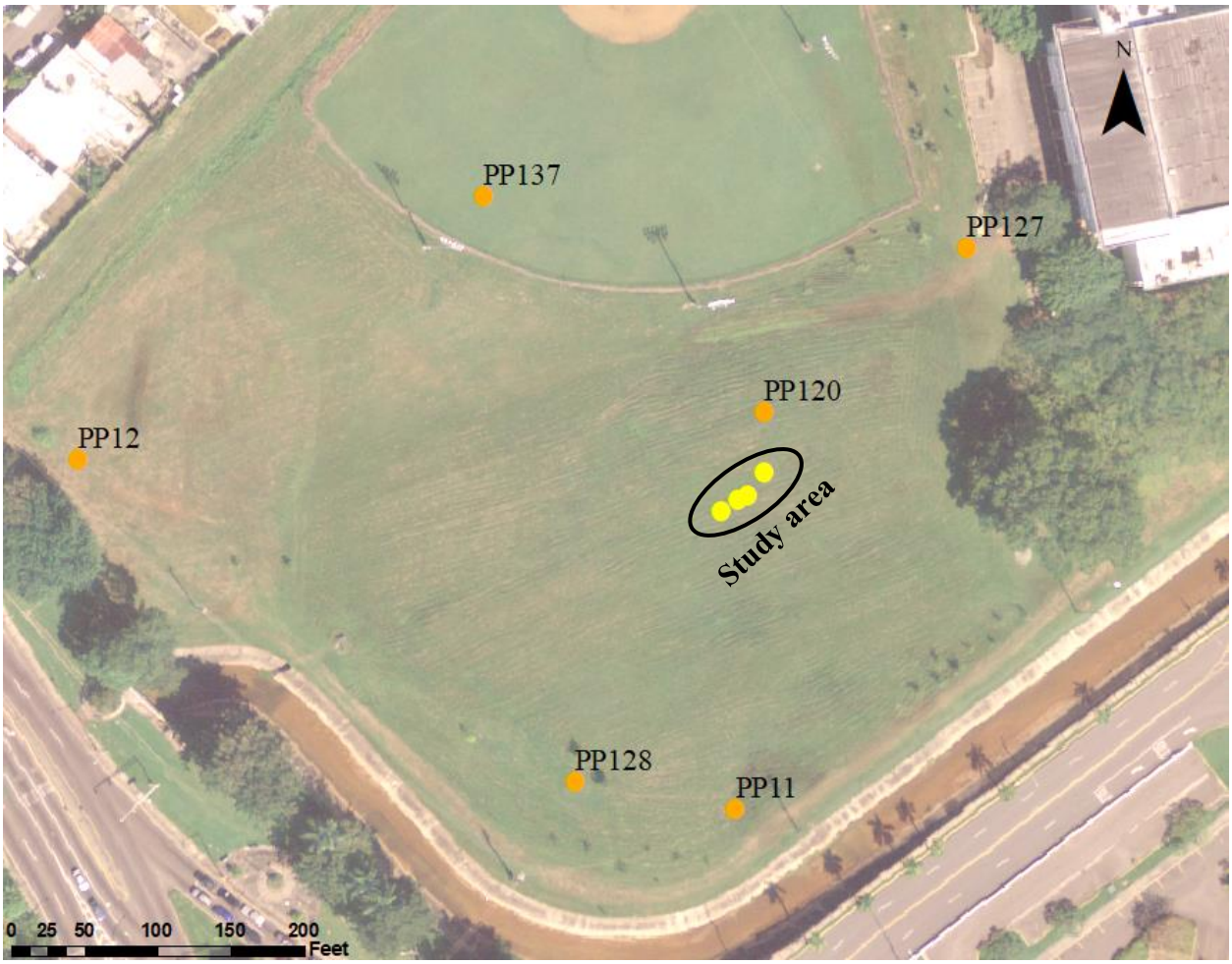

Figure 31. HVSR recording locations for this study and Vázquez (2014), at University of Puerto Rico at Mayagüez

Chapter 5. Discussion of Results and Conclusions

Based on the analysis of the data and the results presented in the previous chapter, the discussion of the Spectral Analysis of Surface Waves (SASW) and Horizontal and Vertical Spectral Ratio (HVSR) are presented. Also, the correlation between the results of the SASW method respect to the Standard Penetration Test (SPT) is discussed. Additionally, the conclusions for this investigation are presented.

5.1 SASW method

The results obtained from the SASW method provided on the dispersion curves (Figures 20 and 21) exhibit a clear velocity inversion of the Rayleigh-waves in the frequency range of 120 Hz to 20 Hz; ranging from 450 m/s at 120 Hz, to 700 m/s at 85 Hz, and 150 m/s at 20 Hz. This behavior was consistent in all dispersion curves, graphs of these dispersion curves are provided in appendix A.

From the results of the inversion process of the experimental dispersion curves, the site was initially characterized by a 9 layers soil model resting over a half-space, which include the physical properties, geometry (thickness of the soil layers) and Shear-wave velocity profile versus depth. On Table 8, the initial model parameter as well as the final model parameters are provided. In Figure 28, the Shear-wave velocity profile versus depth is provided, showing that velocity decreases from approximately 250 m/s at the surface to 115 m/s at 8m depth, where the velocity gradually decreases up to a value of 46.59 m/s at 32m depth are clearly out of context for a reliable values of soil layers model at these depths. Regarding to the obtained shear wave velocity profile

(V_S versus depth), it should be pointed out, that the results can only be validated for the first 6 layers (first 8m of the model), since the results of the SPT tests only reached 8m depth, shown in Figure B3. Also, the last layers of the model (last 24m) the obtained velocities are not realistic for soil layers at those depths. This could have happened because the collected data did not sample properly at those depths, which could be caused by the loss of the signal at those depths. Based on the previous statements, the final soil model was constrained to the first 6 layers.

Table 8. Initial and final model parameter

Layer	**Thickness (m)**	**Density (g/cm^3)**	**Poisson's ratio (v)**	**Initial Vs (m/s)**	**Final Vs (m/s)**
1	1.0	1.4	0.18	110	247.75
2	1.0	1.2	0.2	190	227.30
3	2.0	1.2	0.2	160	187.85
4	1.5	1.1	0.2	190	151.35
5	1.5	1.2	0.2	200	115.00
6*	1.0	1.2	0.2	180	56.71
7*	9.0	1.2	0.2	180	61.07
8*	7.0	1.6	0.22	200	54.60
9*	8.0	1.6	0.22	300	46.59
Half-space*		2.3	0.25	900	46.57

* Non-reliable V_s values, were excluded from the final model

The correlation between the Shear-wave velocity profile versus depth and the SPT tests results shows a consistent behavior among them up to its maximum depth of 8m, see Figure 32. The difference in behavior could be because the SPT tests were performed at an approximate distance of 115m from the study area.

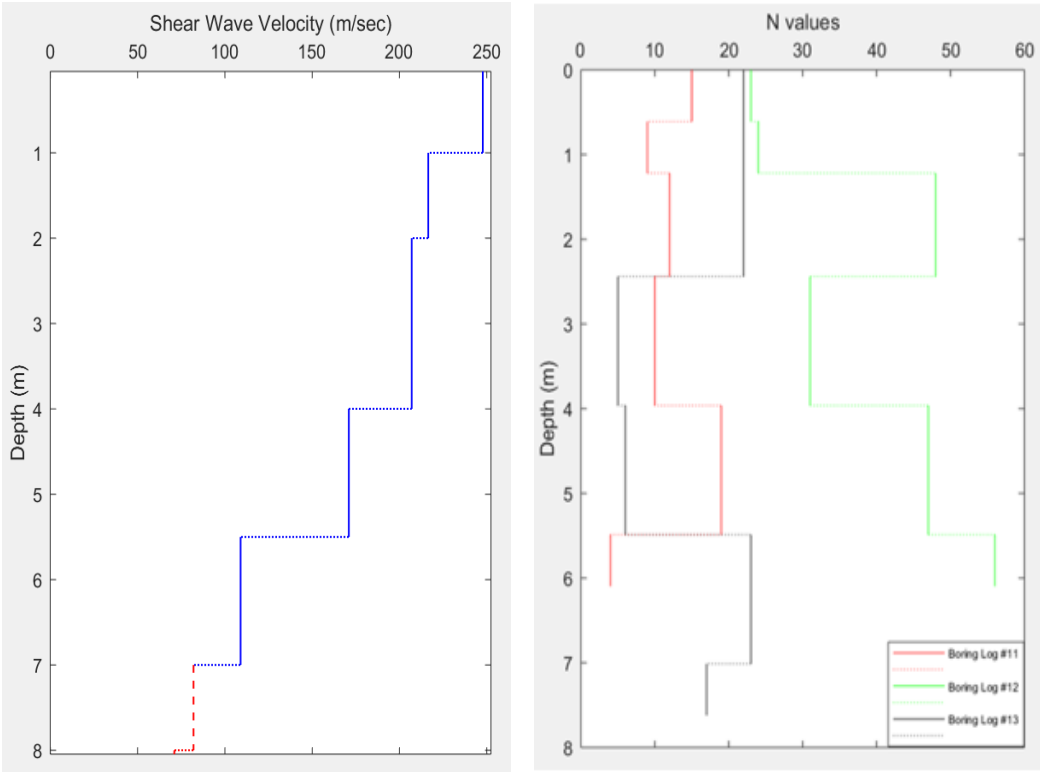

Figure 32. Shear-wave velocity profile and the N-value plots

According to the results obtained during the project, and the soil classification in terms of the American Association of State Highway Officials (AASHTO, 2012) given in Table 9. It was decided to use the AASHTO table because the soil classification can be done using the velocities or the N-values from the SPT results. The soil classification for the different layers present in the studied area corresponds to D and E class types. Table 10 shows the soil classification obtained based on the SASW method.

The average Shear-waves velocity value for the upper 8m of the site was computed using the definition of two standard methods for calculation of V_S up to certain depth ("Vs30m Calculation"), obtaining approximately 178m/s and 166m/s for method 1 and method 2, respectively. The equations for these methods are next provided:

Method 1: $\bar{V}_S = \sum_{i=1}^{n}[V_{S_i} * (\frac{d_i}{7})]$ (5.1)

Method 2: $V_{S_7} = \frac{\sum_{i=1}^{n} d_i}{\sum_{i=1}^{n}(\frac{d_i}{V_{S_i}})}$ (5.2)

where:

i denotes the *i*-th layer thickness (*d*) and Shear-wave velocity (V_S).

From the comparison of V_S obtained by means of Equations 5.1 and 5.2, it is clearly seen that Equation 5.2 provides the more conservative estimation of average V_S values.

Table 9. Soil classification (AASHTO, 2012; Brown et al., 2000; Wair et al., 2012)

Site Class	Soil Profile Name	V_s	SPT N-value
A	Hard Rock	> 5,00 ft/s >1,500 m/s	--
B	Rock	2,500 to 5,000 ft/s 760 to 1,500 m/s	--
C	Very Dense Soil and Soft Rock	1,200 to 2,500 ft/s 360 to 760 m/s	>50 bpf
D	Stiff Soil	600 to 1,200 ft/s 180 to 360 m/s	15 to 50 bpf
E	Soft Soil	<600 ft/s <180 m/s	< 15 bpf
F	Soils Requiring Site-Specific Evaluation	--	--

Table 10. Soil characterization with SASW method

Layer	Thickness (m)	Vs (m/s)	Site Class	Soil Profile Name
1	1.0	247.75	D	Stiff soil
2	1.0	227.30	D	Stiff soil
3	2.0	187.85	D	Stiff soil
4	1.5	151.35	E	Soft soil
5	1.5	115.00	E	Soft soil

5.2 HVSR - Nakamura's method

From the data analysis and the obtained results of the HVSR – Nakamura method, we can appreciate that the estimated dominant fundamental vibration frequency of 1.358 Hz at each instrument location is consistent among them. In addition to characterize the site by the estimation of the dominant fundamental frequency, the site characterization in terms of the site single layer geometry (thickness of the soil layers) and its Shear-wave velocity was obtained using Equation 5.3 (modified from Pierre-Yves and Bouchon, 1980).

$$f_n = \frac{(2n-1)*V_S}{4H}, \tag{5.3}$$

where,

n = the vibration mode, V_S = single layer Shear-wave velocity, and H = the layer thickness.

From the estimated fundamental vibration frequency of 1.358 Hz and using the value of V_S=166m/s from method 2 (Equation 5.2), since using this velocity will be conservative, the estimated single layer thickness is 30.7m. This mean that the fundamental vibration frequency of the site corresponds to a system constrained to 30.7m depth.

5.3 Conclusions

From the discussion and interpretation presented in sections 5.1 and 5.2, it is possible to conclude that the site exhibits a velocity inversion, which was corroborated through the correlation of the N-value results of the SPT test conducted near-by to our study site. From the plot of the N-value versus depth and the sites-soil description, provided in appendix B, the correlation between

the Shear-wave velocity profile versus depth and the N-value plots of three sites of SPT tests shows a consistent behavior among them up to its maximum depth of 8m, which is the maximum sampling depth of the SPT study. As mention before, the velocities of the site decrease as the depth increases, this mean that the velocity is decreasing with larger wavelength. As discussed in section 2.3.1, this is because each layer is composed of different materials.

Regarding to the HVSR Nakamura's method results and its interpretation with the simplified single layer model, the maximum sampling depth of 30.7m with a fundamental vibration frequency of 1.358 Hz, is consistent for a site in which the velocity inversion is observed in the shallow first 8m of the site. With an average velocity of 166m/s it can be concluded that the soil site classification for the studied area is a soft soil (type E).

Chapter 6. Recommendations

As explained in the conclusion, even when the SASW and SPT methods results were consistent, it is recommended to perform an SPT test at the exact point of the study area. The SPT test was not possible to do in this investigation because the proper equipment was not available. This way results obtained with SPT and with both non-invasive methods at the exact same location will provide a more detailed results for comparison between the non-invasive and invasive methods for site characterization. Also, it is recommended to do a bidimensional Shear-wave velocity profile. This way, not only the change in depth will be seen, but also the change in the lateral direction. For the HVRS Nakamura's method it is suggested to explore the possibility of estimating the soil amplification factor and the fundamental periods for the area for micro-zonation purpose.

References

AASHTO. (2012). LRFD Bridge Design Specifications.

Anderson, N., Croxton, N., Rick, H., and Sirles, P. (2008). "Geophysical Methods Commonly Employed for Geotechnical Site Characterization." Washington, DC.

ASTM-D1586. (2008). "Standard Test Method for Standard Penetration Test (SPT) and Split-Barrel Sampling of Soils." ASTM Standard Test Method, D1586–08a, 1–9.

Brown, L. T., Diehl, J. G., and Nigbor, R. L. (2000). "A Simplified Procedure to Measure Average Shear-Wave Velocity to a Depth of 30 Meters (VS30)." (0677), 8.

Burgos, O., Colon, G., Pierre Valle, J., and Ramírez Bonet, J. (2015). Soil Study. Mayagüez, PR.

Curet, A. F. (1986). "Geologic Map of the Mayaguez and Rosario Quadrangles, Puerto Rico."

Foti, S. (2000). "Rayleigh waves." Multistation Method for Geotechnical Characterization Using Surface Waves, Politecnico di Torino Porto.

Huerta, C. (2016). "Ambient vibration and H/V spectral ratio method general aspects of methods." Class notes from Engineering Seismology course, 2016, pp. 1-9.

Huerta, C. (2018). "Personal Communication." Mayagüez, PR.

Lai, C. G., and Rix, G. J. (1998). "Simultaneous inversion of Rayleigh phase velocity and attenuation for near-surface site characterization." Georgia Institute of Technology, 258.

Lin, Y. (2007). "Characterizing Vs Profiles by the SASW Method and Comparison with Other Seismic Methods."

Nazarian, S., and Stoke II, K. H. (1986). In Situ Determination of Elastic Moduli of Pavement Systems by Spectral-Analysis-of- Surface-Waves Method (Theoretical Aspects).

Pezeshk, S., and Zarrabi, M. (2005). "A New Inversion Procedure for Spectral Analysis of Surface Waves Using a Genetic Algorithm." Bulletin of the Seismological Society of America, 95(5), 1801–1808.

Pierre-Yves, B., and Bouchon, M. (1980). "The Seismic Response of Sediment-Filled Valleys. Part 1. the Case of Incident Sh Waves." Bulletin of the Seismological Society of America, 70(4), 1263–1286.

Rix, G. J., and Lai, C. G. (2004). "Elastic, Uncoupled, Fundamental-Mode Surface Wave Inversion Program."

Rix, G. J., Stokoe, Kenneth H, I., and Roesset, J. M. (1991). Experimental Study of Factors Afecting the Spectral-Analysis-of-Surfaces-Waves Method.

Rogers, J. D. (2006). "Subsurface Exploration Using the Standard Penetration Test and the Cone Penetrometer Test." Environmental & Engineering Geoscience, XII(No. 2), 161–179.

Seekins, L. C., Wennerberg, L., Margheriti, L., and Liu, H.-P. (1996). “Site amplification at five locations in San Francisco, California: A comparison of S waves, codas, and microtremors.” Bulletin of the Seismological Society of America, 86(3), 627–635.

Stokoe, K. H., and Santamarina, J. C. (2000). “Seismic-Wave-Based Testing in Geotechnical Engineering.” Proceedings of the GeoEng 2000 Conference, (1887), 1490–1596.

Vázquez, W. (2014). “Micronización del Periodo fundamental de Vibración del Terreno Y Edificios del Recinto Universitario de Mayagüez de la Universidad de Puerto Rico.” Universidad de Puerto Rico Recinto Univercitario de Mayagüez.

Villagómez, J. (2016). “Análisis Espectral de Ondas Superficiales para la Caracterización del Suelo : Estudio de Comparación.” Universidad de Puerto Rico Recinto Universitario de Mayagüez.

“Vs30m Calculation.” (n.d.). <http://www.parkseismic.com/SSC-HowToCalculateVs30m.html> (Sep. 10, 2018).

Wair, B. R., Dejong, J. T., and Shantz, T. (2012). “Guidelines for Estimation of Shear Wave Velocity Profiles.” Pacific Earthquake Engineering, 8(December), 68.

Woods, R. D. (1968). “Screening of Surface Waves in Soils.”

“Yauco Formation, Puerto Rico geologic unit TKy.” (n.d.). <https://mrdata.usgs.gov/geology/pr/prgeo-unit.php?unit=TKy> (Oct. 21, 2018).

Appendix A

This appendix provides the results/plots of the Auto-power spectra in the NW (A) direction, Auto-power spectra in the SE (B), showing the Cross-power spectra, and the dispersion curves for the all distance combinations. Also, the code used in MatLab for the Spectral Analysis of Surface Waves (SASW) is provided.

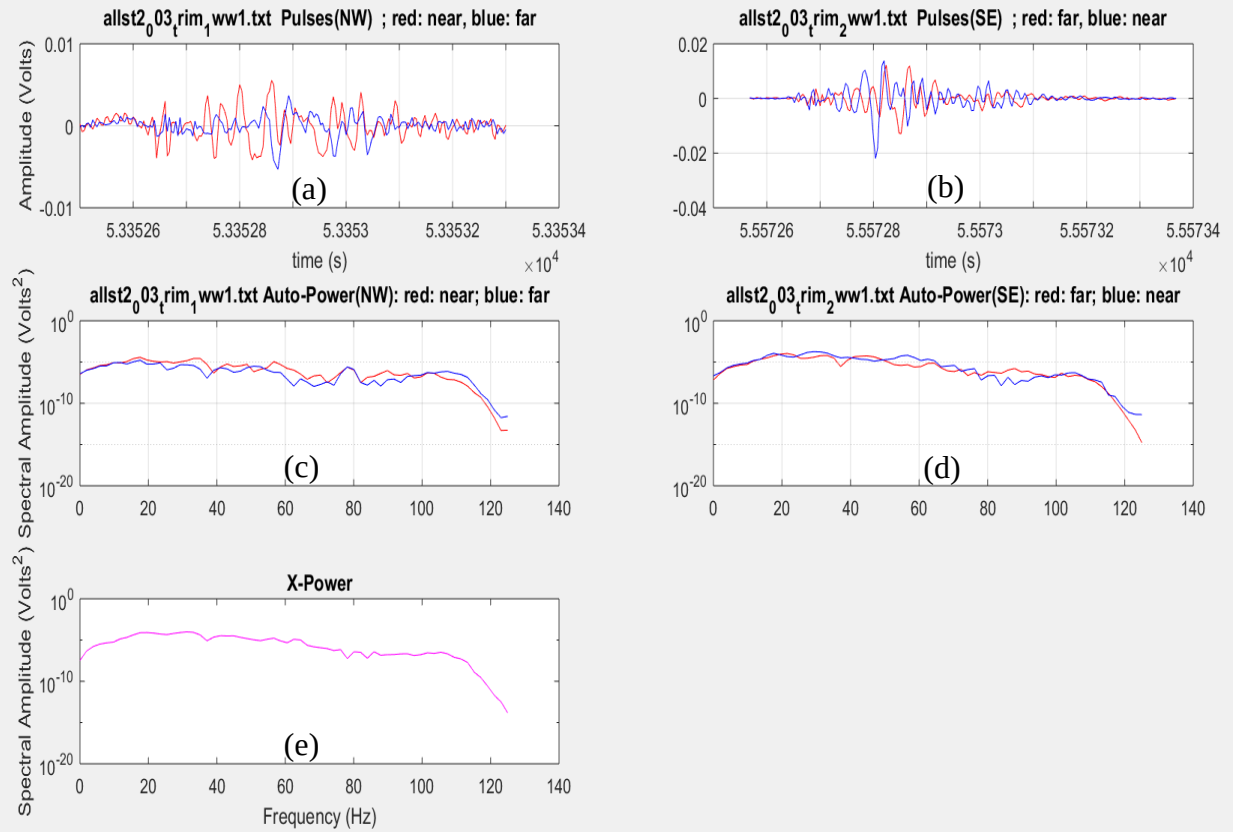

Figure A1. (a) Pulse #1 in the NW (A) direction, (b) Pulse #1 in the SE (B) direction, (c) Auto-power spectra in the NW (A) direction, (d) Auto-power spectra in the SE (B), and (e) shows the Cross-power spectra

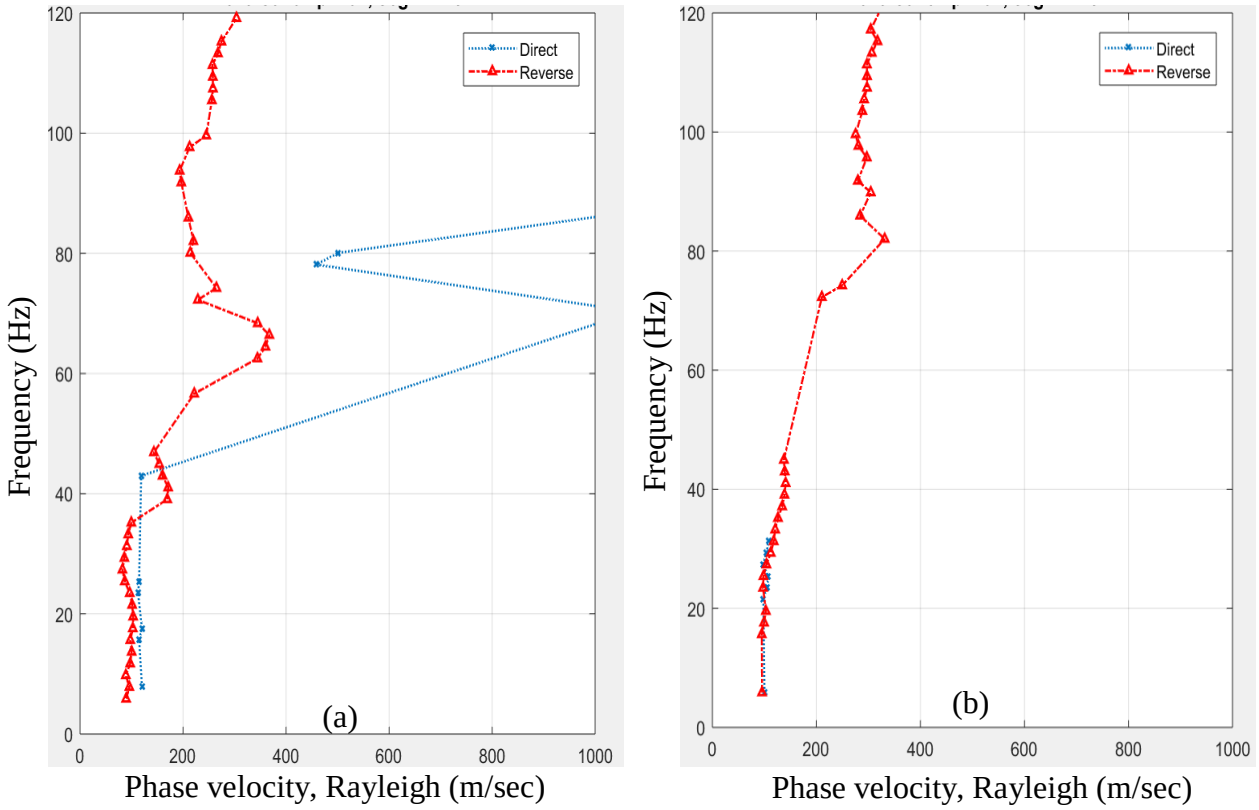

Figure A2. Dispersion curves for the first pulses in each direction, direct (A) and reverse (B) Figure (a) shows the dispersion curves for both directions between instruments #1 and #2, and Figure (b) shows the dispersion curves for both directions between instruments #1 and #3.

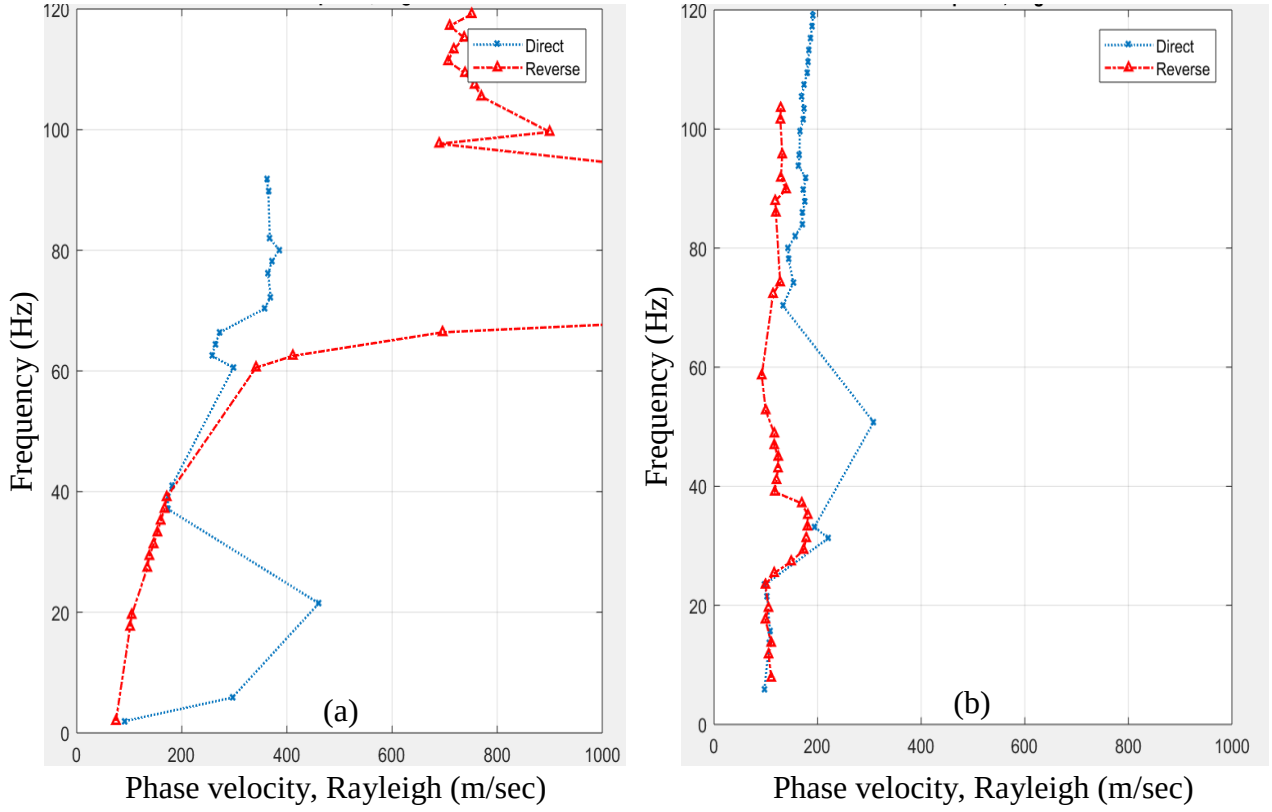

Figure A3. Dispersion curves for the first pulses in each direction (continuation)
Figure (a) shows the dispersion curves for both directions between instruments #1 and #4, and Figure (b) shows the dispersion curves for both directions between instruments #2 and #3

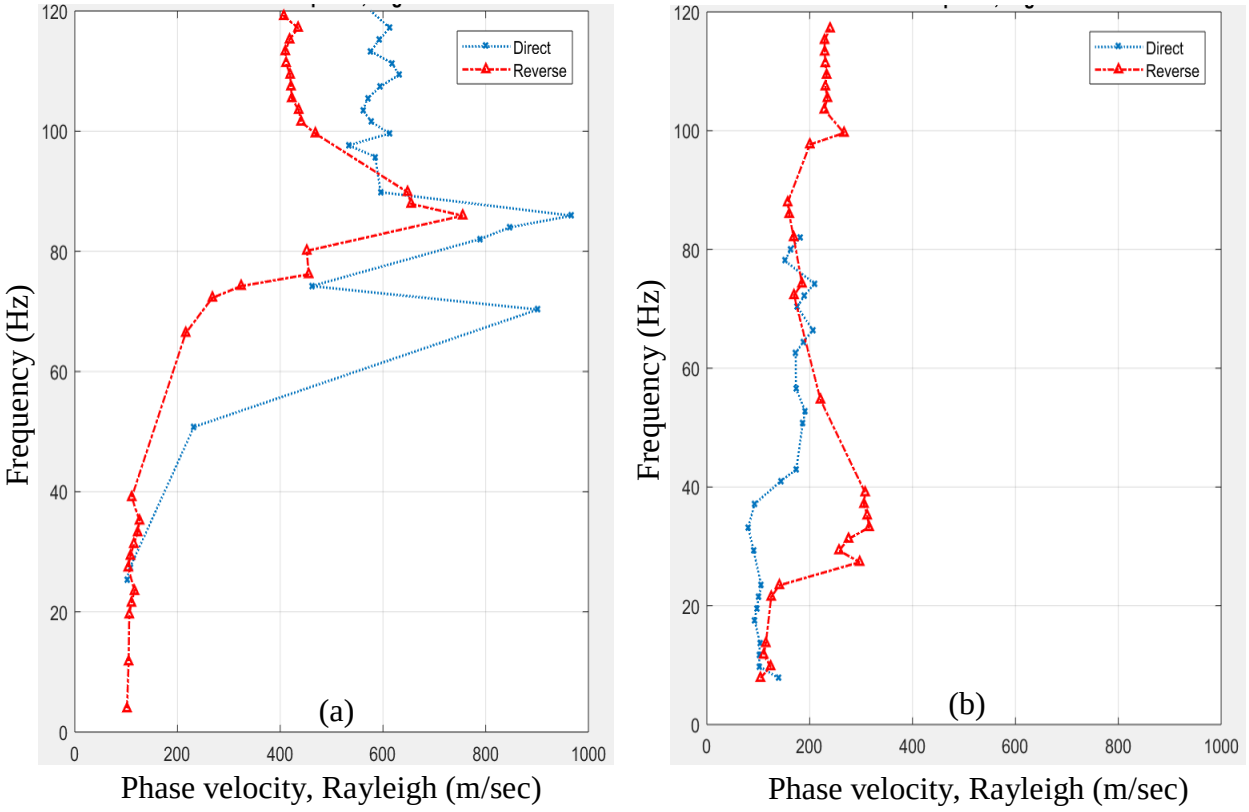

Figure A4. Dispersion curves for the first pulses in each direction (continuation)
Figure (a) shows the dispersion curves for both directions between instruments #2 and #4, and Figure (b) shows the dispersion curves for both directions between instruments #3 and #4

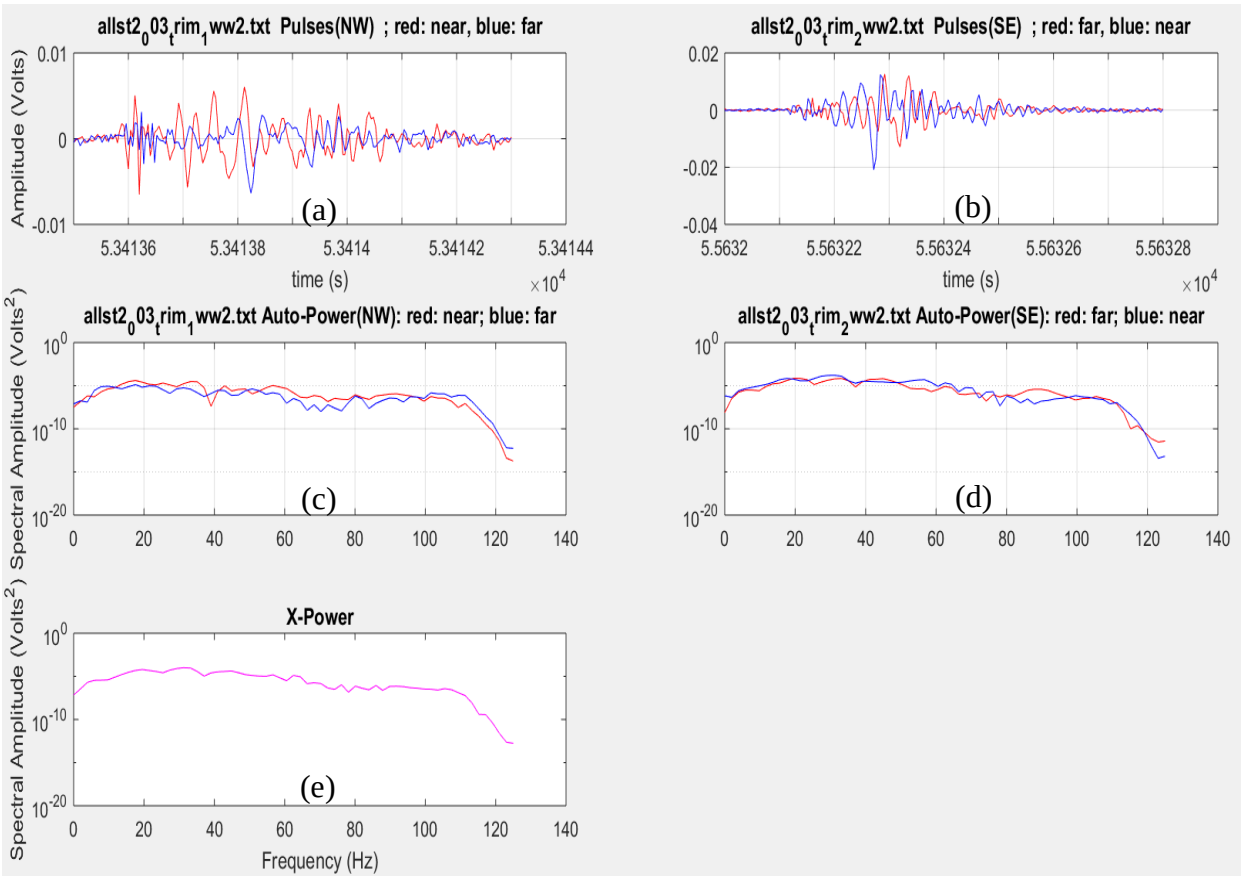

Figure A5. (a) Pulse #2 in the NW (A) direction, (b) Pulse #3 in the SE (B) direction, (c) Auto-power spectra in the NW (A) direction, (d) Auto-power spectra in the SE (B), and (e) shows the Cross power spectra

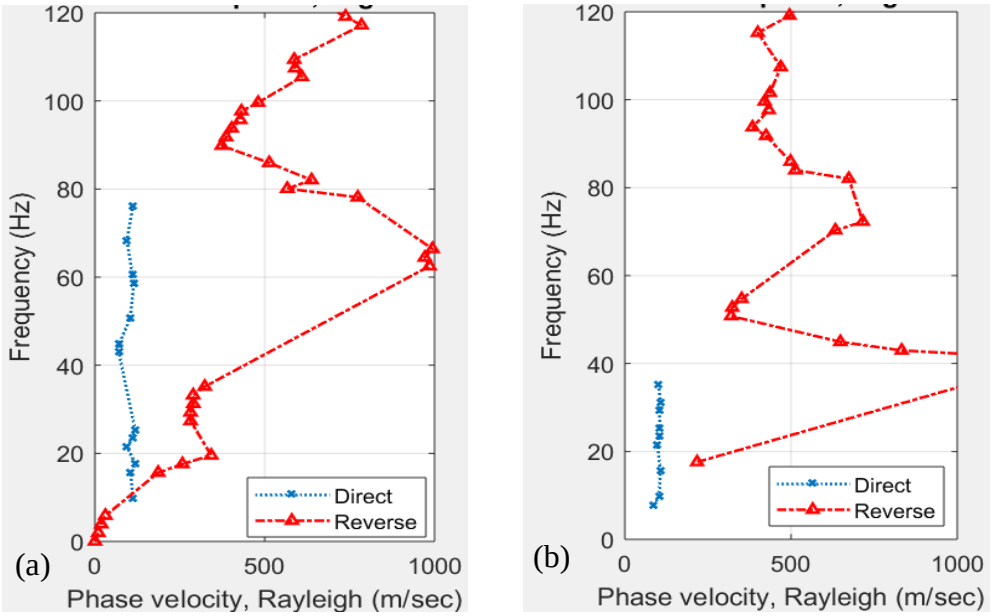

Figure A6. Dispersion curves for the second pulses in each direction, direct (A) and reverse (B) Figure (a) shows the dispersion curves for both directions between instruments #1 and #2, and Figure (b) shows the dispersion curves for both directions between instruments #1 and #3

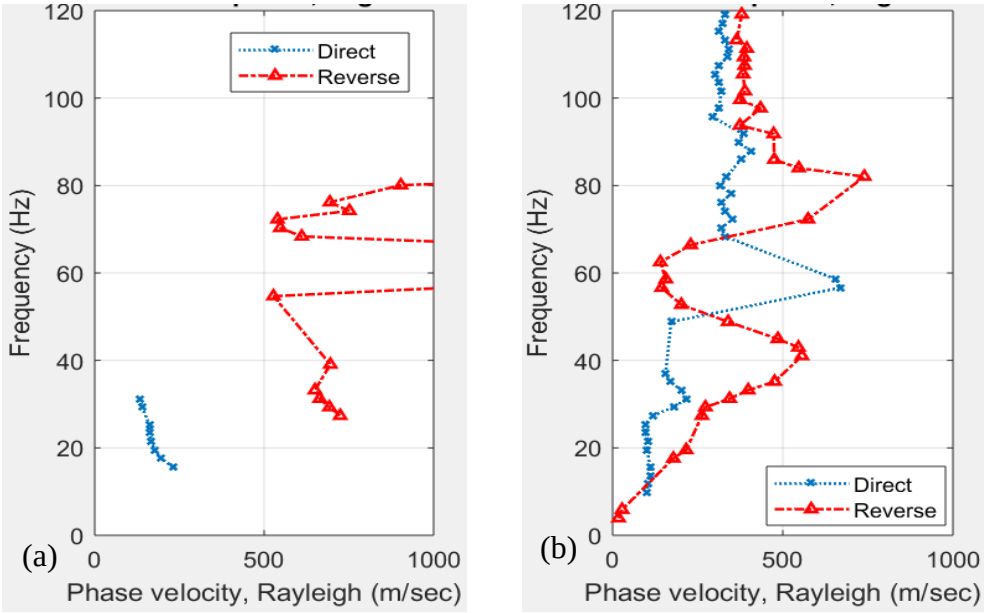

Figure A7. Dispersion curves for the second pulses in each direction (continuation) Figure (a) shows the dispersion curves for both directions between instruments #1 and #4, and Figure (b) shows the dispersion curves for both directions between instruments #2 and #3

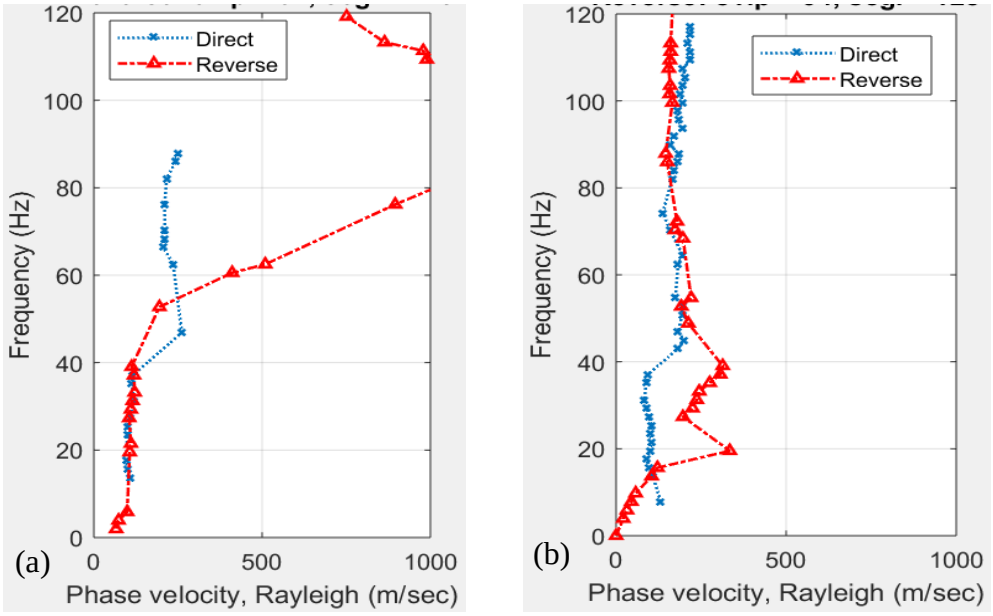

Figure A8. Dispersion curves for the second pulses in each direction (continuation)
Figure (a) shows the dispersion curves for both directions between instruments #2 and #4, and
Figure (b) shows the dispersion curves for both directions between instruments #3 and #4

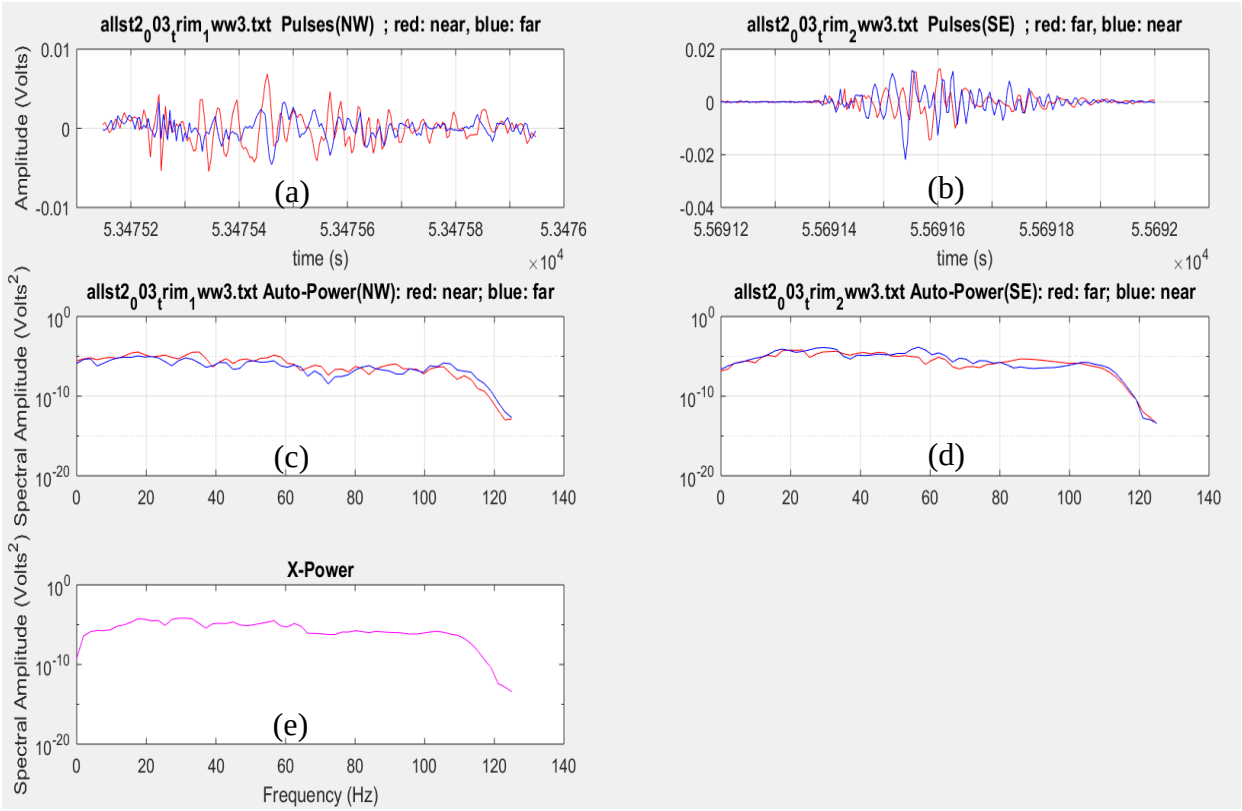

Figure A9. (a) Pulse #3 in the NW (A) direction, (b) Pulse #3 in the SE (B) direction, (c) Auto-power spectra in the NW (A) direction, (d) Auto-power spectra in the SE (B), and (e) shows the Cross power spectra

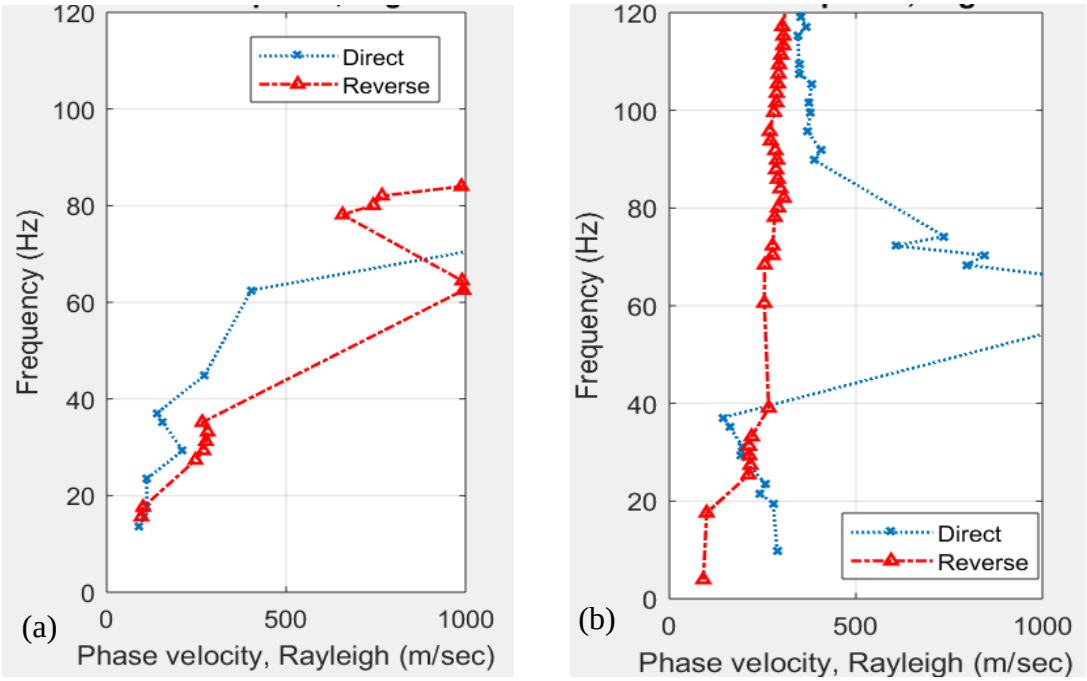

Figure A10. Dispersion curves for the third pulses in each direction, direct (A) and reverse (B) Figure (a) shows the dispersion curves for both directions between instruments #1 and #2, and Figure (b) shows the dispersion curves for both directions between instruments #1 and #3

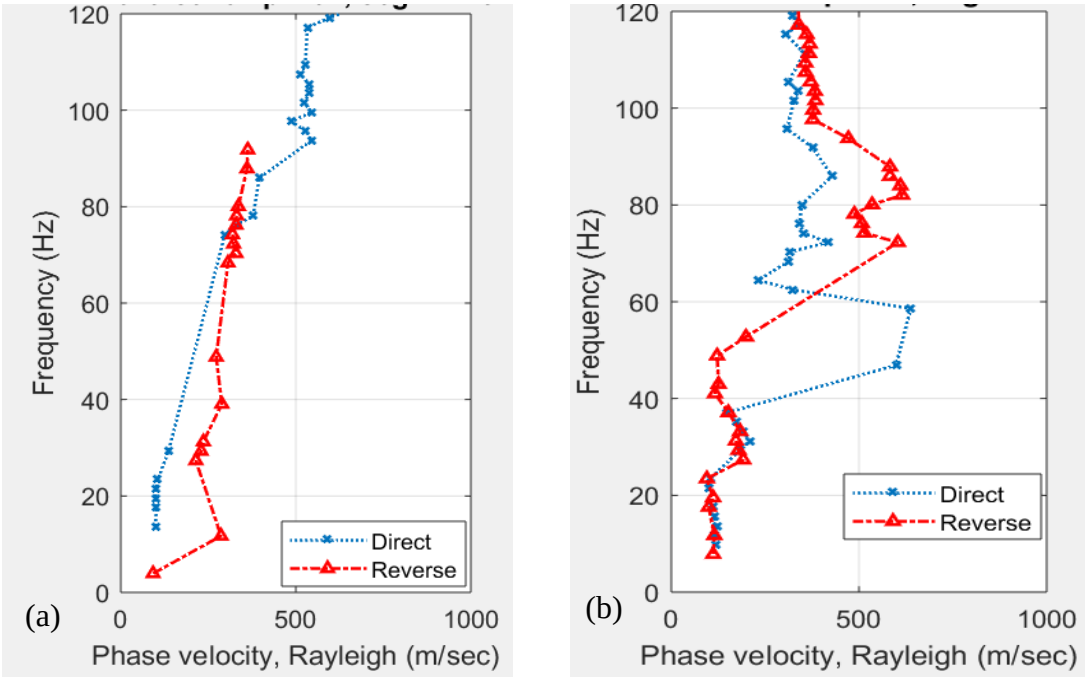

Figure A11. Dispersion curves for the third pulses in each direction (continuation) Figure (a) shows the dispersion curves for both directions between instruments #1 and #4, and Figure (b) shows the dispersion curves for both directions between instruments #2 and #3

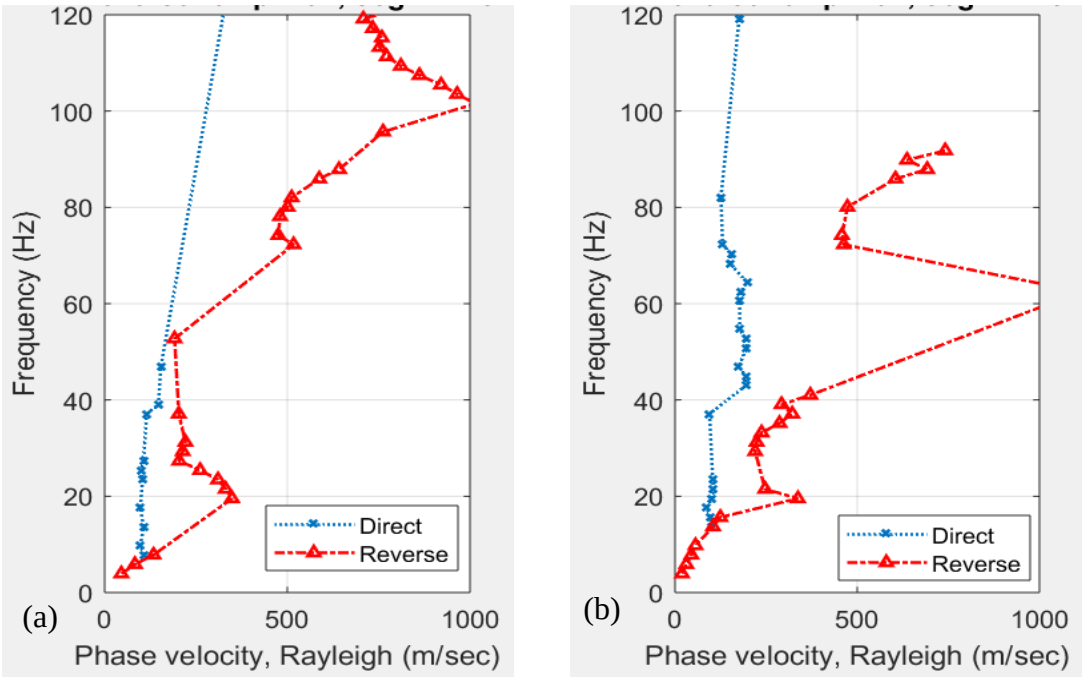

Figure A 12. Dispersion curves for the third pulses in each direction (continuation)
Figure (a) shows the dispersion curves for both directions between instruments #2 and #4, and Figure (b) shows the dispersion curves for both directions between instruments #3 and #4

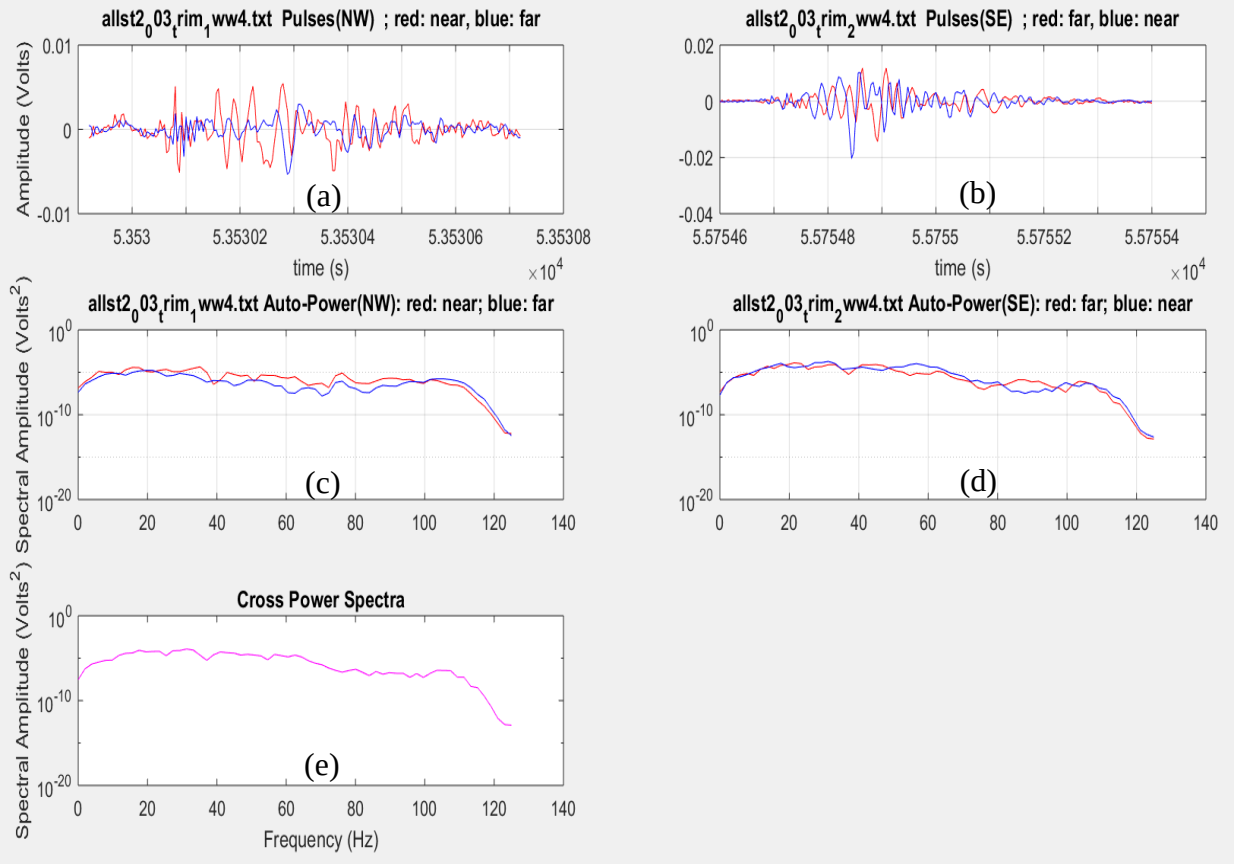

Figure A13. (a) Pulse #4 in the NW (A) direction, (b) Pulse #4 in the SE (B) direction, (c) Auto-power spectra in the NW (A) direction, (d) Auto-power spectra in the SE (B), and (e) shows the Cross power spectra

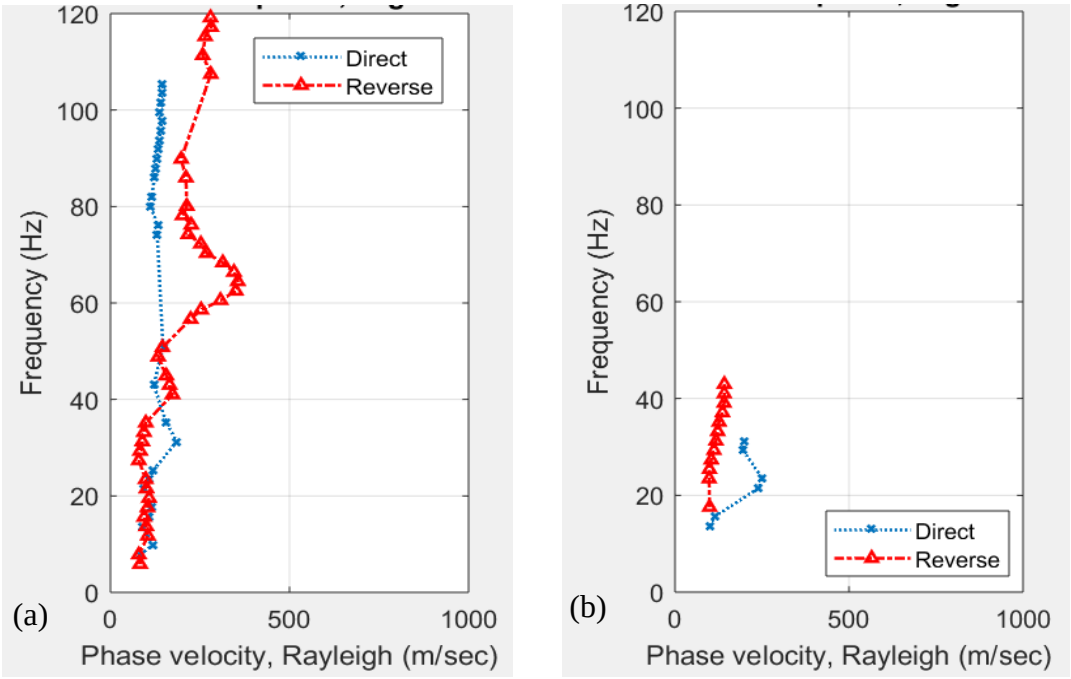

Figure A14. Dispersion curves for the fourth pulses in each direction, direct (A) and reverse (B) Figure (a) shows the dispersion curves for both directions between instruments #1 and #2, and Figure (b) shows the dispersion curves for both directions between instruments #1 and #3

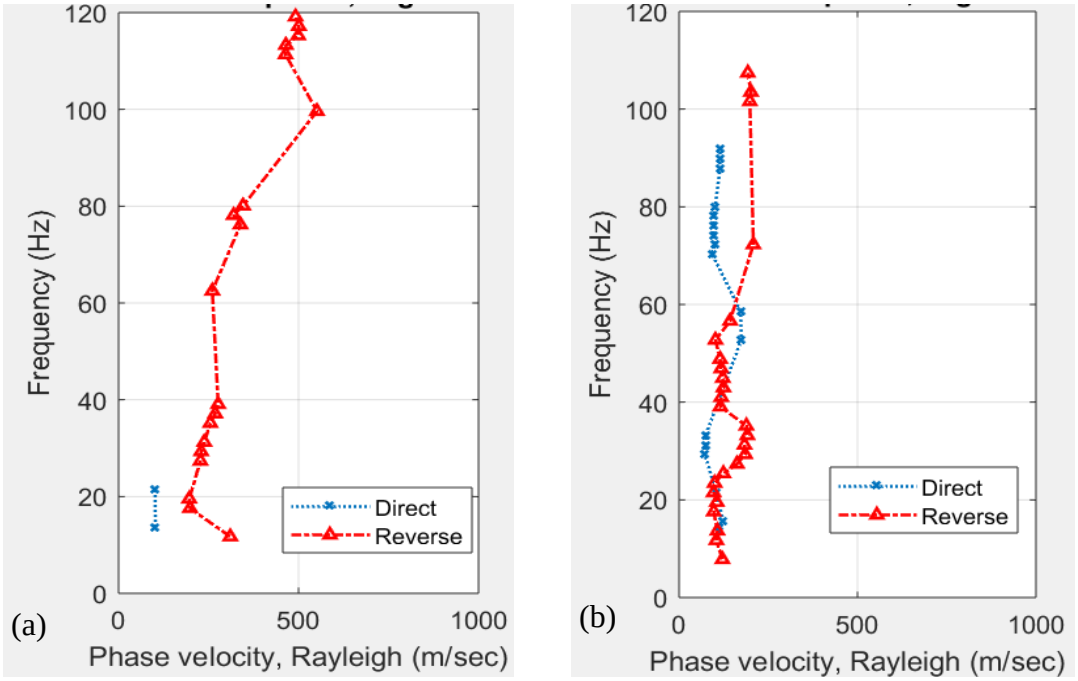

Figure A 15. Dispersion curves for the fourth pulses in each direction (continuation) Figure (a) shows the dispersion curves for both directions between instruments #1 and #4, and Figure (b) shows the dispersion curves for both directions between instruments #2 and #3

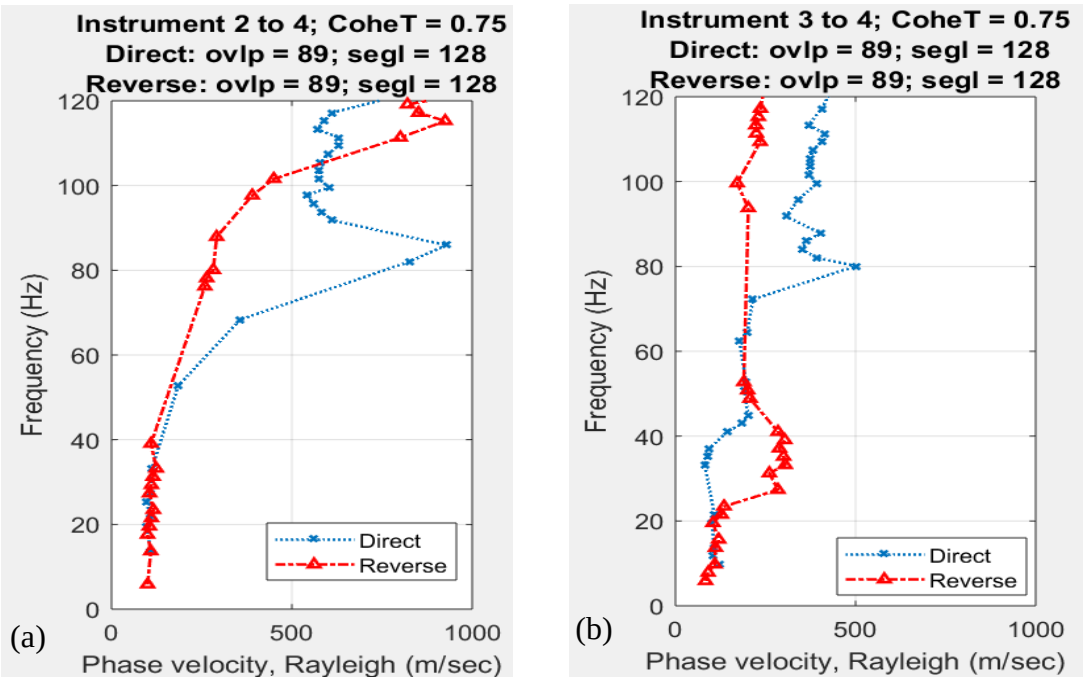

Figure A16. Dispersion curves for the fourth pulses in each direction (continuation)
Figure (a) shows the dispersion curves for both directions between instruments #2 and #4, and Figure (b) shows the dispersion curves for both directions between instruments #3 and #4

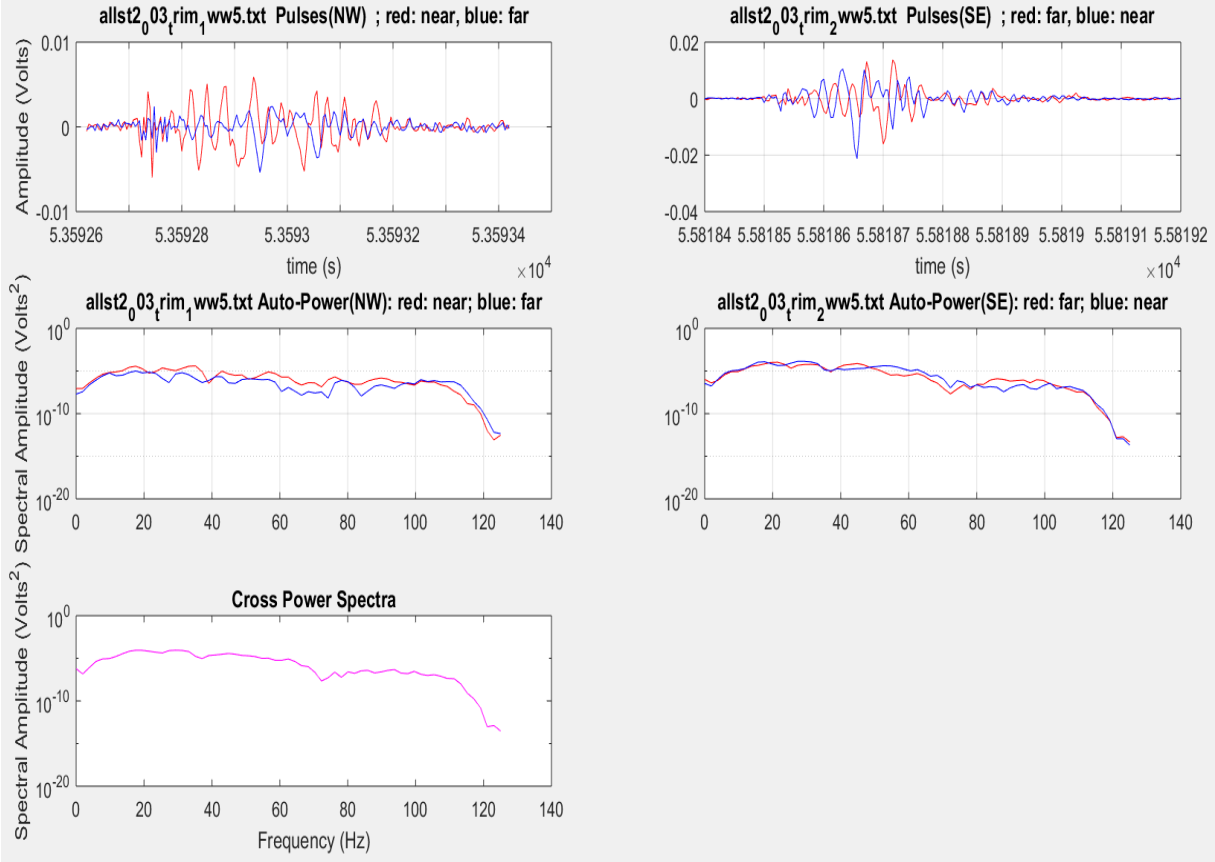

Figure A17. (a) Pulse #5 in the NW (A) direction, (b) Pulse #5 in the SE (B) direction, (c) Auto-power spectra in the NW (A) direction, (d) Auto-power spectra in the SE (B), and (e) shows the Cross power spectra

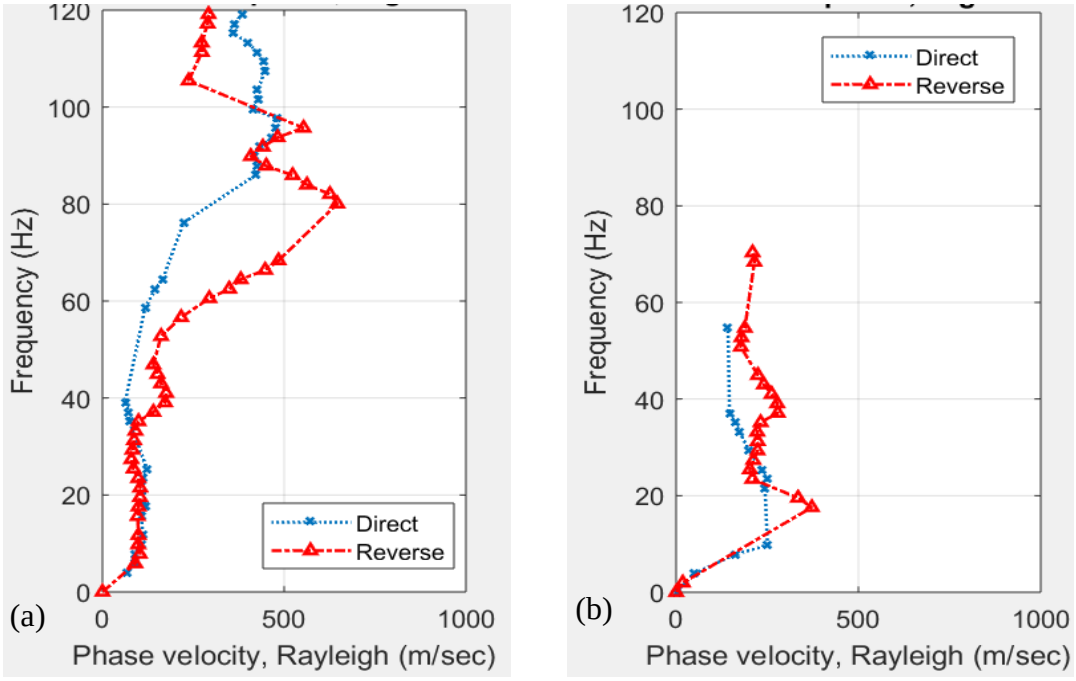

Figure A18. Dispersion curves for the fifth pulses in each direction, direct (A) and reverse (B)
Figure (a) shows the dispersion curves for both directions between instruments #1 and #2, and
Figure (b) shows the dispersion curves for both directions between instruments #1 and #3

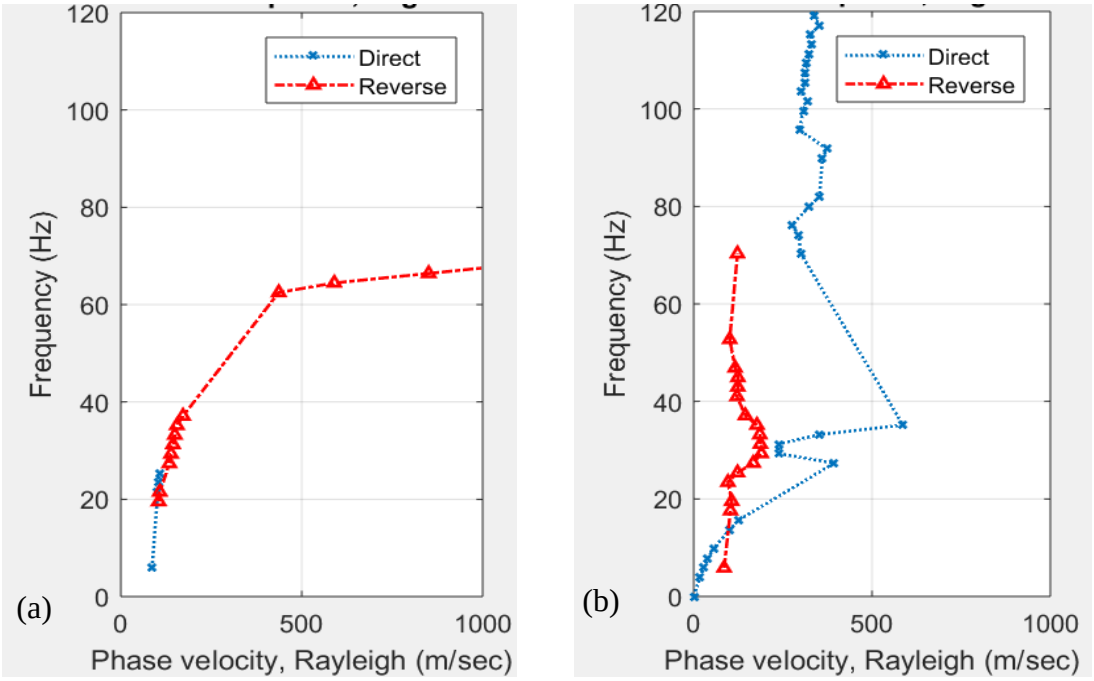

Figure A19. Dispersion curves for the fifth pulses in each direction (continuation)
Figure (a) shows the dispersion curves for both directions between instruments #1 and #4, and
Figure (b) shows the dispersion curves for both directions between instruments #2 and #3

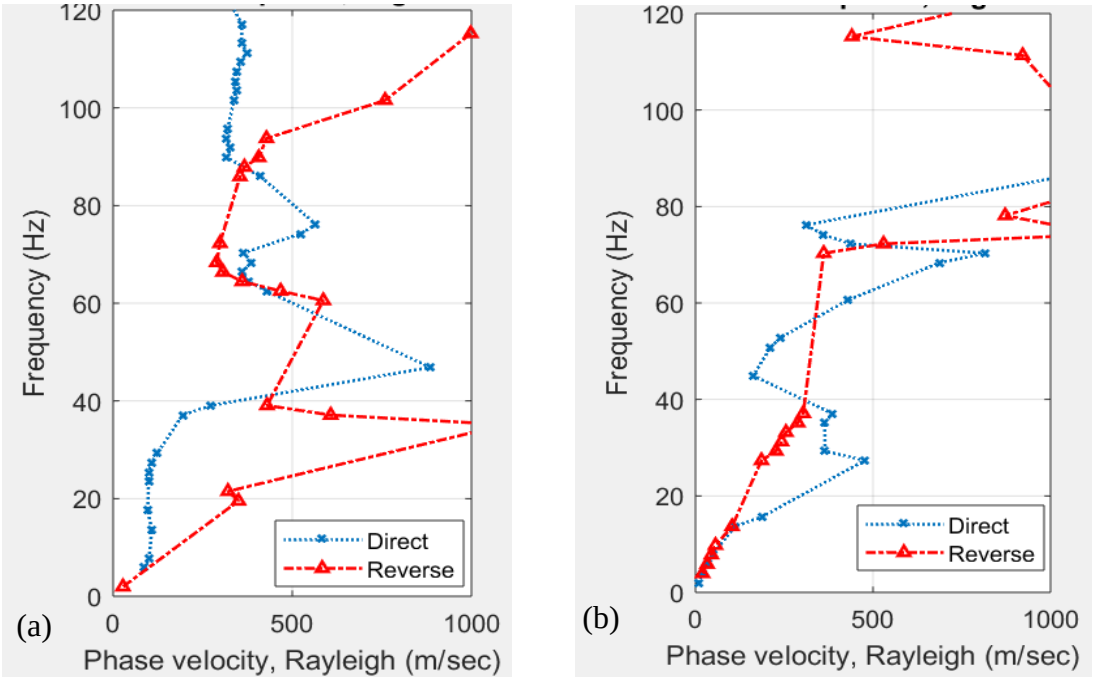

Figure A20. Dispersion curves for the fifth pulses in each direction (continuation)
Figure (a) shows the dispersion curves for both directions between instruments #2 and #4, and Figure (b) shows the dispersion curves for both directions between instruments #3 and #4

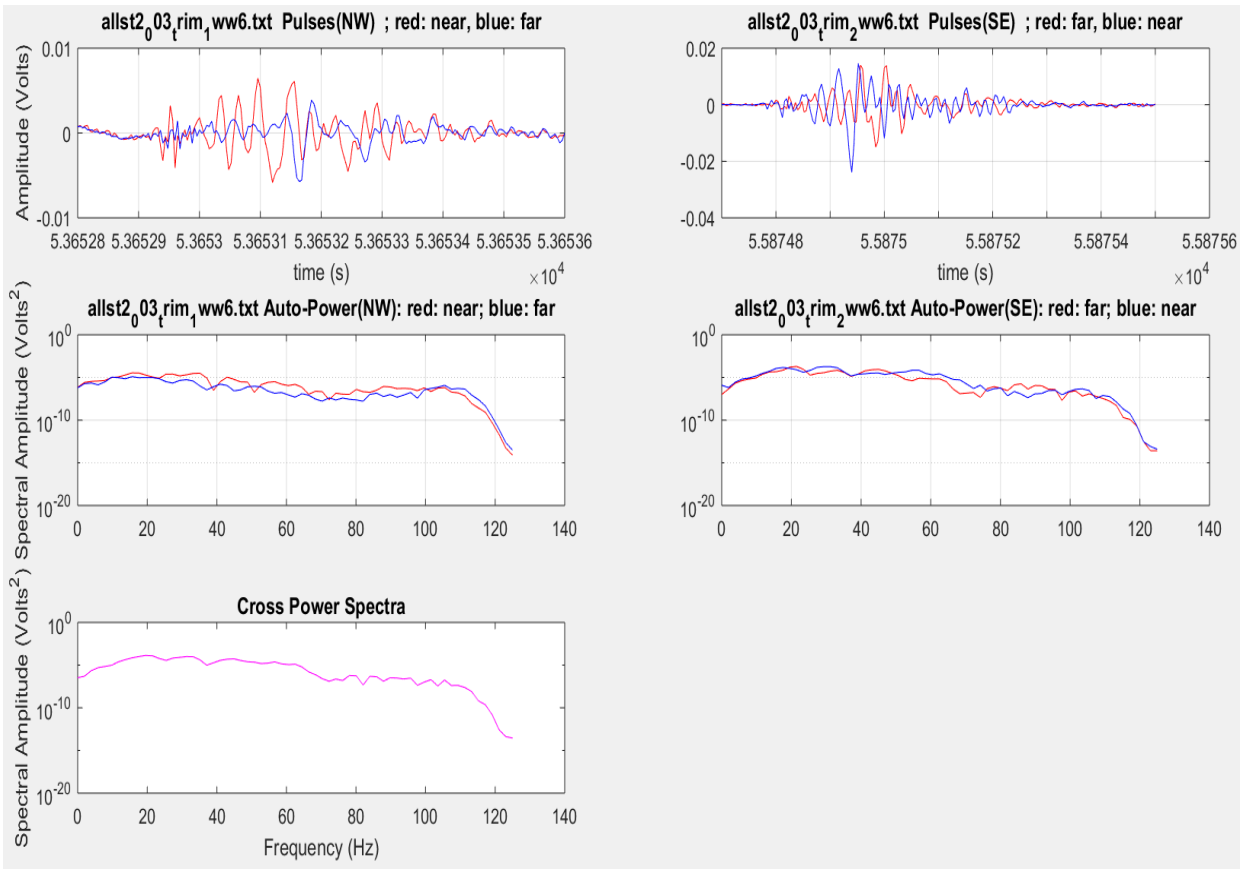

Figure A 21. (a) Pulse #6 in the NW (A) direction, (b) Pulse #6 in the SE (B) direction, (c) Auto-power spectra in the NW (A) direction, (d) Auto-power spectra in the SE (B), and (e) shows the Cross power spectra

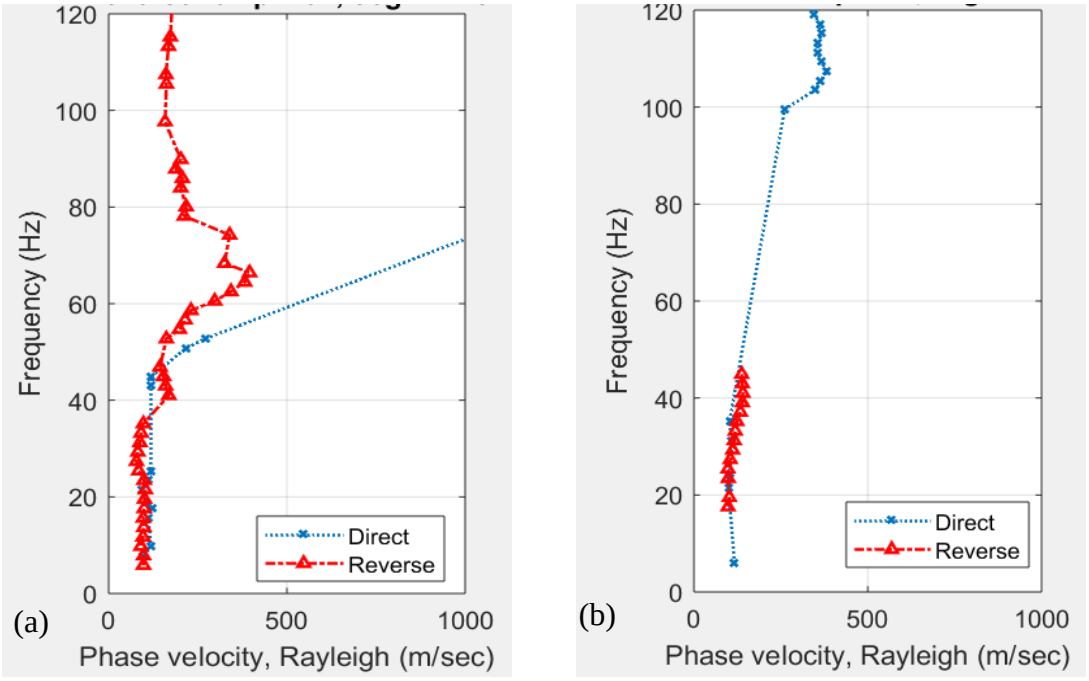

Figure A 22. Dispersion curves for the sixth pulses in each direction, direct (A) and reverse (B) Figure (a) shows the dispersion curves for both directions between instruments #1 and #2, and Figure (b) shows the dispersion curves for both directions between instruments #1 and #3

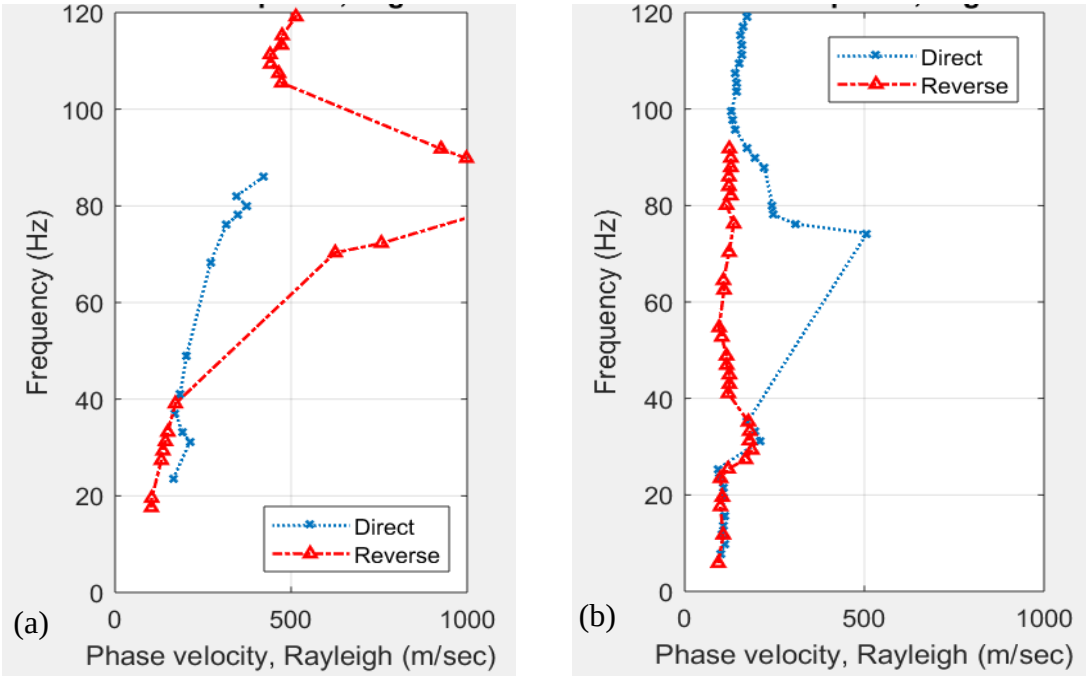

Figure A23. Dispersion curves for the sixth pulses in each direction (continuation) Figure (a) shows the dispersion curves for both directions between instruments #1 and #4, and Figure (b) shows the dispersion curves for both directions between instruments #2 and #3

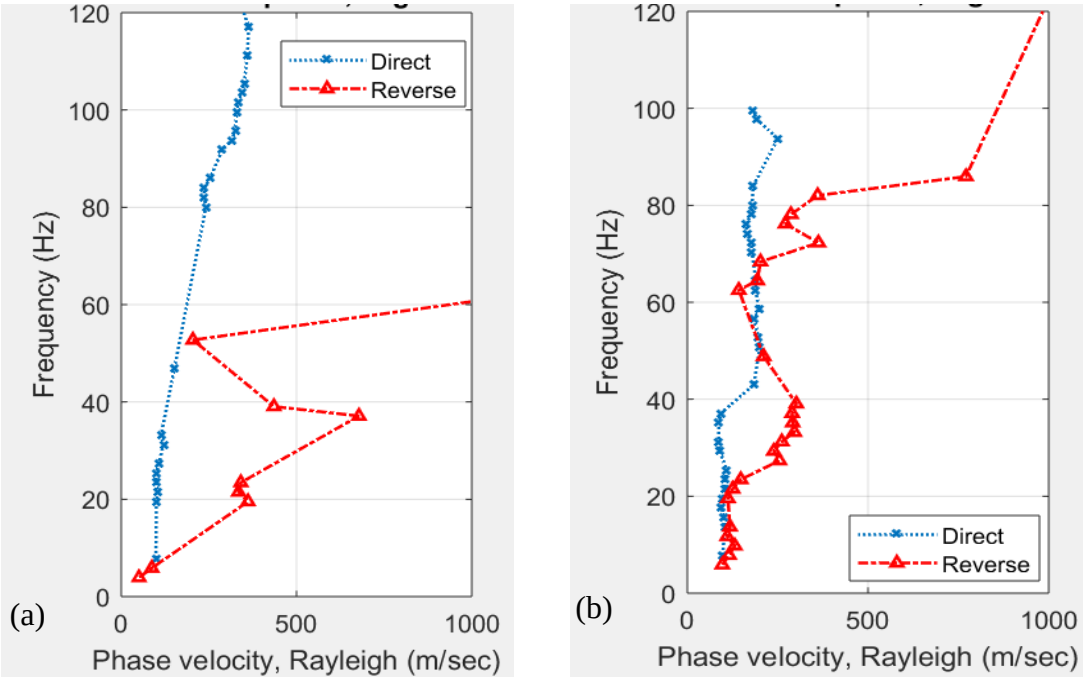

Figure A24. Dispersion curves for the sixth pulses in each direction (continuation)
Figure (a) shows the dispersion curves for both directions between instruments #2 and #4, and Figure (b) shows the dispersion curves for both directions between instruments #3 and #4

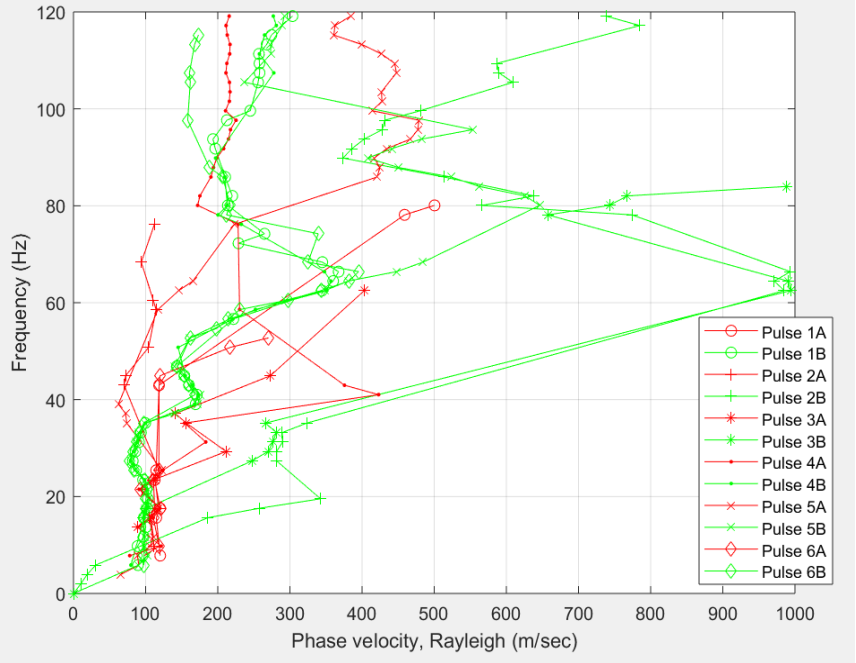

Figure A25. Dispersion curve between instruments #1 and #2

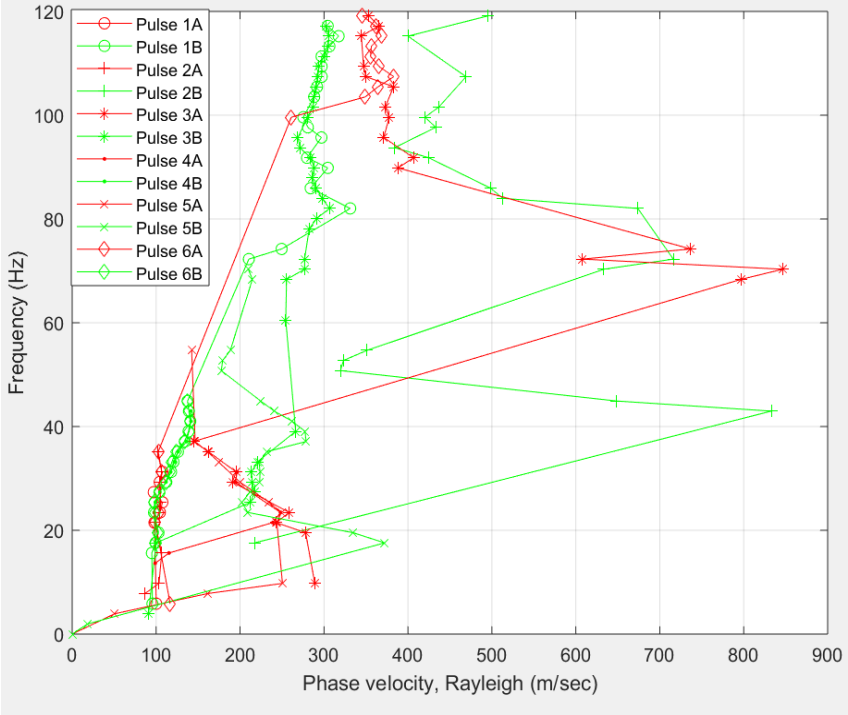

Figure A26. Dispersion curve between instruments #1 and #3

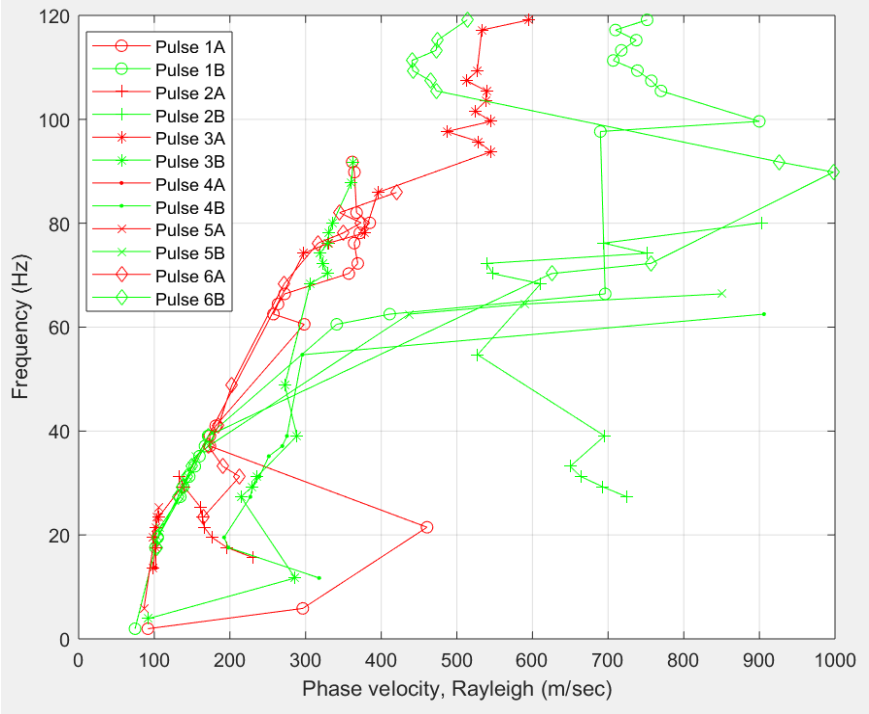

Figure A27. Dispersion curve between instruments #1 and #4

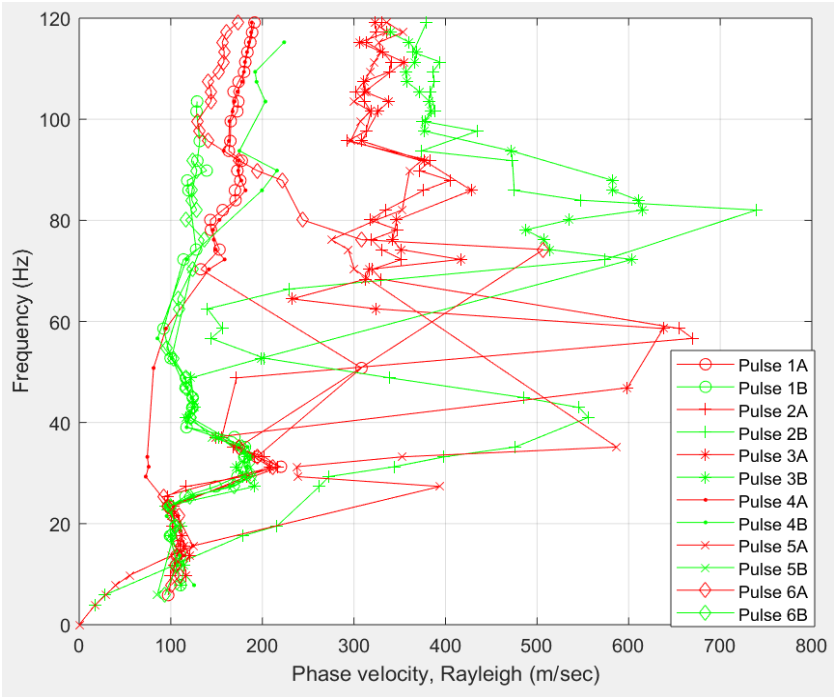

Figure A28. Dispersion curve between instruments #2 and #3

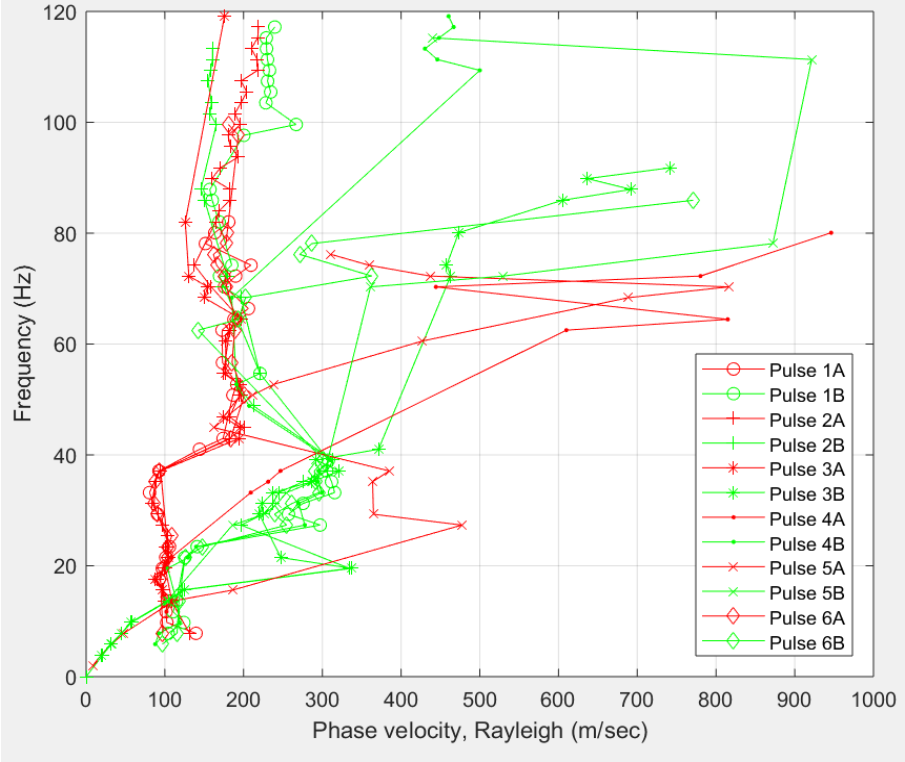

Figure A29. Dispersion curve between instruments #3 and #4

Code to Process the SASW data.

```
%-------------------------------------------------------------------------%
%               INCI 6110 - Engineering Seismology                        %
%               Code to Process SASW Data Test                            %
%                    Dr. Carlos Huertas                                   %
%-------------------------------------------------------------------------%
%                    Revised on May 2018                                  %
%                Used to Analyze Data Taken                               %
%               At UPRM Near Coliseo Mangual                              %
%-------------------------------------------------------------------------%
clear all; clc; close all
rad2deg=180/pi;     %%conversion factor radians to degrees

%-------------------------- Datos de Entrada -----------------------------%
frecmuestreo = 250;                          % Frecuencia de muestreo
ovlap = 0.5;                                 % Overlap portion for windows
ovlap_se = 0.5;                              % Overlap portion for windows
lengsegm = 128;                              % window lenght
lengsegm_se = 128;                           % window lenght
cohe_threshold = 0.75;                       % Coherence

%---------------------- Para cortar los ejes ----------------------------%

trim_f=120;                          % Cortar fecuencias
trim_w=30;                           % Cortar largos de ondas
trim_v=1000;                         % Cortar velocidades

%--------------------------- Archivo con datos----------------------------%

disp ('We  will work doing SASW, using .asc files, ');
disp ('Please, type the file name to work with (no extension)')
filename1 = input(' input_filename1 = ', 's');
filename2 = input(' input_filename2 = ', 's');

filename1 = ([filename1,'.txt']);                % Renaming by adding the extension
filename2 = ([filename2,'.txt']);                % Renaming by adding the extension

ds_source_nearsensor=3*24.384;
%---------------------------
for a = 2:4              %%2 a 4 (representan sensores 1-3) % First sensor to use (column)
   for b = a+1:5         %%3 a 5 (represetan sensores (2-4) % Second sensor to use (column)

      %------ Distancia entre sensores (editar)---------%
```

```
if (a == 2) && (b == 3),     ds = 4.04;   %1-2
elseif (a == 2) && (b == 4), ds = 7.72;   %1-3
elseif (a == 2) && (b == 5), ds = 11.79;  %1-4
elseif (a == 3) && (b == 4), ds = 3.73;   %2-3
elseif (a == 3) && (b == 5), ds = 7.80;   %2-4
elseif (a == 4) && (b == 5), ds = 4.06;   %3-4
end



%---------- Loading and correcting data from files ----------%
% File #1---
data1 = load (filename1);                    % Load file # 1 corresponding to direct hit
data1 = data1(1:end,:);                      % To trim portion of data if necesary
[r1,c1] = size(data1);                       % Number of rows and columns of file #1
m_data1 = mean(data1(:,:),1);                % Mean estimation of each column
data1 = [data1(:,1),data1(:,2)-m_data1(2),...      % Substraction of each with mean value
   data1(:,3)-m_data1(3),data1(:,4)-m_data1(4),...
   data1(:,5)-m_data1(5)];
data_2_use1 = [data1(:,1),data1(:,b),data1(:,a)];  % Selection of sensors

% File #2-----
data2 = load (filename2);                    % Load file2
data2 = data2(1:end,:);                      % Trim portion of data
[r2,c2] = size(data2);                       % Number of rows and columns of file2
m_data2 = mean(data2(:,:),1);                % Mean estimation of each column
data2 = [data2(:,1),data2(:,2)-m_data2(2),...      % Substraction of each with mean value
   data2(:,3)-m_data2(3),data2(:,4)-m_data2(4),...
   data2(:,5)-m_data2(5)];
data_2_use2 = [data2(:,1),data2(:,b),data2(:,a)];  % Selection of sensors


%---------- Graphing Signals in time domain ----------%

figure
subplot(3,2,1); plot(data_2_use1(:,1),data_2_use1(:,2),'r',
data_2_use1(:,1),data_2_use1(:,3),'b'); grid
xlabel('time (s)'); ylabel('Amplitude (Volts)'); title([filename1,'  Pulses(NW)  ; red: near,
blue: far'])
subplot(3,2,2); plot(data_2_use2(:,1),data_2_use2(:,2),'r',
data_2_use2(:,1),data_2_use2(:,3),'b'); grid;
xlabel('time (s)'); title([filename2,'  Pulses(SE)  ; red: far, blue: near'])

%---------- Power Spectra ----------%
```

```
%Segm. length (choose a sample number)
overlapi = floor(lengsegm*ovlap);                % Overlap number
labeoblap = num2str(overlapi);                   % label for plot
labeseglength = num2str(lengsegm);               % label for plot

%Segm. length (choose a sample number)
overlapi_se = floor(lengsegm_se*ovlap_se);       % Overlap number
labeoblap_se = num2str(overlapi_se);             % label for plot
labeseglength_se = num2str(lengsegm_se);         % label for plot

[da1da1,f1] = psd(data_2_use1(:,2),lengsegm,...  % Auto_power spectra for file 1 (near)
   frecmuestreo,hanning(lengsegm),...
   overlapi,'mean');
[da2da2,f2] = psd(data_2_use1(:,3),lengsegm,...
   frecmuestreo,hanning(lengsegm),...
   overlapi,'mean');                             % Auto_power spectra for file 1 (far)

[db1db1,f1_se] = psd(data_2_use2(:,2),lengsegm_se,...%Auto_power spectra for file 2
(near)
   frecmuestreo,hanning(lengsegm_se),...
   overlapi_se,'mean');
[db2db2,f2_se] = psd(data_2_use2(:,3),lengsegm_se,...%Auto_power spectra for file 2 (far)
   frecmuestreo,hanning(lengsegm_se),...
   overlapi_se,'mean');

%----------- Graphing Auto Power Spectra ------------------------%
subplot(3,2,3); semilogy(f1,da1da1,'r', f2,da2da2,'b'); grid; %hold on
ylabel('Spectral Amplitude (Volts^2)');
title([filename1,' Auto-Power(NW): red: near; blue: far']); %%','overlap: ',labeoblap,';
seglength: ',labeseglength])

subplot(3,2,4); semilogy(f1_se,db1db1,'r', f2_se,db2db2,'b'); grid; %hold on
title([filename2,' Auto-Power(SE): red: far; blue: near']); %%','overlap_se: ',labeoblap_se,';
seglength_se: ',labeseglength_se])

%%
%-------------------- Cross Power Spectra ------------------------%
[da1da2,f_a] = csd(data_2_use1(:,2),data_2_use1(:,3),... % X-power spectra file 1
   lengsegm,frecmuestreo,hanning(lengsegm),overlapi,'mean');
da1da2 = da1da2(1:end);                  % To remove data if necesarry
f_a = f_a(1:end);                        % To remove data if necesarry
[C_da1da2,f_c_a] = cohere(data_2_use1(:,2),...   % Coherence
   data_2_use1(:,3),lengsegm,...
   frecmuestreo,hanning(lengsegm),...
   overlapi,'mean');
```

```
C_da1da2 = C_da1da2(1:end);
f_c_a = f_c_a(1:end);
fas_da1da2 = angle(da1da2);
fas_da1da2_unwrap = unwrap(fas_da1da2,(5/7)*pi);    % ¿Porqué 5/7 de pi?

subplot(3,2,5); semilogy(f_a,abs(da1da2),'g'); grid; %hold on  % Graficado de Cross Power
Spectra


[db1db2,f_b] = csd(data_2_use2(:,3),data_2_use2(:,2),...  %X-power spectra
   lengsegm_se,frecmuestreo,hanning(lengsegm_se),...
   overlapi_se,'mean');
db1db2 = db1db2(1:end);
f_b = f_b(1:end);
[C_db1db2,f_c_b] = cohere(data_2_use2(:,3),data_2_use2(:,2),lengsegm_se,...
   frecmuestreo,hanning(lengsegm_se),overlapi_se,'mean');
C_db1db2 = C_db1db2(1:end);
f_c_b = f_c_b(1:end);
fas_db1db2=angle(db1db2);
fas_db1db2_unwrap=unwrap(fas_db1db2,(5/7)*pi); % ¿Porqué 5/7 de pi?

subplot(3,2,5); semilogy(f_b,abs(db1db2),'m');     % Graficado de Cross Power Spectra
segunda direccion
xlabel('Frequency (Hz)'); ylabel('Spectral Amplitude (Volts^2)');
title(['Cross Power Spectra']) %, NW:Green; overlap: ',labeoblap,' seglength:
',labeseglength,', SE:magenta; overlap_se: ',labeoblap_se,' seglength_se: ',labeseglength_se])

%%
%---------------------- Grafica de Coherencia y Fase ----------%
figure
subplot(4,1,1); df_f_c_a=f_c_a(2)-f_c_a(1);
line_colo_fa='r'; line_colo_ca='g'; line_type_b='-'; sibol_b='o'; line_width=1.25;
[a1,h11,h22]=plotyy(f_c_a(1:end),fas_da1da2(1:end)*rad2deg,...
   f_c_a(1:end), C_da1da2(1:end)); grid on;
set(get(a1(1),'Ylabel'),'String','Phase (Degrees)'); set(h11,'Color',line_colo_fa,...
   'LineStyle',line_type_b,'LineWidth',line_width,'Marker',sibol_b,'MarkerSize',1.5);
set(get(a1(2),'Ylabel'),'String','Coherence'); set(h22,'Color',line_colo_ca,'LineStyle',...
   line_type_b,'LineWidth',line_width);
ay11=gca; ylimits=get(ay11,'YLim'); yinc=(ylimits(2)-ylimits(1))/8;
set(ay11,'YTick',[ylimits(1):yinc:ylimits(2)]);
title([filename1,' NW, ','overlap: ',labeoblap,'; seglength: ',labeseglength])

subplot(4,1,2); plot(f_c_a(1:end),fas_da1da2(1:end)*rad2deg,'r',...
   f_c_a(1:end),fas_da1da2_unwrap(1:end)*rad2deg); grid on
```

```
    subplot(4,1,3);
    df_f_c_b=f_c_b(2)-f_c_b(1);
    line_colo_fb='r'; line_colo_cb='g'; line_type_r='-'; sibol_r='o'; line_width=1.25;
    [a1,h11,h22]=plotyy(f_c_b(1:end),fas_db1db2(1:end)*rad2deg,...
       f_c_b(1:end),C_db1db2(1:end)); grid on
    set(get(a1(1),'Ylabel'),'String','Phase (Degrees)'); set(h11,'Color',line_colo_fb,...
       'LineStyle',line_type_r,'LineWidth',line_width,'Marker',sibol_r,'MarkerSize',1.5);
    set(get(a1(2),'Ylabel'),'String','Coherence'); set(h22,'Color',line_colo_cb,'LineStyle',...
       line_type_r,'LineWidth',line_width);
    ay11=gca; ylimits=get(ay11,'YLim'); yinc=(ylimits(2)-ylimits(1))/8;
    set(ay11,'YTick',[ylimits(1):yinc:ylimits(2)]);
    title([filename2,' SE, ','overlap_se: ',labeoblap_se,'; seglength_se: ',labeseglength_se])
    xlabel('Frequency (Hz)')

    subplot(4,1,4); plot(f_c_b(1:end),fas_db1db2(1:end)*rad2deg,'r',...
       f_c_b(1:end),fas_db1db2_unwrap(1:end)*rad2deg); grid on
    %-----------------------------------------------------------------%
%%
    array_freq_cohe_phase_a=[f_c_a,C_da1da2,fas_da1da2_unwrap*rad2deg]; %array with:
freq, coherence,phase(in degrees) for "a"
    array_freq_cohe_phase_b=[f_c_b,C_db1db2,fas_db1db2_unwrap*rad2deg]; %array with:
freq, coherence,phase(in degrees) for "b"

    aa=sortrows(array_freq_cohe_phase_a,2);      %sorting the coherence for "a" in ascending
order
    bb=sortrows(array_freq_cohe_phase_b,2);      %sorting the coherence for "b" in ascending
order
    array_f_vraf=[]; array_f_vrbf=[];

    lab_cohere=num2str(cohe_threshold);
%%
    for icount = 1:length(aa)
       if aa(icount,2) >= cohe_threshold
          ta_f = abs(aa(icount,3))/(360*aa(icount,1));
          vra_f = ds/ta_f;
          wave_length_a=vra_f/aa(icount,1);
          array_f_vraf=[array_f_vraf;aa(icount,1),wave_length_a,vra_f,aa(icount,2)]; end
    end
    %%%%%%%%%%%%% Filtro para las longitudes de ondas %%%%%%%%%%%%
    icount_v_f1 = size(array_f_vraf,1);
    for icount=1:icount_v_f1
       if  array_f_vraf(icount,2) > (4.5*ds) | array_f_vraf(icount,2) < ds/3     %%% Eq-2.6, pag.
19, APPLICATIONS AND LIMITATIONS OF THE SPECTRAL-ANALYSIS-OF-SURFACE-
WAVES METHOD
```

```
% % % % %            if  array_f_vraf(icount,2) > (3*ds)      %%% Eq-2.12, pag. 20, APP. &
LIMIT. of SASW METHOD
            array_f_vraf(icount,:)=NaN;
         end
      end

%%%%%%%%%%%%%%%%%%%%%%%%%%%%%%%%%%%%%%%%%%%%%%%%%%%%
      srt_array_f_vraf=sortrows(array_f_vraf,1);
      srt_array_l_vraf=sortrows(array_f_vraf,2);
%%
      for icount= 1:length(bb)
         if bb(icount,2) >= cohe_threshold   %%select values w/coherence
            tb_f=abs(bb(icount,3))/(360*bb(icount,1));  %compuete travel time
            vrb_f=ds/tb_f;    %%cumpute phase velocity
            wave_length_b=vrb_f/bb(icount,1);   %compute wave-length
            array_f_vrbf=[array_f_vrbf;bb(icount,1),wave_length_b,vrb_f,bb(icount,2)]; end
      end
      %%%%%%%%%% Filtro para las longitudes de ondas %%%%%%%%%%%%%%%%
      icount_v_f1=size(array_f_vrbf,1);
      for icount=1:icount_v_f1
         % % % % %     if  wave_length_b(icount) > (3*(2*(str2num(filename2(5:6))))) |
wave_length_b(icount) < (str2num(filename2(5:6)));
         if  array_f_vrbf(icount,2) > (4.5*ds) | array_f_vrbf(icount,2) < ds/3;      % Eq-2.6, pag.
19, APPLICATIONS AND LIMITATIONS OF THE SPECTRAL-ANALYSIS-OF-SURFACE-
WAVES METHOD
% % % % %            if  array_f_vrbf(icount,2) > (3*ds)       %%% Eq-2.12, pag. 20, APP. &
LIMIT.  of SASW METHOD
            array_f_vrbf(icount,:)=NaN;
         end
      end

%%%%%%%%%%%%%%%%%%%%%%%%%%%%%%%%%%%%%%%%%%%%%%%%%%%%
      srt_array_f_vrbf=sortrows(array_f_vrbf,1); %sorting array frequemcyin ascending order as
a group.
      srt_array_l_vrbf=sortrows(array_f_vrbf,2); %sorting array wavelemgth in ascending order
as a group.
%%
      %%%%%%%%%% graficado de frecuencia y Wavelenght %%%%%%% % % figure(33)
      subplot(1,2,1)
      plot(srt_array_f_vraf(1:end,3),srt_array_f_vraf(1:end,1),':x',...                 %%%graficado
de frecuencia
         srt_array_f_vrbf(1:end,3),srt_array_f_vrbf(1:end,1),'r-.^',...
         'LineWidth',line_width,'MarkerSize',4); grid on, %%hold on
      xlim([0,trim_v]);ylim([0,trim_f]);                                %%%% Para cortar ejes de Y/X
      xlabel('Phase velocity, Rayleigh (m/sec)'), ylabel('Frequency (Hz)');
```

```
      legend('Direct','Reverse');
      title({['Instrument ',num2str(a-1),' to ',num2str(b-1),'; CoheT = ',lab_cohere];[' Direct: ovlp
= ',labeoblap,'; segl = ',labeseglength,]...
         ;['Reverse: ovlp = ',labeoblap_se,'; segl = ',labeseglength_se]})

      subplot(1,2,2); plot(srt_array_l_vraf(1:end,3),srt_array_l_vraf(1:end,2),':x',...
%%%graficado de  Wavelenght
         srt_array_l_vrbf(1:end,3),srt_array_l_vrbf(1:end,2),'r-.^','LineWidth',line_width,...
         'MarkerSize',4); grid on, axis ij, , %%hold on
      xlim([0,trim_v]);ylim([0,trim_w]);                                    %%%% Para
cortar ejes de Y/X
      xlabel('Phase velocity, Rayleigh (m/sec)'), ylabel('Wavelength (m)')
      legend('Direct','Reverse');
      title({['Instrument ',num2str(a-1),' to ',num2str(b-1),'; Coherence = ',lab_cohere];[' Direct:
ovlp = ',labeoblap,'; segl = ',labeseglength,]...
         ;['Reverse: ovlp = ',labeoblap_se,'; segl = ',labeseglength_se]})

      fileprueba1 = [filename1(17:20) '_cols_' num2str(a) '_and_' num2str(b) '_frec_a'];
      fileprueba2 = [filename1(17:20) '_cols_' num2str(a) '_and_' num2str(b) '_frec_b'];
      fileprueba3 = [filename1(17:20) '_cols_' num2str(a) '_and_' num2str(b) '_waveln_a'];
      fileprueba4 = [filename1(17:20) '_cols_' num2str(a) '_and_' num2str(b) '_waveln_b'];
      file2save1 = [srt_array_f_vraf(1:end,3),srt_array_f_vraf(1:end,1)];
      file2save2 = [srt_array_f_vrbf(1:end,3),srt_array_f_vrbf(1:end,1)];
      file2save3 = [srt_array_l_vraf(1:end,3),srt_array_l_vraf(1:end,2)];
      file2save4 = [srt_array_l_vrbf(1:end,3),srt_array_l_vrbf(1:end,2)];

      % num_decimals = 1;
      % file2save1 = round(file2save1.*(10^num_decimals))./(10^num_decimals);
      % file2save2 = round(file2save2.*(10^num_decimals))./(10^num_decimals);
      % file2save3 = round(file2save3.*(10^num_decimals))./(10^num_decimals);
      % file2save4 = round(file2save4.*(10^num_decimals))./(10^num_decimals);

      save(fileprueba1, 'file2save1', '-ascii');
      save(fileprueba2, 'file2save2', '-ascii');
      save(fileprueba3, 'file2save3', '-ascii');
      save(fileprueba4, 'file2save4', '-ascii');
   end
end
```

Program used to obtain the dispersion curve.

```
% Programa para graficar curvas de dispersion de todos los golpes juntos

% grafica los golpes directos y de reverza en figuras a parte.
%-------------------------------------------------------------------------%
clc; clear all; close all;
%-----------------------Entrar Datos-----------------------------------%

sms_f = 6.5;                    % para suavizar curva de frecuencia
sms_w = 6;                      % para suavizar curva de largos de ondas
source= 'Weight (all)';           % nombre de la fuente


wave_c = 125;                    % cortar largos de onda
frec_c = 60;                    % cortar frecuencias
vel_c = 1000;                    % cortar velocidades

path_to_save_disp_curv ='C:\Users\name\Desktop\SASW_WW\Dispcurves3\separadas\'
%-------------------------------------------------------------------------%

dat_a_f_s = [];
dat_b_f_s = [];
dat_a_f_1 = [];
dat_b_f_1 = [];

dat_a_w_s = [];
dat_b_w_s = [];
dat_a_w_1 = [];
dat_b_w_1 = [];

array_round_f = [];
array_round_w = [];
icount = 0;

array_dat_a_b_w=[];
nan_matrix_vel=[];


%-------- Leer y Crear Matriz con Nombres de Archivos


for i = 1:6                % Numero de Golpes (1-6)
    for j = 2:4            % Columnas 2 a 4 (representan sensores 1-3)
        for k = j+1%:5  % Columnas 3 a 5 (represetan sensores (2-4)
```

```
%%
            %%%%%%%%%%%%%%%% Frecuencias %%%%%%%%%%%%%%
            icount = icount + 1;
            filename_a_f = ['1ww' num2str(i),'_cols_' num2str(j) '_and_' num2str(k) '_frec_a'];
% Archivos de Frecuencias tiro directo (a)
            filename_b_f = ['1ww' num2str(i),'_cols_' num2str(j) '_and_' num2str(k) '_frec_b'];
% Archivos de Frecuencias tiro reversa (b)
            dat_a_f=load(filename_a_f,'-ascii');                              % Cargar Archivos
(a)
            dat_b_f=load(filename_b_f,'-ascii');                              % Cargas Archivos
(b)
            dat_a_f_s = [dat_a_f_s; dat_a_f];                                 % Crear Matriz con
todos los datos de Frecuencias (a)
            dat_b_f_s = [dat_b_f_s; dat_b_f];                                 % Crear Matriz con
todos los datos de Frecuencias (b)
            dat_a_f_1 = [dat_a_f_1; filename_a_f];                              % Crear Matriz
con nombre de archivos de Frecuencias (a)
            dat_b_f_1 = [dat_b_f_1; filename_b_f];                              % Crear Matriz
con nombre de archivos de Frecuencias (b)

            %%%%%%%%%%%%%%%%%%%%%% Wavelenght %%%%%%%%%%%%%%

            filename_a_w = ['1ww' num2str(i),'_cols_' num2str(j) '_and_' num2str(k) '_waveln_a'];
% Archivos de Largos de Onda tiro directo (a)
            filename_b_w = ['1ww' num2str(i),'_cols_' num2str(j) '_and_' num2str(k) '_waveln_b'];
% Archivos de Largos de Onda tiro directo (b)
            dat_a_w = load(filename_a_w,'-ascii');                              % Cargar
Archivos (a)
            dat_b_w = load(filename_b_w,'-ascii');                              % Cargas
Archivos (b)
            dat_a_w_s = [dat_a_w_s; dat_a_w];                                   % Crear Matriz
con todos los datos de Largos de Onda(a)
            dat_b_w_s = [dat_b_w_s; dat_b_w];                                   % Crear Matriz
con todos los datos de Largos de Onda(b)
            dat_a_w_1 = [dat_a_w_1; filename_a_w];                                % Crear
Matriz con nombre de archivos de largo de Onda (a)
            dat_b_w_1 = [dat_b_w_1; filename_b_w];                                % Crear
Matriz con nombre de archivos de largo de Onda (b)

      end
   end
end
%%%%%%%%%%%%%%%%%%%%%%%%%%%%%%%%%%%%%%%%%%%%%%
```

```
% % % % % dat_a_b_f = [dat_a_f_s; dat_b_f_s];                    % Matriz con todos
los datos (frecuencias)
% % % % % dat_a_b_w = [dat_a_w_s; dat_b_w_s];                    % Matriz con
todos los datos (Wavelenght)
% % % % %
% % % % %
% % % % % dat_a_b_ff = [dat_a_f_1;dat_b_f_1];                    % Matriz con todos
los nombres de archivos (frecuencias)
% % % % % dat_a_b_fw = [dat_a_w_1;dat_b_w_1];                    % Matriz con
todos los nombres de archivos (Wavelenght)

[rfa, cfa] = size (dat_a_f_1);                                  % Número de filas y columnas de la
matriz de nombres (frecuencias_a)
[rwa, cwa] = size (dat_a_w_1);                                  % Número de filas y columnas de la
matriz de nombres (Wavelenght_a)
[rfb, cfb] = size (dat_a_f_1);                                  % Número de filas y columnas de la
matriz de nombres (frecuencias_b)
[rwb, cwb] = size (dat_a_w_1);                                  % Número de filas y columnas de la
matriz de nombres (Wavelenght_b)
%% Computos relacionados a Wavelenght direccion a (directo)

num_dig=1;                                                      % Lugares decimales a tener datos
redondeados
dat_a_w_s(any(isnan(dat_a_w_s), 2), :) = [];                    % Para remover valores NaN de
los datos de Wavelenght
dat_a_w_s = round(dat_a_w_s.*(10^num_dig))./(10^num_dig);       % Redondeo de
valores de Wavelenght
[no_repeat_lamdas,m,n] = unique(dat_a_w_s(:,2), 'rows');        % Para remover valores
repetidos de Wavelenght
sort_lamdas_array = sort(dat_a_w_s(m,2),'ascend');              % Para organizar en orden
ascendiente los datos de Wavelenght
nan_matrix_vel=nan([length(sort_lamdas_array),rwa+3]);          % Construcción de
matriz de NaNs para Wavelenght con deasedo número de columnas

%%%%%%%%%%%%%% Para abrir archivos (Wvlng)%%%%%%%%%%%%%%

for icon=1:size(dat_a_w_1,1)                                    % Desde 1 hasta el largo de la matriz
de nombre (Wvln)
   temp_dat=load(dat_a_w_1(icon,:),'-ascii');                   % Cargar archivos Wvln
      temp_dat(any(isnan(temp_dat), 2), :) = [];                % Remover NaNs de archivos de
Wvln
      temp_dat = round(temp_dat*(10^num_dig))./(10^num_dig);    % Redondear alugares
decimales determinado por variable (num_dig)

      %%%%%%% Para lleanr matriz de NaNs %%%%%%%%%%%%%%%%%%%%
```

```
    for icon_posit=1:length(temp_dat);                    % Desde 1 hasta largo del archivo
cargado
       lamda_loc=sampnum_position(sort_lamdas_array,temp_dat(icon_posit,2));   % Llama a
función samp_num que asinga posicion
       nan_matrix_vel(lamda_loc,icon+1)=temp_dat(icon_posit,1);       % Llenar matriz de
NaNs con velocidades en su posicion
    end
end

%%%%%%%%%%%%%%%%%%%%%%%%%%%%%%%%%%%%%%%%%%%%%%%%


mean_vel=nanmean(nan_matrix_vel,2);                              % Determinar el promedio de
las velocidades que correponen a mismo Wvln
median_vel=nanmedian(nan_matrix_vel,2);                            % Determinar la media de las
velocidades que correponen a mismo Wvln

nan_matrix_vel(:,1)=sort_lamdas_array;                            % Llenar la matriz de NaNs con
las frecuencias unicas en primera columna
nan_matrix_vel(:,size(dat_a_w_1,1)+2)= mean_vel;                     % Llenar la matriz de NaNs
con los promedios en penultima columna
nan_matrix_vel(:,size(dat_a_w_1,1)+3)= median_vel;                     % Llenar la matriz de
NaNs con la media en la ultima columna


%%%%%%%%%% Para remover de la matriz de NaN Wvln  %%%%%%%%%%
for icount_remove=1:size(nan_matrix_vel,1)
if nan_matrix_vel(icount_remove,1) >= wave_c || nan_matrix_vel(icount_remove,1) <= 0;,
nan_matrix_vel(icount_remove,1)=NaN;
  nan_matrix_vel(icount_remove,:)=NaN;, end
end

%%%%%%%%%% Para remover de la matriz de datos Wvln  y velocidades%%%%%%%%
for icount_remove=1:size(dat_a_w_s,1)
if dat_a_w_s(icount_remove,2) >= wave_c || dat_a_w_s(icount_remove,1) >= vel_c ||
dat_a_w_s(icount_remove,1) <= 0;,  dat_a_w_s(icount_remove,2)=NaN;
  dat_a_w_s(icount_remove,:)=NaN;, end
end

for i=1:size(nan_matrix_vel,1)
     for j=2:size(nan_matrix_vel-3,2)
        if nan_matrix_vel(i,j)>=vel_c;,
           nan_matrix_vel(i,j)=NaN;
        end
```

```
        end
end

nan_matrix_vel(isnan(nan_matrix_vel(:,rwa+2)),:)=[];                    % Para remover las filas
con todos valores NaN

xi=nan_matrix_vel(:,1);                                                 % Datos de Wavelength
epsilon = ((xi(end)-xi(1))/(numel(xi)-1))^3/100;                        % Precision de ajuste
p=1/(1+epsilon*10^sms_w);                                               % Suavizado largos de ondas
xxi= nan_matrix_vel(1:length(nan_matrix_vel),1);                        % Valores de Wvln para
ajuste
ybad_mean=nan_matrix_vel(:,rwa+2);                                      % Valores promedios de
velocidad (penultima col)
ybad_median=nan_matrix_vel(:,rwa+3);                                    % Valores de mediana de
velocidad (ultima col)
yy_mean = csaps(xi,ybad_mean,p,xxi);                                    % Curva suavizada con los
promedios
yy_median = csaps(xi,ybad_median,p,xxi);

%%%%%%%%% Para remover de ajustes valores de Wvln mayores %%%%%%%%%%%
for icount_remove=1:length(xxi)
if xxi(icount_remove,1) >= wave_c || xxi(icount_remove,1) <= 0;,  xxi(icount_remove,1)=NaN;
   xxi(icount_remove,:)=NaN;, end
end

%%%%%%%%%%%%%%%%% Graficos Wvln %%%%%%%%%%%%%%%%%%%%
figure
plot(dat_a_w_s(:,1),dat_a_w_s(:,2),'rx');, hold on, grid on             % Grafica de todos los valores
de Wvln
axis ij
plot(nan_matrix_vel(:,rwa+2),nan_matrix_vel(:,1), '-g','LineWidth',1);, hold on, grid on     %
Grafica de los promedios
axis ij
plot(nan_matrix_vel(:,rwa+3),nan_matrix_vel(:,1), '-b','LineWidth',1); hold on, grid on      %
Grafica de las medianas
axis ij
plot(yy_mean, xxi, 'y', 'LineWidth', 2.5 );, hold on;, , grid on        % Curva suavizada de los
promedios
plot(yy_median, xxi, 'r', 'LineWidth', 2.5 );, hold on;, , grid on      % Curva suavizada de las
medianas
title({['Wavelength vs. Phase Velocity; Direct ', '; Source = ',source]});
legend('A','Mean','Median','Smoothed Mean','Smoothed Median');

   %-------------------------Para guardar-------------------------%
```

```
    sm_mean   = [xxi yy_mean];                    % matriz con largos de onda y promedio de
velocidades suavizada
    sm_median = [xxi yy_median];                  % Matriz con largos de onda y medianas de
velocidades suavizada
% % % %      save([path_to_save_disp_curv, 'dc_all_wv_a'],'nan_matrix_vel','-ascii')
% % % %      save([path_to_save_disp_curv, 'dc_rev_mean_wv_a'],'sm_mean','-ascii')
% % % %      save([path_to_save_disp_curv,'dc_rev_median_wv_a'],'sm_median','-ascii')


num_dig=1;                                        % Lugares decimales a tener datos
redondeados
dat_b_w_s(any(isnan(dat_b_w_s), 2), :) = [];                % Para remover valores NaN de
los datos de Wavelenght
dat_b_w_s = round(dat_b_w_s.*(10^num_dig))./(10^num_dig);        % Redondeo de
valores de Wavelenght
[no_repeat_lamdas,m,n] = unique(dat_b_w_s(:,2), 'rows');         % Para remover valores
repetidos de Wavelenght
sort_lamdas_array = sort(dat_b_w_s(m,2),'ascend');               % Para organizar en orden
ascendiente los datos de Wavelenght
nan_matrix_vel=nan([length(sort_lamdas_array),rwb+3]);           % Construcción de
matriz de NaNs para Wavelenght con deasedo número de columnas

%%%%%%%%%%%%%%% Para abrir archivos (Wvlng)%%%%%%%%%%%%%%

for icon=1:size(dat_b_w_1,1)                      % Desde 1 hasta el largo de la matriz
de nombre (Wvln)
   temp_dat=load(dat_b_w_1(icon,:),'-ascii');           % Cargar archivos Wvln
      temp_dat(any(isnan(temp_dat), 2), :) = [];        % Remover NaNs de archivos de
Wvln
      temp_dat = round(temp_dat*(10^num_dig))./(10^num_dig);     % Redondear alugares
decimales determinado por variable (num_dig)

      %%%%%%% Para lleanr matriz de NaNs%%%%%%%%%%%%%%%%%%%%%

      for icon_posit=1:length(temp_dat);              % Desde 1 hasta largo del archivo
cargado
         lamda_loc=sampnum_position(sort_lamdas_array,temp_dat(icon_posit,2));   % Llama a
función samp_num que asinga posicion
         nan_matrix_vel(lamda_loc,icon+1)=temp_dat(icon_posit,1);       % Llenar matriz de
NaNs con velocidades en su posicion
      end
end

%%%%%%%%%%%%%%%%%%%%%%%%%%%%%%%%%%%%%%%%%%%%%%%%%%%%%%%%
```

```
mean_vel=nanmean(nan_matrix_vel,2);                    % Determinar el promedio de
las velocidades que correponen a mismo Wvln
median_vel=nanmedian(nan_matrix_vel,2);                % Determinar la media de las
velocidades que correponen a mismo Wvln

nan_matrix_vel(:,1)=sort_lamdas_array;                 % Llenar la matriz de NaNs con
las frecuencias unicas en primera columna
nan_matrix_vel(:,size(dat_b_w_1,1)+2)= mean_vel;       % Llenar la matriz de NaNs
con los promedios en penultima columna
nan_matrix_vel(:,size(dat_b_w_1,1)+3)= median_vel;     % Llenar la matriz de
NaNs con la media en la ultima columna


%%%%%%%%%% Para remover de la matriz de NaN Wvln  %%%%%%%%%%
for icount_remove=1:length(nan_matrix_vel)
if nan_matrix_vel(icount_remove,1) >= wave_c || nan_matrix_vel(icount_remove,1) <= 0;,
nan_matrix_vel(icount_remove,1)=NaN;
  nan_matrix_vel(icount_remove,:)=NaN;, end
end

%%%%%%%%%% Para remover de la matriz de datos Wvln  y velocidades%%%%%%%%
for icount_remove=1:length(dat_b_w_s)
if dat_b_w_s(icount_remove,2) >= wave_c || dat_b_w_s(icount_remove,1) >= vel_c ;,
dat_b_w_s(icount_remove,2)=NaN;
  dat_b_w_s(icount_remove,:)=NaN;, end
end

for i=1:size(nan_matrix_vel,1)
      for j=2:size(nan_matrix_vel-3,2)
         if nan_matrix_vel(i,j)>=vel_c;,
            nan_matrix_vel(i,j)=NaN;
         end
      end
end

nan_matrix_vel(isnan(nan_matrix_vel(:,rwb+2)),:)=[];   % Para remover las filas
con todos valores NaN

xi=nan_matrix_vel(:,1);                                % Datos de Wavelength
epsilon = ((xi(end)-xi(1))/(numel(xi)-1))^3/100;       % Precision de ajuste
p=1/(1+epsilon*10^sms_w);                              % Suavizado largos de ondas
xxi= nan_matrix_vel(1:length(nan_matrix_vel),1);       % Valores de Wvln para
ajuste
```

```
ybad_mean=nan_matrix_vel(:,rwb+2);                    % Valores promedios de
velocidad (penultima col)
ybad_median=nan_matrix_vel(:,rwb+3);                  % Valores de mediana de
velocidad (ultima col)
yy_mean = csaps(xi,ybad_mean,p,xxi);                  % Curva suavizada con los
promedios
yy_median = csaps(xi,ybad_median,p,xxi);

%%%%% Para remover de ajustes valores de Wvln mayores %%%%%%%%%%%%
for icount_remove=1:length(xxi)
if xxi(icount_remove,1) >= wave_c || xxi(icount_remove,1) <= 0;,  xxi(icount_remove,1)=NaN;
   xxi(icount_remove,:)=NaN;, end
end

%%%%%%%%%%%%%%%%%% Graficos Wvln %%%%%%%%%%%%%%%%%%%%
figure
plot(dat_b_w_s(:,1),dat_b_w_s(:,2),'rx');, hold on, grid on          % Grafica de todos los valores
de Wvln
axis ij
plot(nan_matrix_vel(:,rwb+2),nan_matrix_vel(:,1), '-g','LineWidth',1);, hold on, grid on     %
Grafica de los promedios
axis ij
plot(nan_matrix_vel(:,rwb+3),nan_matrix_vel(:,1), '-b','LineWidth',1); hold on, grid on      %
Grafica de las medianas
axis ij
plot(yy_mean, xxi, 'y', 'LineWidth', 2.5 );, hold on;, , grid on       % Curva suavizada de los
promedios
plot(yy_median, xxi, 'r', 'LineWidth', 2.5 );, hold on;, , grid on      % Curva suavizada de las
medianas
xlabel('Phase velocity, Rayleigh (m/sec)'), ylabel('Wavelength (m)')
title({['Wavelength vs. Phase Velocity; Reverse ', '; Source = ',source]});
legend('B','Mean','Median','SmMean','SmMedian');

  %-------------------------Para guardar-------------------------%
    sm_mean   = [xxi yy_mean];                    % matriz con largos de onda y promedio de
velocidades suavizada
    sm_median = [xxi yy_median];                  % Matriz con largos de onda y medianas de
velocidades suavizada
% % % %       save([path_to_save_disp_curv, 'dc_all_wv_b'],'nan_matrix_vel','-ascii')
% % % %       save([path_to_save_disp_curv, 'dc_rev_mean_wv_b'],'sm_mean','-ascii')
% % % %       save([path_to_save_disp_curv, 'dc_rev_median_wv_b'],'sm_median','-ascii')
%% Computos relacionados a frecuencias

num_dig=1;                                        % Lugares decimales a tener datos
redondeados
```

```
dat_a_f_s(any(isnan(dat_a_f_s), 2), :) = [];                    % Para remover valores NaN de
los datos de Frecuencia
dat_a_f_s = round(dat_a_f_s.*(10^num_dig))./(10^num_dig);       % Redondeo de valores
de Frecuencia
[no_repeat_frec,m,n] = unique(dat_a_f_s(:,2), 'rows');          % Para remover valores
repetidos de Frecuencia
sort_frec_array = sort(dat_a_f_s(m,2),'ascend');                % Para organizar en orden
ascendiente los datos de Frecuencia
nan_matrix_vel_f=nan([length(sort_frec_array),rfa+3]);          % Construcción de matriz
de NaNs para Frecuencias con deasedo número de columnas

%%%%%%%%%%%%%%%% Para abrir archivos (frec)%%%%%%%%%%%%%%%%%

for icon=1:size(dat_a_f_1,1)                                    % Desde 1 hasta el largo de la matriz
de nombre (Frec)
   temp_dat_f=load(dat_a_f_1(icon,:),'-ascii');                 % Cargar archivos Frec
      temp_dat_f(any(isnan(temp_dat_f), 2), :) = [];            % Remover NaNs de archivos
de Frec
      temp_dat_f = round(temp_dat_f*(10^num_dig))./(10^num_dig);  % Redondear
alugares decimales determinado por variable (num_dig)

      %%%%%%%%%% Para llenar matriz de NaNs %%%%%%%%%%%%%%%%%%

      for icon_posit=1:length(temp_dat_f);                      % Desde 1 hasta largo del archivo
cargado
         frec_loc=sampnum_position(sort_frec_array, temp_dat_f(icon_posit,2));   % Llama a
función samp_num que asinga posicion
         nan_matrix_vel_f(frec_loc,icon+1)=temp_dat_f(icon_posit,1);     % Llenar matriz de
NaNs con velocidades en su posicion
      end
end

%%%%%%%%%%%%%%%%%%%%%%%%%%%%%%%%%%%%%%%%%%%%%%%%%%%%%%%%%

mean_vel_f=nanmean(nan_matrix_vel_f,2);                         % Determinar el promedio de
las velocidades que correponen a mismo Frec
median_vel_f=nanmedian(nan_matrix_vel_f,2);                     % Determinar la media de
las velocidades que correponen a mismo Frec

nan_matrix_vel_f(:,1)=sort_frec_array;                          % Llenar la matriz de NaNs con
las frecuencias unicas en primera columna
nan_matrix_vel_f(:,size(dat_a_f_1,1)+2)= mean_vel_f;            % Llenar la matriz de
NaNs con los promedios en penúltima columna
nan_matrix_vel_f(:,size(dat_a_f_1,1)+3)= median_vel_f;          % Llenar la matriz de
NaNs con la media en la última columna
```

```
%%%%%%%%%% Para remover de la matriz de NaN frecuencias  %%%%%%%%%%
for icount_remove=1:size(nan_matrix_vel_f,1)
if nan_matrix_vel_f(icount_remove,1) >= frec_c || nan_matrix_vel_f(icount_remove,1) <= 0;,
nan_matrix_vel_f(icount_remove,1)=NaN;
  nan_matrix_vel_f(icount_remove,:)=NaN;, end
end

%%%%%%% Para remover de la matris de datos frec mayores y velocidades %%%%%%%%
for icount_remove=1:size(dat_a_f_s,1)
if dat_a_f_s(icount_remove,2) >= frec_c || dat_a_f_s(icount_remove,1) >= vel_c ||
dat_a_f_s(icount_remove,1) <= 0;,  dat_a_f_s(icount_remove,2)=NaN;
  dat_a_f_s(icount_remove,:)=NaN;, end
end

for i=1:size(nan_matrix_vel_f,1)
       for l=2:size(nan_matrix_vel_f-3,2)
          if nan_matrix_vel_f(i,l)>=vel_c;,
             nan_matrix_vel_f(i,l)=NaN;
          end
       end
end
nan_matrix_vel_f(isnan(nan_matrix_vel_f(:,rfa+2)),:)=[];                  % Para remover las
filas con todos valores NaN
xi_f=nan_matrix_vel_f(:,1);                                    % Datos de Frecuencia
epsilon_f = ((xi_f(end)-xi_f(1))/(numel(xi_f)-1))^3/100;              % Precisión de ajuste
% % % % % p =  1 - 1/(1+epsilon);
p_f=1/(1+epsilon_f*10^sms_f);                                  % Suavizado frecuencia
xxi_f= nan_matrix_vel_f(1:size(nan_matrix_vel_f,1),1);                % Valores de Wvln para
ajuste
ybad_mean_f=nan_matrix_vel_f(:,rfa+2);                            % Valores promedios de
velocidad (penúltima col)
ybad_median_f=nan_matrix_vel_f(:,rfa+3);                          % Valores de mediana de
velocidad (última col)
yy_mean_f = csaps(xi_f,ybad_mean_f,p_f,xxi_f);                    % Curva suavizada con los
promedios
yy_median_f = csaps(xi_f,ybad_median_f,p_f,xxi_f);                % Curva suavizada con las
medianas

%%%%%%% Para remover de ajustes valores de frecuencia %%%%%%%%%%%%%%%
for icount_remove=1:length(xxi_f)
if xxi_f(icount_remove,1) >= frec_c | xxi_f(icount_remove,1) <= 0;,
xxi_f(icount_remove,1)=NaN;
```

```
   xxi_f(icount_remove,:)=NaN;, end
end

%%%%%%%%%%% Graficos Wvln %%%%%%%%%%%%%%%%%%%%%%
figure
   plot(dat_a_f_s(:,1),dat_a_f_s(:,2),'rx');, hold on, grid on            % Grafica de todos los valores
de Wvln
   plot(nan_matrix_vel_f(:,rfa+2),nan_matrix_vel_f(:,1), '-g','LineWidth',1);, hold on, grid on
% Grafica de los promedios
   plot(nan_matrix_vel_f(:,rfa+3),nan_matrix_vel_f(:,1), '-b','LineWidth',1); hold on, grid on
% Grafica de las medianas
   plot(yy_mean_f, xxi_f, 'y', 'LineWidth', 2.5 );, hold on;, , grid on   % Curva suavizada de los
promedios
   plot(yy_median_f, xxi_f, 'r', 'LineWidth', 2.5 );, hold on;, , grid on  % Curva suavizada de las
medianas
   xlabel('Phase velocity, Rayleigh (m/sec)'), ylabel('Frequency (Hz)');
   title({['Frequency vs. Phase Velocity; Direct ', '; Source = ',source], ''})
   legend('A','Mean','Median','Smoothed Mean','Smoothed Median');

%-------------------------Para guardar-------------------------%
    sm_mean   = [xxi_f yy_mean_f];                    % matriz con largos de onda y promedio de
velocidades suavizada
    sm_median = [xxi_f yy_median_f];                   % Matriz con largos de onda y medianas
de velocidades suavizada
    %%save([path_to_save_disp_curv, 'dc_all_freq_a'],'nan_matrix_vel','-ascii')
    save([path_to_save_disp_curv, 'dc_rev_mean_freq_a'],'sm_mean','-ascii')
    save([path_to_save_disp_curv, 'dc_rev_median_freq_a']','sm_median','-ascii')

num_dig=1;                                             % Lugares decimales a tener datos
redondeados
dat_b_f_s(any(isnan(dat_b_f_s), 2), :) = [];                    % Para remover valores NaN de
los datos de Frecuencia
dat_b_f_s = round(dat_b_f_s.*(10^num_dig))./(10^num_dig);          % Redondeo de
valores de Frecuencia
[no_repeat_frec,m,n] = unique(dat_b_f_s(:,2), 'rows');             % Para remover valores
repetidos de Frecuencia
sort_frec_array = sort(dat_b_f_s(m,2),'ascend');                % Para organizar en orden
ascendiente los datos de Frecuencia
nan_matrix_vel_f=nan([length(sort_frec_array),rfb+3]);             % Construcción de matriz
de NaNs para Frecuencias con deasedo número de columnas

%%%%%%%%%%%%%%%%%% Para abrir archivos (frec)%%%%%%%%%%%%%%%

for icon=1:size(dat_b_f_1,1)                           % Desde 1 hasta el largo de la matriz
de nombre (Frec)
```

```
   temp_dat_f=load(dat_b_f_1(icon,:),'-ascii');                    % Cargar archivos Frec
      temp_dat_f(any(isnan(temp_dat_f), 2), :) = [];                 % Remover NaNs de archivos
de Frec
      temp_dat_f = round(temp_dat_f*(10^num_dig))./(10^num_dig);        % Redondear
alugares decimales determinado por variable (num_dig)

      %%%%%% Para llenar matriz de NaNs %%%%%%%%%%%%%%%%%%%%%%

      for icon_posit=1:length(temp_dat_f);                        % Desde 1 hasta largo del archivo
cargado
         frec_loc=sampnum_position(sort_frec_array, temp_dat_f(icon_posit,2));   % Llama a
función samp_num que asinga posicion
         nan_matrix_vel_f(frec_loc,icon+1)=temp_dat_f(icon_posit,1);     % Llenar matriz de
NaNs con velocidades en su posicion
      end
end

%%%%%%%%%%%%%%%%%%%%%%%%%%%%%%%%%%%%%%%%%%%%%%%%%%%%%%%%

mean_vel_f=nanmean(nan_matrix_vel_f,2);                          % Determinar el promedio de
las velocidades que correponen a mismo Frec
median_vel_f=nanmedian(nan_matrix_vel_f,2);                       % Determinar la media de
las velocidades que correponen a mismo Frec

nan_matrix_vel_f(:,1)=sort_frec_array;                           % Llenar la matriz de NaNs con
las frecuencias unicas en primera columna
nan_matrix_vel_f(:,size(dat_b_f_1,1)+2)= mean_vel_f;               % Llenar la matriz de
NaNs con los promedios en penúltima columna
nan_matrix_vel_f(:,size(dat_b_f_1,1)+3)= median_vel_f;             % Llenar la matriz de
NaNs con la media en la última columna



%%%%%%%%%% Para remover de la matriz de NaN frecuencias  %%%%%%%%%%
for icount_remove=1:size(nan_matrix_vel_f,1)
if nan_matrix_vel_f(icount_remove,1) >= frec_c || nan_matrix_vel_f(icount_remove,1) <= 0;,
nan_matrix_vel_f(icount_remove,1)=NaN;
  nan_matrix_vel_f(icount_remove,:)=NaN;, end
end

%%%%%% Para remover de la matris de datos frec mayores y velocidades %%%%%%%%
for icount_remove=1:size(dat_b_f_s,1)
if dat_b_f_s(icount_remove,2) >= frec_c || dat_b_f_s(icount_remove,1) >= vel_c ||
dat_b_f_s(icount_remove,1) <= 0;,  dat_b_f_s(icount_remove,2)=NaN;
  dat_b_f_s(icount_remove,:)=NaN;, end
```

```
end

for i=1:size(nan_matrix_vel_f,1)
        for l=2:size(nan_matrix_vel_f-3,2)
           if nan_matrix_vel_f(i,l)>=vel_c;,
              nan_matrix_vel_f(i,l)=NaN;
           end
        end
end
nan_matrix_vel_f(isnan(nan_matrix_vel_f(:,rfb+2)),:)=[];                    % Para remover las
filas con todos valores NaN
xi_f=nan_matrix_vel_f(:,1);                                          % Datos de Frecuencia
epsilon_f = ((xi_f(end)-xi_f(1))/(numel(xi_f)-1))^3/100;                 % Precisión de ajuste
% % % % % p =  1 - 1/(1+epsilon);
p_f=1/(1+epsilon_f*10^sms_f);                                        % Suavizado frecuencia
xxi_f= nan_matrix_vel_f(1:size(nan_matrix_vel_f,1),1);                   % Valores de Wvln para
ajuste
ybad_mean_f=nan_matrix_vel_f(:,rfb+2);                               % Valores promedios de
velocidad (penúltima col)
ybad_median_f=nan_matrix_vel_f(:,rfb+3);                             % Valores de mediana de
velocidad (última col)
yy_mean_f = csaps(xi_f,ybad_mean_f,p_f,xxi_f);                       % Curva suavizada con los
promedios
yy_median_f = csaps(xi_f,ybad_median_f,p_f,xxi_f);                   % Curva suavizada con las
medianas

%%%%%%%%%% Para remover de ajustes valores de frecuencia %%%%%%%%%%%%%
for icount_remove=1:length(xxi_f)
if xxi_f(icount_remove,1) >= frec_c | xxi_f(icount_remove,1) <= 0;,
xxi_f(icount_remove,1)=NaN;
  xxi_f(icount_remove,:)=NaN;, end
end

%%%%%%%%%%%%%%%%%%%% Graficos Wvln %%%%%%%%%%%%%%%%%%
figure
   plot(dat_b_f_s(:,1),dat_b_f_s(:,2),'rx');, hold on, grid on          % Grafica de todos los valores
de Wvln
   plot(nan_matrix_vel_f(:,rfb+2),nan_matrix_vel_f(:,1), '-g','LineWidth',1);, hold on, grid on
% Grafica de los promedios
   plot(nan_matrix_vel_f(:,rfb+3),nan_matrix_vel_f(:,1), '-b','LineWidth',1); hold on, grid on
% Grafica de las medianas
   plot(yy_mean_f, xxi_f, 'y', 'LineWidth', 2.5 );, hold on;, , grid on   % Curva suavizada de los
promedios
   plot(yy_median_f, xxi_f, 'r', 'LineWidth', 2.5 );, hold on;, , grid on  % Curva suavizada de las
medianas
```

```
    xlabel('Phase velocity, Rayleigh (m/sec)'), ylabel('Frequency (Hz)');
    title({['Frequency vs. Phase Velocity: Reverse ', '; Source = ',source], ''})
    legend('B','Mean','Median','Smoothed Mean','Smoothed Median');

%-------------------------Para guardar-------------------------%
     sm_mean   = [xxi_f yy_mean_f];                    % matriz con largos de onda y promedio de
velocidades suavizada
     sm_median = [xxi_f yy_median_f];          % Matriz con largos de onda y medianas de
velocidades suavizada
     %%save([path_to_save_disp_curv, 'dc_freq_b'],'nan_matrix_vel','-ascii')
     save([path_to_save_disp_curv, 'dc_rev_mean_freq_b'],'sm_mean','-ascii')
     save([path_to_save_disp_curv, 'dc_rev_median_freq_b'],'sm_median','-ascii')
```

Appendix B

SPT Method

Standard Penetration Test (SPT), is an in-situs and invasive procedure that provides a soil sample. The SPT results used in this investigation were obtained from a study performed by Burgos et al., 2015 (Figure B1).

The drilling method used by Burgos et al. (2015)was the hollow stem auger. To take a sample, a borehole was made. The ASTM-D1586 (2008) say that the sample had to be taken using a split-barrel sampler with an inside diameter of 1-1/2 in or 1-3/8 in. The samplers were driven in the soil dropping a 140lb hammer from a height of 30in. The blow count of the split-barrel sampler were recorded every time it reached 6 inches, until a total of 18 inches were obtained, (ASTM-D1586, 2008). First, samples were taken every two feet until the borehole reached 6 feet, for borings 11 and 12. Then a sample was taken every 2 to 3 feet. The procedure was repeated until a depth of 20 feet or 25 feet was reached. Figure B2 shows the resulting information for the boring log 11, 12 and 13.

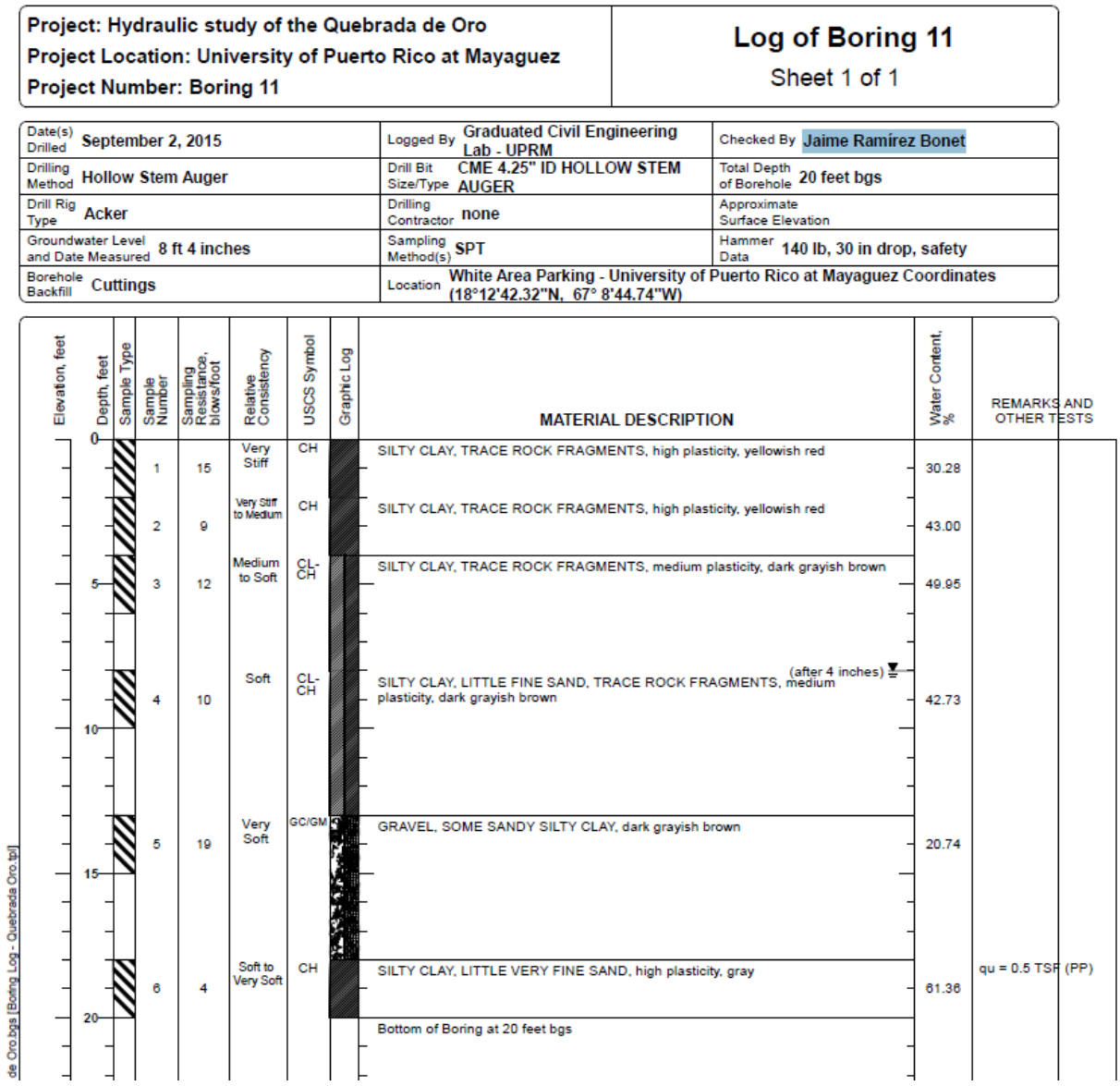

Figure B1. SPT results for boring 11 (Burgos et al., 2015)

Based on the information presented in borings 11, 12 and 13 a profile of N-values vs. depth was created as presented in Figure B2. Figure B3 shows the locations where the boring logs where made.

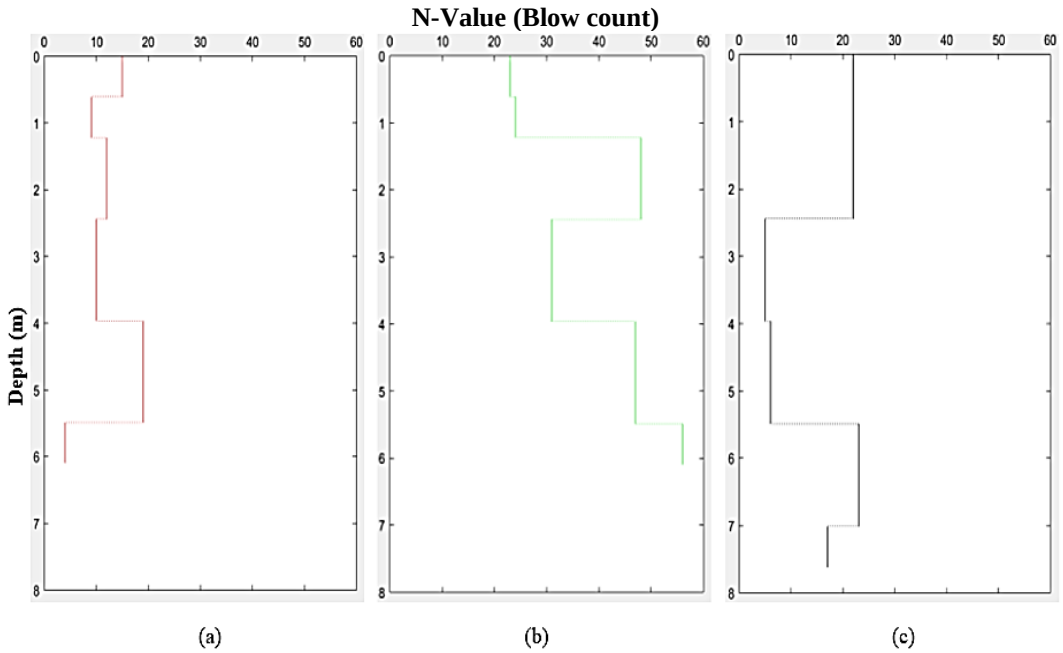

Figure B2. N-value vs. Depth, (a) Boring Log #11, (b) Boring Log #12 and (c) Boring Log #13

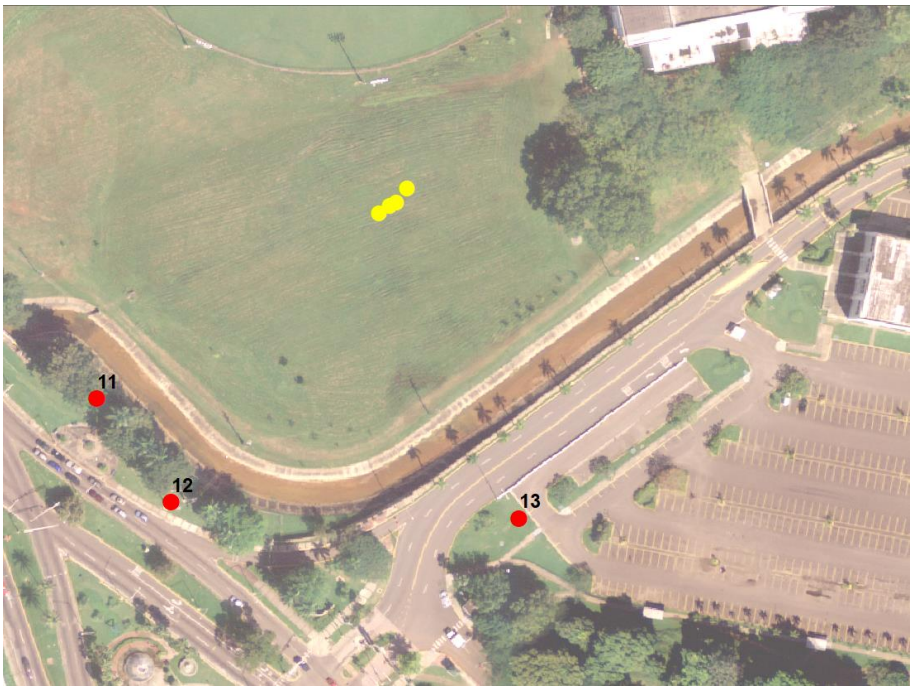

Figure B3. Location of the bore-hole of SPT results (red) and study area (yellow)

Appendix C

This appendix provides the results/plots and the MatLab code for the Horizontal and Vertical Spectral Ratio (HVSR) – Nakamura method.

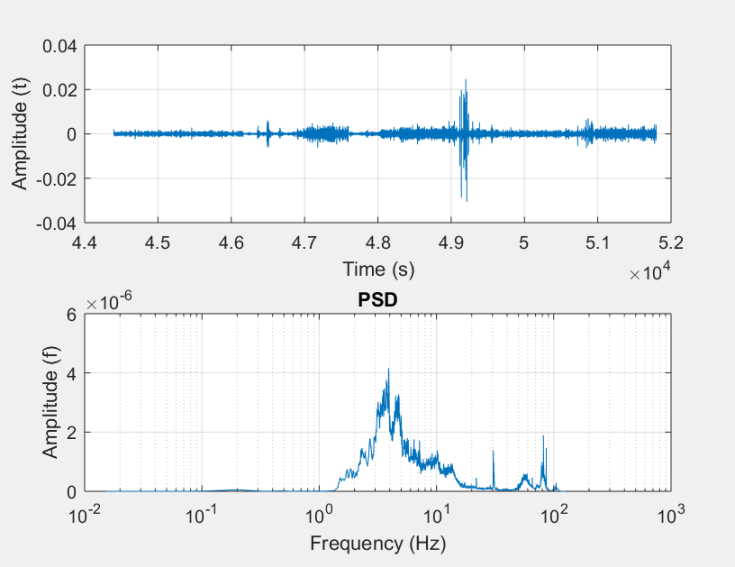

Figure C1. (a) Recorded signal, and (b) power spectral density for instrument #1 in the horizontal direction, H1 (EW)

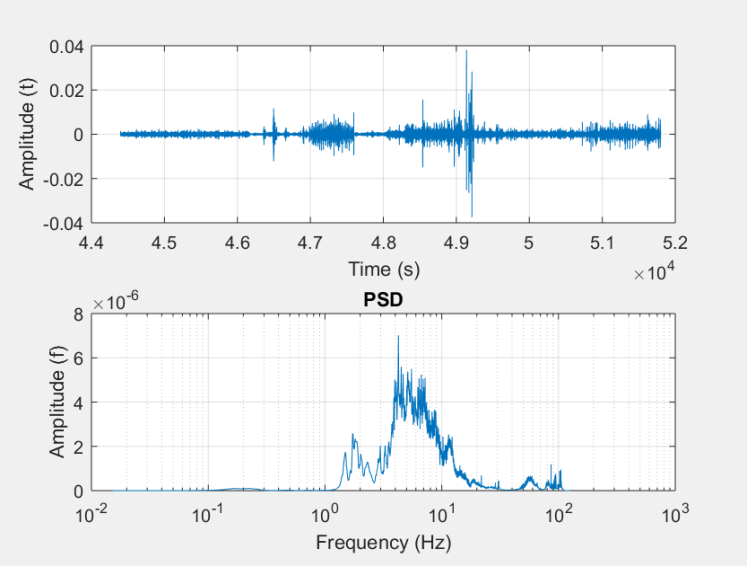

Figure C2. (a) Recorded signal, and (b) power spectral density for instrument #1 in the horizontal direction, H1 (NS)

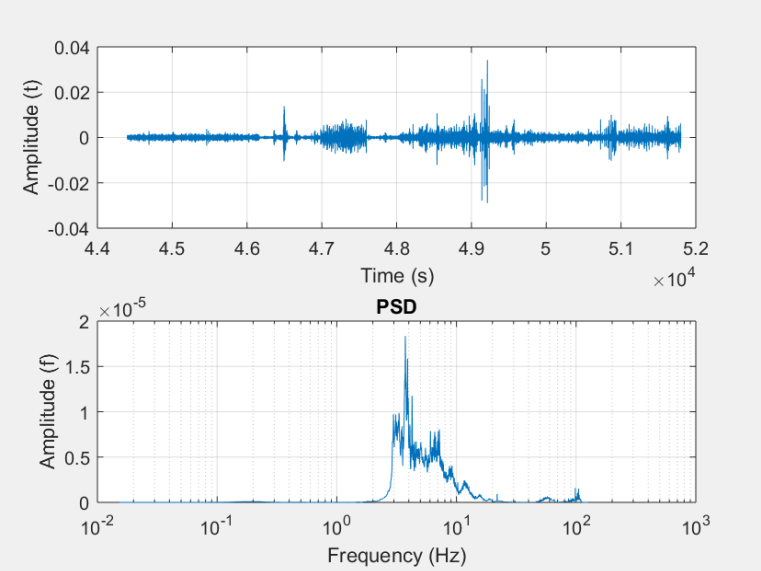

Figure C3. (a) Recorded signal, and (b) power spectral density for instrument #1 in the vertical direction (depth)

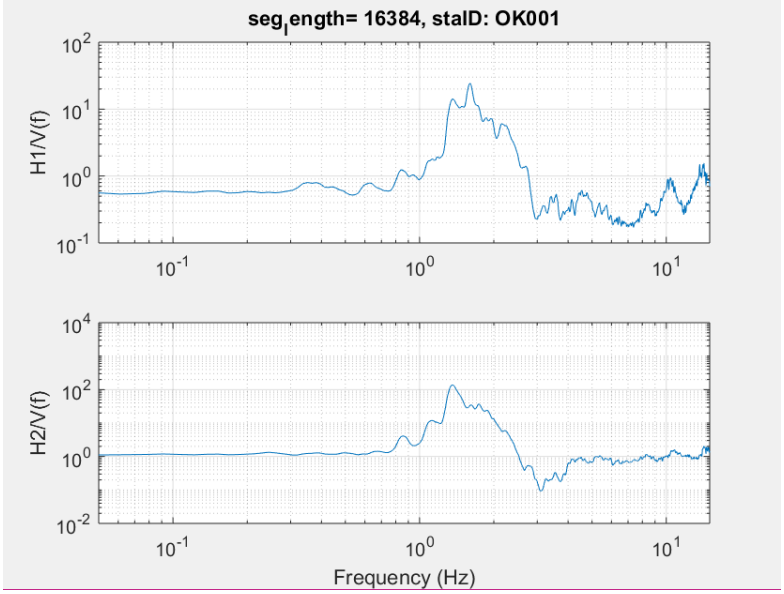

Figure C4. Fourier spectral quotients for both horizontal directions (instrument #1)

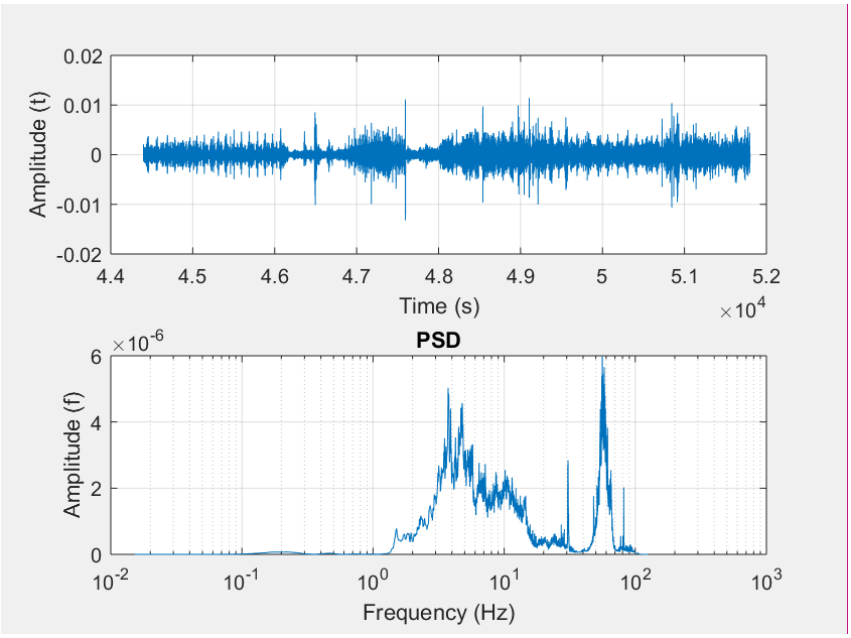

Figure C5. (a) Recorded signal, and (b) power spectral density for instrument #2 in the horizontal direction, H1 (EW)

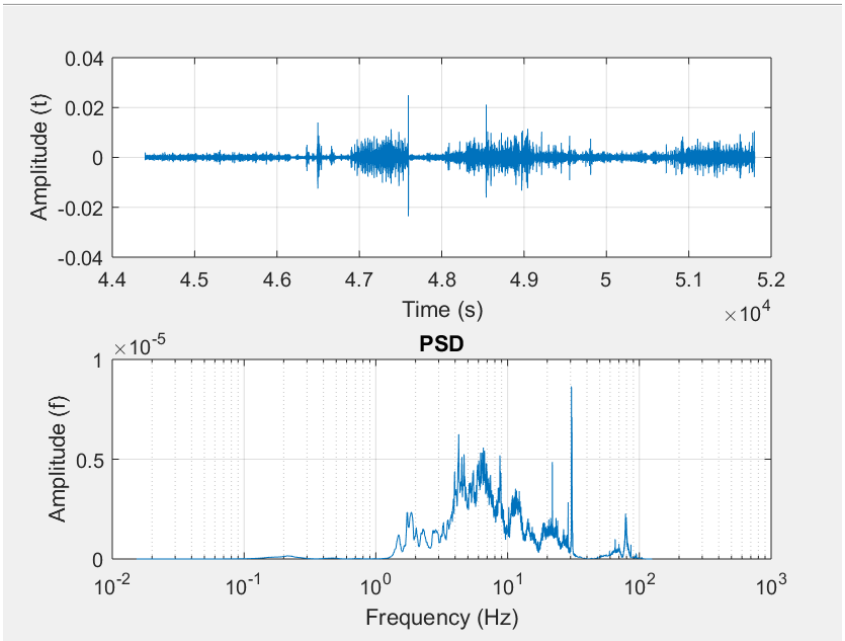

Figure C6. (a) Recorded signal, and (b) power spectral density for instrument #2 in the horizontal direction, H2 (NS)

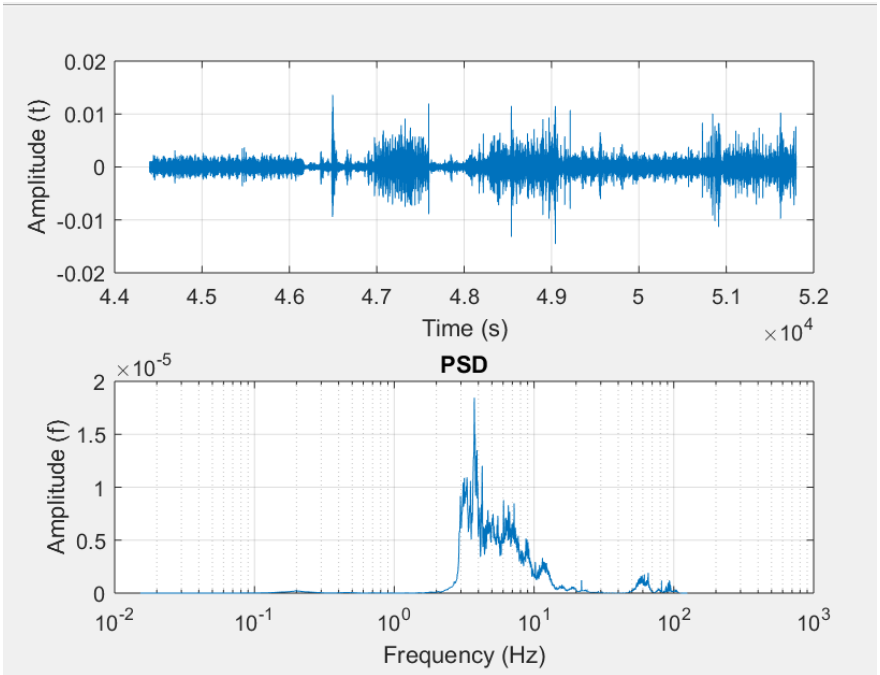

Figure C7. (a) Recorded signal, and (b) power spectral density for instrument #2 in the vertical direction (depth)

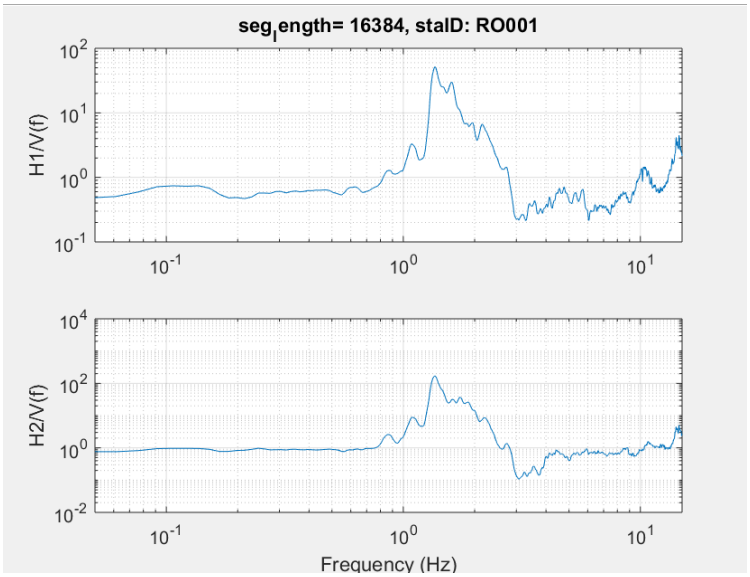

Figure C8. Fourier spectral quotients for both horizontal directions (instrument #2)

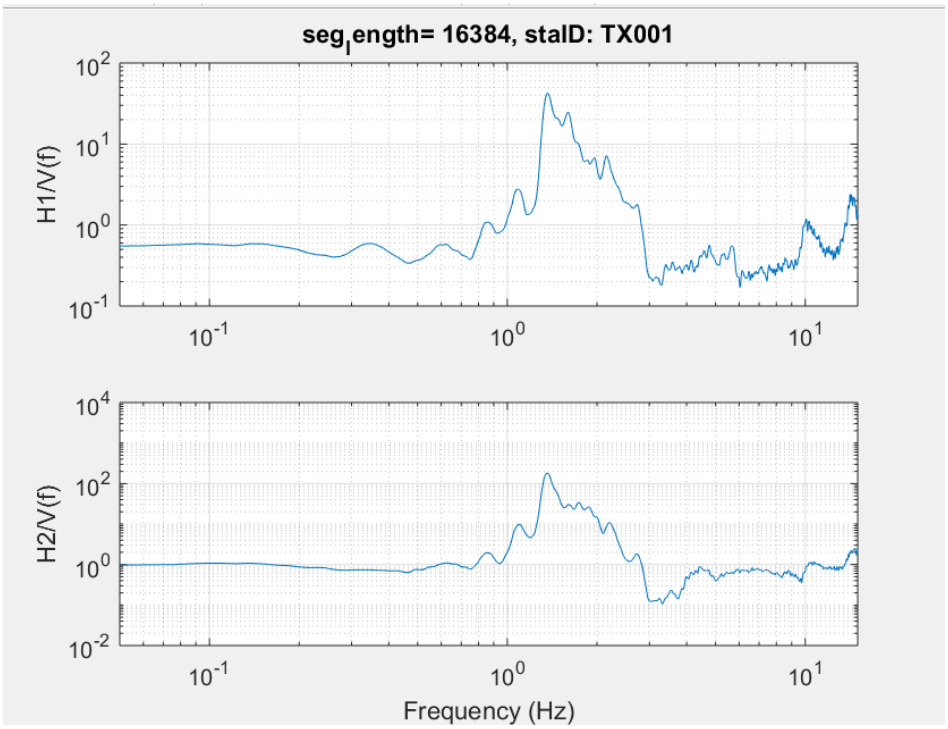

Figure C9. Fourier spectral quotients for both horizontal directions (instrument #3)

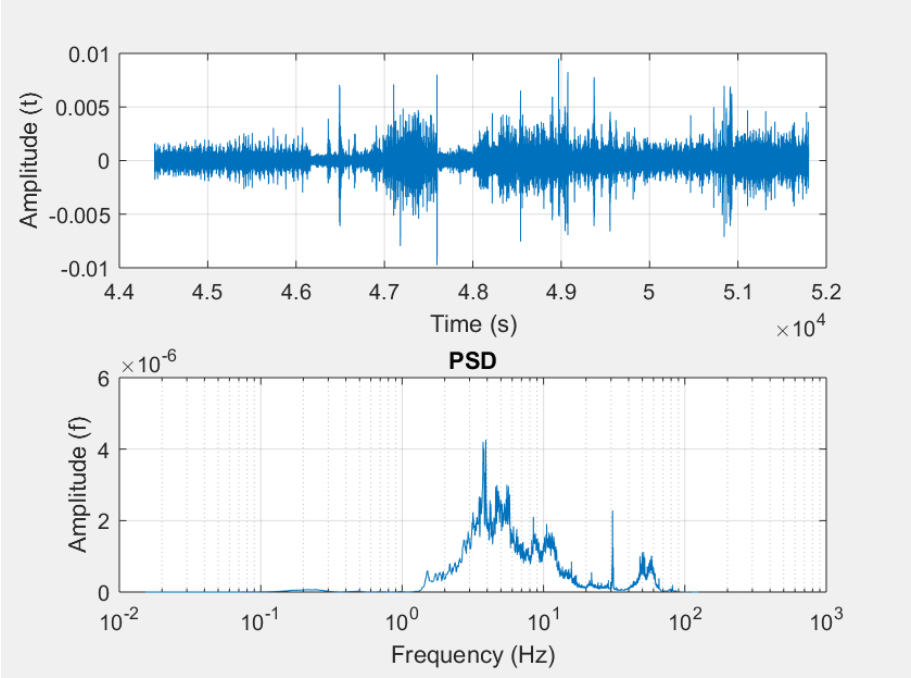

Figure C10. (a) Recorded signal, and (b) power spectral density for instrument #4 in the horizontal direction, H1 (EW)

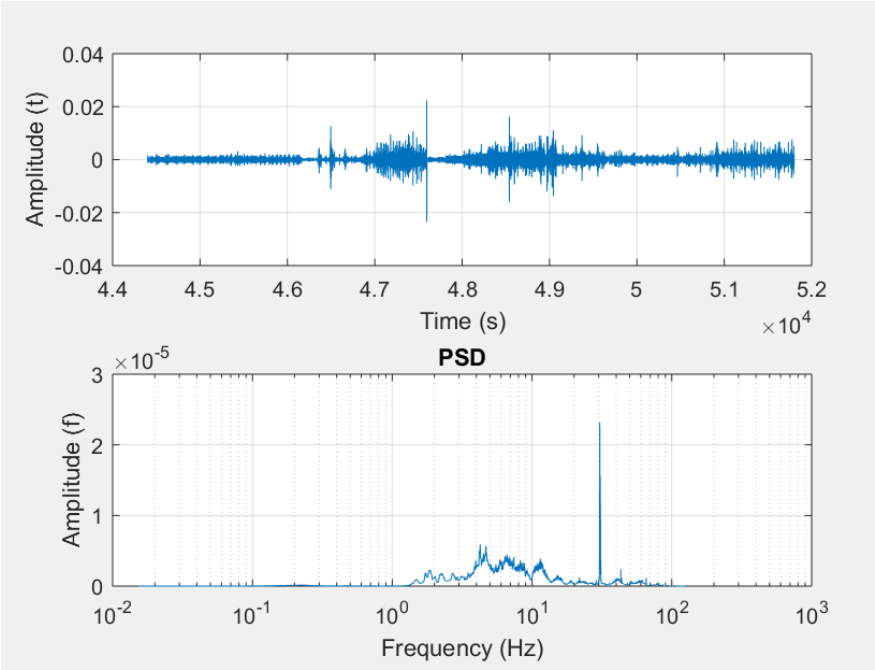

Figure C11. (a) Recorded signal, and (b) power spectral density for instrument #4 in the horizontal direction, H2 (NS)

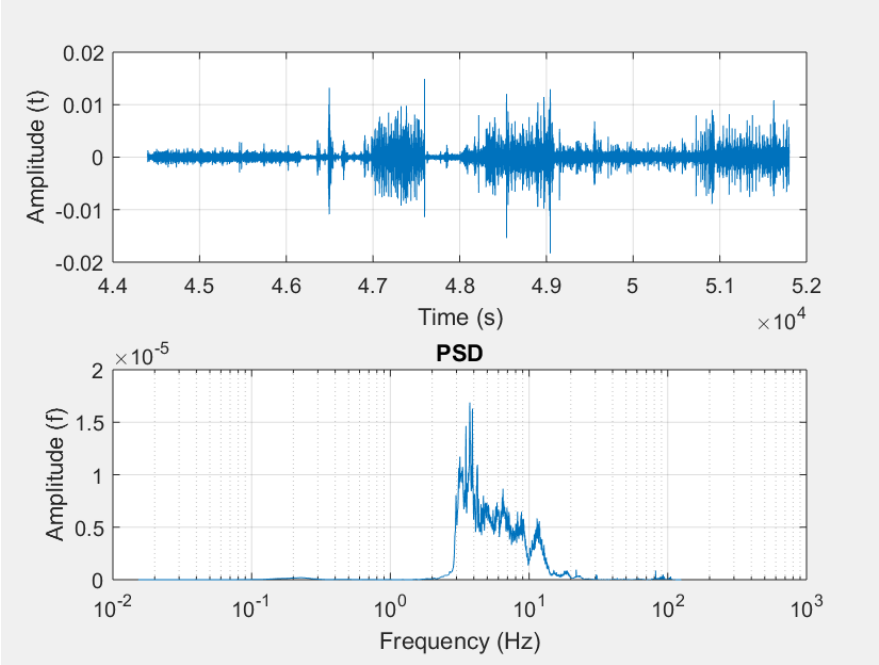

Figure C12. (a) Recorded signal, and (b) power spectral density for instrument #4 in the vertical direction (depth)

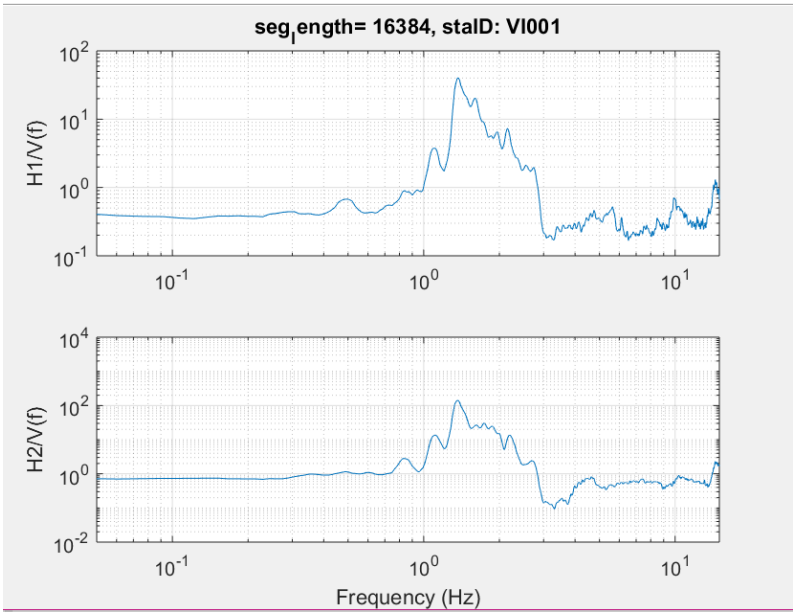

Figure C13. Fourier spectral quotients for both horizontal directions (instrument #4)

Code to Process the HVSR data per instrument.

```
clear all
%%code to plot time series and compute FFT and or PSD as well as H/V spectral ratios...%%
%% By Dr. Carlos Huerta %%

seg_length=16384;   %%segments length for doing the average process
ovlap=0.5;  %%the overlap in terms of fraction of percent
overlap=floor(seg_length*(ovlap));  %%overlap number of points
frecmuestreo=250;  %%Sampling frequency in (Hz)

          for icount=1:3
       if icount == 1, fname=['VI001_00',int2str(icount)];, end
       if icount == 2, fname=['VI001_00',int2str(icount)];, end
       if icount == 3, fname=['VI001_00',int2str(icount)];, end

   dat=load([fname,'.txt'], '-ascii');

   tim_vect=dat(:,1);

   id_save_file_corr=0;
   [dat]=base_line_corr(dat(:,2),[fname,'.txt'],id_save_file_corr);
   dat=[tim_vect,dat];
   dat_trim=dat(1:length(dat),:);  %%here to trim or not to trim portion of time series.

   [rows,columns]=size(dat_trim);



   data_mean=mean(dat_trim(:,2));, dat_trim(:,2)=dat_trim(:,2)-data_mean;

      figure(1)
   subplot(2,3,icount);, plot(dat(:,1),dat(:,2),'r');, grid on
   subplot(2,3,icount+3);, plot(dat_trim(:,1),dat_trim(:,2),'g');, grid on

           figure(icount+10)                                    %Registro en dominio de tiempo
    subplot(2,1,1);, plot(dat_trim(:,1),dat_trim(:,2));, grid on

           xlabel('Time (s)');, ylabel('Amplitude (t)');
    [auto_p,fsamp] =
psd(dat_trim(:,2),seg_length,frecmuestreo,hanning(seg_length),overlap,'mean');  %auto_power
spectra (psd)

            figure(icount+10)
```

```
            subplot(2,1,2);, semilogx(fsamp,auto_p); grid on
            xlabel('Frequency (Hz)');, ylabel('Amplitude (f)');, title('PSD');
if icount == 1, for_ratio_c1=auto_p;, end
if icount == 2, for_ratio_c2=auto_p;, end
if icount == 3, for_ratio_c3=auto_p;, end

        end

 %-----------------do spectral ratios next block-------------------------%
 sp_rat_c1_2_c3=for_ratio_c1./for_ratio_c3;   %%here doing H1/V
 sp_rat_c2_2_c3=for_ratio_c2./for_ratio_c3;   %%here doing H2/V

 nit=1;, Np=length(sp_rat_c1_2_c3);  %%parameter to smooth the H/V spectral ratios
 [sp_rat_c1_2_c3]=to_smooth_w_points(sp_rat_c1_2_c3,nit,Np);
 [sp_rat_c2_2_c3]=to_smooth_w_points(sp_rat_c2_2_c3,nit,Np);

figure(33)
subplot(2,1,1), loglog(fsamp,sp_rat_c1_2_c3);, grid on

% % % % % subplot(2,1,1), loglog(fsamp,sp_rat_c1_2_c3);, grid on

% % % % %  xlabel('Frequency (Hz)');,
 ylabel('H1/V(f)');, title(['seg_length= ',num2str(seg_length),', staID: ',fname(1:5)])
xlim([0.05 15]);
subplot(2,1,2), loglog(fsamp,sp_rat_c2_2_c3);, grid on

% % % % % subplot(2,1,2), loglog(fsamp,sp_rat_c2_2_c3);, grid on

xlabel('Frequency (Hz)');, ylabel('H2/V(f)');, %%title('Spectral Ratio (Nakamura)')
xlim([0.05 15]);

coef_spec_h1 = [fsamp,sp_rat_c1_2_c3'];
coef_spec_h2 = [fsamp,sp_rat_c2_2_c3'];
file_save_h1 = [fname(1:5) '_coef_spec_H1'];
file_save_h2 = [fname(1:5) '_coef_spec_H2'];
path= 'C:\Users\name\Desktop\datos\Nakamura\CORRECCION\';

% % % save([path, file_save_h1], 'coef_spec_h1', '-ascii')
% % % save([path, file_save_h2], 'coef_spec_h2', '-ascii')
```

Code to plot the spectral ratios and average for the HVSR method.

```
clear all
%code to plot SPRHV at Coliseo

file_nameh1v=['OK001_coef_spec_H1';'RO001_coef_spec_H1';'TX001_coef_spec_H1';'VI001_
coef_spec_H1'];
file_nameh2v=['OK001_coef_spec_H2';'RO001_coef_spec_H2';'TX001_coef_spec_H2';'VI001_
coef_spec_H2'];

color_use=['r','g','b','k'];

 for icount =1:4
     dat1=load(file_nameh1v(icount,:), '-ascii');
     dat2=load(file_nameh2v(icount,:), '-ascii');

  figure(1)
    subplot(2,1,1)

    if icount==1
% % % % %     semilogx(dat1(:,1),dat1(:,2),color_use(icount));, hold on, grid on;,axis([0.1 20 0
400]);
    loglog(dat1(:,1),dat1(:,2),color_use(icount));, hold on, grid on;,axis([0.1 20 0 400]);

      %xlabel('Frequency (Hz)');
    dat_1=dat1(:,1);,
    dat_2=dat1(:,2);, end;

    if icount==2
% % % % %     semilogx(dat1(:,1),dat1(:,2),color_use(icount));, hold on, grid on;,axis([0.1 20 0
40]);
    loglog(dat1(:,1),dat1(:,2),color_use(icount));, hold on, grid on;,axis([0.1 20 0 400]);

      %xlabel('Frequency (Hz)');
       dat_3=dat1(:,1);,
       dat_4=dat1(:,2);, end;
    if icount==3
% % % % %     semilogx(dat1(:,1),dat1(:,2),color_use(icount));, hold on, grid on;,axis([0.1 20 0
40]);
       loglog(dat1(:,1),dat1(:,2),color_use(icount));, hold on, grid on;,axis([0.1 20 0 400]);

      %xlabel('Frequency (Hz)');
       dat_5=dat1(:,1);,
       dat_6=dat1(:,2);, end;
```

```
   if icount==4
% % % % %     semilogx(dat1(:,1),dat1(:,2),color_use(icount));, hold on, grid on;,axis([0.1 20 0
40]);
   loglog(dat1(:,1),dat1(:,2),color_use(icount));, hold on, grid on;,axis([0.1 20 0 400]);

       %xlabel('Frequency (Hz)');,
       dat_7=dat1(:,1);,
       dat_8=dat1(:,2);, end

%%%%%%%%%%%% Segunda Grafica (direccion H2)

     if icount==1
       dat_1a=dat2(:,1);,
       dat_2a=dat2(:,2);, end;

     if icount==2
       dat_3a=dat2(:,1);,
       dat_4a=dat2(:,2);, end;

     if icount==3
       dat_5a=dat2(:,1);,
       dat_6a=dat2(:,2);, end

     if icount==4
       dat_7a=dat2(:,1);,
       dat_8a=dat2(:,2);, end

   subplot(2,1,2)
% % %      semilogx(dat2(:,1),dat2(:,2),color_use(icount));, hold on, grid on
         loglog(dat2(:,1),dat2(:,2),color_use(icount));, hold on, grid on

           xlabel('Frequency (Hz)');, ylabel('Amplitude SRHV');,axis([0.1 20 0 400]); %Datos de la
grafica (x&y labels y especificacion de los ejes.

 end


% % % % % %  Calculos para obtener el promedio de los coeficientes espectrales y graficarlo.
% % % % %         frec1= dat_1 + dat_3 + dat_5 + dat_7;,
       amplit1= dat_2 + dat_4 + dat_6+ dat_8;,

% % % % %             avg_f1 = frec1/4;,
          avg_ampt1 = amplit1/4;,
```

```
% % % % %        frec2= dat_1a + dat_3a + dat_5a + dat_7a;,
      amplit2= dat_2a + dat_4a + dat_6a + dat_8a;,

% % % % %            avg_f2 = frec2/4;,
         avg_ampt2 = amplit2/4;,

% % % % %  avrg= avg_f1 + avg_f2;,
% % % % %  avrg1=avrg/2;,
 avrg_ampt= avg_ampt1 + avg_ampt2;,
 avrg_ampt1= avrg_ampt/2;,
 format long;,
 max=find(max(avrg_ampt1))


figure (1)
subplot(2,1,1)
% % % % %     semilogx(avg_f1(:,1),avg_ampt1(:,1), 'm','Linewidth',1.5);, hold on, grid on;,
% % % % %          loglog(avg_f1(:,1),avg_ampt1(:,1), 'm','Linewidth',1.5);, hold on, grid on;,
              loglog(dat_1(:,1),avg_ampt1(:,1), ':b','Linewidth',1.5);, hold on, grid on;,


         axis([0.1 15 0 80]);,    %xlabel({'(a)'});,axis([0.1 15 0 80]);,
         legend('Station #1','Station #2','Station #3','Station #4','Average');,
         title({'Spectral Ratio (Nakamura)','H1/V'});,
         ylabel({'Amplitude SRHV'});

 subplot(2,1,2)
% % % % %     semilogx(avg_f2(:,1),avg_ampt2(:,1), 'm','Linewidth',1.5);, hold on, grid on;,
% % % % %          loglog(avg_f2(:,1),avg_ampt2(:,1), 'm','Linewidth',1.5);, hold on, grid on;,
       loglog(dat_1a(:,1),avg_ampt2(:,1), ':g','Linewidth',1.5);, hold on, grid on;,

         xlabel({'Frequency (Hz)'});, ylabel({'Amplitude SRHV'});,axis([0.1 20 0 220]);
%xlabel({'Frequency (Hz)','(b)',''});, ylabel({'A(f)'});,axis([0.1 20 0 220]);
         legend('Station #1','Station #2','Station #3','Station #4', 'Average')
         title({'H2/V'});


 figure (2)
 subplot(1,1,1)
% % % % %       semilogx(avrg1(:,1),avrg_ampt1(:,1), 'm','Linewidth',1.5);, hold on, grid on;,
% % % % % %              loglog(avrg1(:,1),avrg_ampt1(:,1), 'm','Linewidth',1.5);, hold on, grid
on;,
            loglog(dat_1(:,1),avrg_ampt1(:,1), ':k','Linewidth',1.5);, hold on, grid on;,
            loglog(dat_1(:,1),avg_ampt1(:,1), ':b','Linewidth',1.5);, hold on, grid on;,
            loglog(dat_1(:,1),avg_ampt2(:,1), ':g','Linewidth',1.5);, hold on, grid on;,
```

```
xlabel('Frequency (Hz)');, ylabel('Amplitude SRHV');,axis([0.1 20 0 200]);,
legend('Average (H1/V & H2/V)', 'Average (H1/V)', 'Average (H2/V)');,
title('Spectral Ratio (Nakamura)');,


% % % % % % Codigo para guardar los promedios en un file

coef_spec_h1 = [dat_1(:,1),avg_ampt1];     %[avg_f1,avg_ampt1];
coef_spec_h2 = [dat_1(:,1),avg_ampt2];     %[avg_f2,avg_ampt2];
coef_spec_h1_h2 = [dat_1(:,1),avrg_ampt1];
file_save_h1 = ['avrg_coef_spec_H1'];
file_save_h2 = ['avrg_coef_spec_H2'];
file_save_h1_h2 = ['avrg_coef_spec_H1_H2'];

path= 'C:\Users\name\Desktop\datos\Nakamura\CORRECCION\';,
% % % save([path, file_save_h1], 'coef_spec_h1', '-ascii')
% % % save([path, file_save_h2], 'coef_spec_h2', '-ascii')
% % % save([path, file_save_h1_h2], 'coef_spec_h1_h2', '-ascii')
```